Black holes and vacua in string theory

A non-supersymmetric study

Cohen Maldonado, D.B.

Black Holes and Vacua in String Theory

Diego B. Cohen-Maldonado

BLACK HOLES AND VACUA IN STRING THEORY

A Non-supersymmetric Study

Diego B. Cohen-Maldonado

Black Holes and Vacua in String Theory

A Non-supersymmetric Study

Black Holes and Vacua in String Theory

A Non-supersymmetric Study

Academisch Proefschrift

ter verkrijging van de graad van doctor

aan de Universiteit van Amsterdam

op gezag van de Rector Magnificus

prof. dr. ir. K.I.J. Maex

ten overstaan van een door het College voor Promoties ingestelde commissie,

in het openbaar te verdedigen in de Agnietenkapel

op donderdag 7 maart 2019, te 10.00 uur

door

Diego Benjamin Cohen Maldonado

geboren te Santiago

PROMOTIECOMMISSIE

PROMOTOR

prof. dr. J. de Boer	Universiteit van Amsterdam

CO-PROMOTOR

Dr. A. Castro Anich	Universiteit van Amsterdam
Dr. B.S.E Vercnocke	KU Leuven

OVERIGE LEDEN

prof. dr. E.P. Verlinde	Universiteit van Amsterdam
prof. dr. E.L.M.P Laenen	Universiteit van Amsterdam
prof. dr. S.J.G. Vandoren	Universiteit Utrecht
dr. B.W. Freivogel	Universiteit van Amsterdam
dr. I. Bena	CEA/Saclay

This work has been accomplished at the Institute for Theoretical Physics (ITFA) of the University of Amsterdam, and it was funded by the "Becas Chile" scholarship programme of the Chilean government (CONICYT PAI/INDUSTRIA 79090016).

FACULTEIT DER NATUURWETENSCHAPPEN, WISKUNDE EN INFORMATICA

“Do not train a child to learn by force or harshness; but direct them to it by what amuses their minds, so that you may be better able to discover with accuracy the peculiar bent of the genius of each.”

— Plato

Publications

THIS THESIS IS BASED ON THE FOLLOWING PUBLICATIONS:

[1] Tomás Andrade, Alejandra Castro, and Diego Cohen-Maldonado,
"The Spectrum of Static Subtracted Geometries,"
Class.Quant.Grav. 34 (2017) no.9, 095009, arXiv:1611.09330 [hep-th].

Presented in Chapter **5**.

[2] Diego Cohen-Maldonado, Juan Diaz, Thomas van Riet, and Bert Vercnocke,
"Observations on fluxes near anti-branes,"
JHEP 1601 (2016) 126, arXiv:1507.01022 [hep-th].

Presented in Chapter **8**.

[3] Diego Cohen-Maldonado, Juan Diaz and Fridrik Freyr Gautason,
"Polarised antibranes from Smarr relations,"
JHEP 1605 (2016) 175, arXiv:1603.05678 [hep-th].

Presented in Chapter **9**.

OTHER PUBLICATIONS BY THE AUTHOR:

[4] Diego Cohen-Maldonado, Juan Diaz, Thomas van Riet, and Bert Vercnocke,
"From black holes to flux throats : Polarization can resolve the singularity,"
Fortsch.Phys. 64 (2016) 317-321, arXiv:1511.07453 [hep-th].

[5] Máximo Bañados and Diego Cohen-Maldonado,
"Short note on gravity with tensor auxiliary fields,"
Phys.Rev. D89 (2014) no.4, 047505, arXiv:1309.6177 [hep-th].

Acknowledgements

These acknowledgments took me more time than expected. They also came out more sentimental that my initial intentions. I was planning to make them flatter, on the edge of failing a Turing test. But, apparently, I needed to give lots of "thank yous"; I wanted to tell everybody how much I appreciate what they have done for me. Inevitably, these acknowledgments departed from its initially intended robotic writing and grew into emotions, flesh, and bones. My lack of control over these acknowledgments has a clear origin. For me, the Ph.D. process went way beyond my research and a degree. It was a die-reborn-growth process. I left my hometown, Santiago, arriving in a place that I only knew by pictures. I knew nobody. I was welcomed by strangers. The Ph.D. came as a bucket of cold water – it was time to grow. Probably the reader can relate to this. It is very hard to find somebody in an international field like ours that has not been through the same. For some of you, more than once, and with complications added (e.g. two body problem). I would say that there is not much room to write about these matters in a science thesis. It makes you appear overly emotional in a field that reason is the most valued asset. But I just felt it was necessary. Because if there is a test I want to pass easily, is Turing's.

Outside the Horizon: The Academic Path

In this section, I would like to thank the persons that walked me through the laborious steps and challenges in academia. We, in a combined effort, managed to land this thesis plane, that was circling around for longer and with less fuel than expected. This is the *outside of the horizon*, where measurements can be made: a thesis was required, and a thesis it was.

I start with the usual suspects, the people whose help and presence were crucial. Thanks, Alejandra Castro, for your guidance and teachings during these five years. I appreciate all those moments you demonstrate to care. Thanks for the many times that I was lost and you put me back on track. Thanks for your precious help. Thanks, Bert Vercnocke, for immersing me in the complex-yet-beautiful branes' world. Thank you for your academical and life guidance. Thanks, both of you, for the extra effort and time that this thesis required. Thanks to the committee members for carefully reviewing and approving this thesis. Thanks for joining me during its defense. Despite receiving the first notice more than a year ago, they decided to be present with no further remarks. Thank you for your time and patience.

No publications, no thesis. I had the opportunity of working along pleasant, bright, and lively people. Thank you so much for joining forces together Alejandra Castro, Tomas Andrade, Juan Diaz, Bert Vernocke, Thomas van Riet, and Fridrik Gautason. Thanks, Juan Pedraza, Manus Visser, and Watse

Sybesma for the short time I worked among you on a project that, unfortunately, I had to step out. Thanks, Andrea Puhm, for your help and time invested in the project that we wanted to work on.

When arriving in Amsterdam, I brought along a Chilean wine. I wanted to show my appreciation to the secretary, Anne-Marieke Crommentuijn, that helped me greatly to make a safe touchdown from a house in Chile to a house in Amsterdam. I gave her the wine. Looking back, I should have brought a full container. The amounts of help and support I have received from the staff of the IoP and UvA is priceless. Thanks, Anne-Marieke Crommentuijn, Nataly Wells, Klaartje Wartenbergh, Joost van Mameren, and Mirjam Meier. This thesis would not be there, literally, without your help.

One of the (many) paradoxes of the Ph.D. life, is being afraid of asking questions – when it is actually what you should be doing. Fortunately, the IoP postdocs were extremely kind and ready to help everytime I knocked at their door. Thanks, Juan Jottar, Juan Pedraza, Damian Galante, Nabil Iqbal (who was a postdoc back then), Marcos Crichigno, Alex Belin, and Marcel Vonk.

It is said that my English "are not the better." This thesis went through intense proof-reading. Not this section though – this is where **I** write. Thanks to my proofreaders Lauren Greenspan, Watse Sybesma, Eva Llabres, and Tomas Andrade. Despite having the busy schedule that any theoretical physicist can relate to, they squeezed this thesis in it. *Thanks you again for you preciousus helpfulness*. Watse Sybesma also helped me greatly during the writing of the "Samenvatting" section. Dankjewel W.

I would need another thesis, named "Students and Friendships in Science park: A Non-academic Study", to describe mine/our social circle around the UvA. Meeting other students (in Science Park) and hanging out with them (not in Science Park) has been one of the most rewarding experiences during the past years. Thanks Fotis Dimitrakopoulos, Natascia Pinzani, Irfan Ilgin, Daniel Mayerson, Jaco de Swart, Robert Jefferson, Laurens Kabir, Eva Llabres, Jorrit Kruthoff, Manus Visser, Sam van Leuven, Gerben Oling, Sagar Lockhande, Francesca Ferrari, Sabrina Cotogno, Michael Wiechers, Ido Niesen, Sergio Tapia, Henry de Cagny, Benjamin Daiber, and Fernando Rejon-Barrera. After these years, I am lucky enough (?) to keep on seeing many of those faces. Let's hope that after this thesis there will be enough time to meet in *insert name of the city where you live nowadays*.

I was first exposed to physics in the Universidad de Chile and Universidad Catolica de Chile, a bit more than a decade ago. These professors showed me the beauty that is found in the physical description of nature. Thanks, Gonzalo Gutierrez, Gonzalo Palma, Nelson Zamorano, Max Banados, and Jaime Roessler. You are, like it or not, responsible for starting a process that ends in this document. Thank you so much for pushing me forward at the beginning.

Inside the Horizon: The Emotional Path

In this section, I would like to thank the persons that helped me to withstand the steps and challenges in academia, and that in a combined effort managed to land this thesis pilot, that was up there in the clouds with more confusion and less control than expected. This is the *inside of the horizon*, where measurements cannot be quantified (?): a thesis was delivered, with a healthy mind intact.

Arriving in Amsterdam was hard. The first few months I was browsing quite often for return tickets. I was looking into a way to transfer my grant back to Chile and continue my Ph.D. over there. Severely homesick. Luckily, I came across people that helped me to overcome it. I want to thank Eelke Krol, who is no longer with us, for all his professional advice and support. Without him, probably I would be writing this in Spanish, if only. Thanks, Fotis Dimitrakopoulos, Natascia Pinzani, Laurens Kabir, Michael Wiechers, Nataly Cisternas, and Antonia Cohen-Maldonado, who took good care of me during those difficult moments. Thanks, Claudia Oviedo and Sebastian Olivares, whose advice was crucial. Thanks to my family, that were continuously supporting me from Chile.

During my Ph.D. I never stopped sporting, *mens sana in corpore sano*. This was initially encouraged by Eelke Krol. Besides the gym, I frequently played water polo during these years – despite not being very good at it. I felt so much better after every training. This feeling remains until today. Thanks, Michael Wiechers, for inviting me to join the team. Thanks, JAWS, for accepting and training me in English. Thanks also for inviting me to all the social events related to the team, and the unrelated ones as well. Sadly, this might be my last year with you guys. Nevertheless, I hope to keep on seeing you around the Amsterdam streets/pools.

After one year of arriving in Amsterdam, I moved to a large flat, that I call "the Anfieldcastle." Some of you might have been lucky enough to visit for dinners, birthday parties, Ph.D. celebrations and more – even a "completada." But that flat would be nothing without its residents, with whom I shared almost every day of my life since my arrival. Thanks, Eva Llabres, Michael Wiechers and Laurens Kabir for making everyday living an interesting experience. Thanks also to our short-stay flatmates: Adolfo Toloza, Paulina Martinez, Ilan Oxman, Ismael Palacios, Cony Quiroz, and Ricardo del Fuego. Thanks to the current flatmates, Michael Wiechers, Ina Cheibas, and Bernat Salbanya. Even though the inhabitants have changed, the vibe and harmony remain; I still love to live in that place.

I could not go that often to Chile; thus, Chile came to me. Amsterdam grew a little Chile, with residents and visitors. Thanks, Hernan Gonzalez, Sebastian Honores, Nataly Cisternas, Carlos Alcalde, Magdalena Flores, Conrado Bosman, Hernan Labbe, Natalia Rivera, Paloma Opazo, Camilo Ulloa, Pablo Inostroza, Cony Quiroz, Ilan Oxman, Javiera Vergara, Gonzalo Palomo, Adolfo Toloza, Paulina Martinez, Andres Huhner, Ismael Palacios, Constanza Moncada, and Marcos Perez. I cannot way to prepare some piscolas again with you guys. Thanks also to the ones who, even though not Chileans, I cannot unentangle from this group: Eva Llabres, Bernat Salbanya, Michael Mulet, Pablo Gracia, Miguel Ortega, Guillermo Garcia, Vanessa Catalano, Farah Gaddar, Alejandra Herrera, and Damian Galante.

During the writing of this thesis, at some point became clear that it was time to get a haircut, a trim, a tie and look for a job/working permit. I would like to say thanks to the Credit Risk Modelling team in Rabobank, more specifically the Stress Testing team, who welcomed and guide me through the complex world of finance and banking. My managers, Umesh Ramdaras, Reintje Maasdam, and Mieke van Riel, gave me enough room to finish this thesis and prompted me for its completion. Indeed, a big chunk of this thesis has been writing in the Rabo towers, Utrecht. Thank you very much.

While this thesis was ongoing, it inspired another book: "Femke en het zwarte gat dat haar sok

opvrat" which in English translates to "Femke and the black hole that washed up her sock." The book tells the story of Femke, a little girl, whose sock is stolen by a black hole. She goes after it, eventually facing the thief. It is a beautiful project that I am very glad to have worked on. Thank you, Watse Sybesma, for pushing forward this project, an idea originally born in the Brazil edition of the DRSTP. Thanks, Antonia Cohen-Maldonado, for joining the project and give its beauty and design. Thanks, Jacqueline de Vree, Jan Pieter van der Schaar, and Marcel Vonk for your priceless input while the making of the book. I hope that this is not the last adventure of Femke.

Not only the people based in Europe maintained my spirit alive. Remotely, many others were present. I appreciate every single opportunity that we have to meet/talk/text during these years. Thanks Ariel Franco, Matias Ibaceta, Benjamin Astroza, Romina Nespolo, Diamela Diaz, Juan Pablo Aguirre, Claudio Araos, Nicolas Pino, Jose Manuel Gonzalez, Pablo Echiburu, Diego Martinez, Johan Heyer, Milen Duarte, Santiago Hormazabal, Tomas Cohen, Luis Gonzalez, Luciano del Valle, Nicole Miller, Nicolas Donoso, Erick Burgos, Gloria Segovia, Diego Guzman, Rodrigo Lopez, Macarena Munoz, Alejandro Bernardin, Yasmin Navarrete, Pasquinell Urbani, Felipe "Pipin" Gonzalez, Miguel Pino, Claudia Oviedo, Sebastian Olivares, Giovanna Cottin, Gabriel Torrealba, Lita Becker, Matias Bennet, and Marcos Perez. Every time I happen to meet/contact you, it seems that it has passed no day since the last time.

Amsterdam also revealed to me its Mokum-Alef dual. I started to join celebrations like Hanukkah, Rosh Hashanah, and Pesaj. I want to thanks the hosts/guests Ido Niesen and his mother, Ilan Oxman, and Damian Galante. Maybe this year I will do my homework and put the correct dates on the calendar. Thank you all for this new part of my life.

The last year of writing was the toughest one. During it, many showed they care about this thesis. Some ask many times *the question* and patiently listened to the answer. Some gave me advise and time management insights. Some just gave me a hug. Thanks, Gerben Oling, Sam van Leuven, Eva Llabres, Ina Cheibas, Irfan Ilgin, Lucas Besters, Bart Litjens, Fotis Dimitrakopulos, Xinyi Zhao, Jesse Bouman, Thomas Kuijpers, Marcos Perez, Odysseas Tasioudis, Orestis Chatzaras, Martin van Daatselaar, Erik Oude Steenhof, Thomas Rockx, Veenam Panda, and Watse Sybesma. You were there with the right words at the right moment. Thank you all.

The Vacuum: The Beginning of both Paths.

In this section, I would like to thank all the persons that made the steps and challenges of the academic world to be meaningful and meaningless at the same time. There would be no reason to land a single-pilot plane at a deserted airport. This is *the vacuum*, the starting point of anything that can or cannot be measured: a thesis was required, and I was not alone.

My life has been built on the shoulders of Giants – my family. They have encouraged me to read, to experience, to laugh, to respect, and care for the others. They never made me feel ashamed of my mistakes; they taught me how to learn from them. They stood by me during tough times and celebrated with me in happy ones. My family, even not perfect, is the best family I could wish for. As my grandfather used to say: "perfect is an enemy of the good."

This thesis will not have been possible without Lia Maldonado, my mother, who has become my role model of how parenting should be. Her bravery and strength can only be compared with her love. She always knew how to scare away the ghosts I carried along. Thanks for showing me the important matters in life. My father, Gregory Cohen, who taught me about literature, poetry, movies, physics, theatre, and pushed me to be intellectually curious in all the possible ways. As he once said: "You are a physicist. But not only that." I love you both. I could not have asked for a better childhood that you provided me.

My sister, Antonia Cohen-Maldonado, who has been my accomplice all this time, and that took care of me, back then in Chile, and here in Europe. From whom I have always received honest advise. She show me in early in life, during my bachelor, many mistakes that I came to acknowledge now when finishing this thesis. Thank you for being there. My sister Rocio Almeyda, that defended me fiercely when needed. She also gave me good lessons as well. I still remember how afraid she was when I left. Referring to northern Europe, she said "those countries are too cold, too dark. Be cautious about it." She lived in Berlin several years in the past. Thanks for your caring. I think that now we agree that in these countries, summer happens as well.

In Amsterdam, I gained a new family member. Eva Llabres-Llambias became my new sister for me. With mutual support and trust, we boosted up what Amsterdam and this Ph.D. program had to offer to us. I wish you the best of luck in Paris. Thank you so much for being next to me these five years, and counting. As you said in your thesis acknowledgments: it would not have been half as fun without you.

I want to thank Leon Cohen and Edy Herrera, to have been there in the most turbulent times during my life. Both in Santiago and in Amsterdam. Thank you so much. I also appreciate the visit of my cousins Tomas Cohen, Cristobal Cohen, and Benjamin Cohen. Thank for walking me around in my new home. I also want to thanks Alejandro Siebert, Victoria Siebert, Manuel Escobar, Lia Escobar, Francisca Escobar, and Tia Muchi. I enjoyed very much seeing you when I was visiting home.

During these five years, my family went through big changes. Most of them I sadly missed. I want to thank the ones who left us: Elsa Parada, Manuel Almeyda, tia Toya, tia Bebe, Leon Cohen-Steingard, Blanca Munoz. I will miss you, but I keep your treasured lessons and memories with me. And I want to welcome the new generation, Abril Ramos, Emilia Ramos, Estela, Emiliana, Martin Escobar. Maybe one day you'll reach to this thesis, whatever the reasons are.

I want to thank immensely to Ina Cheibas. Thank you so much, for being next to me these (a bit more than) two years. You are the reason why I wanted to stay in Amsterdam so badly, a decision that I have no regrets of. This last year has been a roller coaster for us. You said to me once:"I feel I am in a competition with your other girlfriend, namely thesis." I am sorry for that. You were by far the one who was exposed the most to my mood swings, frustrations, excitements, fears etc ? all those beautiful things that make us human. It was exhausting. There is so much to make for, and I cannot wait for it. Thank you very much. You have been vital for me.

I want to thank the reader that make it all the way here. The emotional outburst is finished. I would say: let us jump into physics.

Samenvatting

Gedurende de afgelopen decennia heeft men met behulp van supersymmetrie en snaartheorie veel belangrijk nieuwe inzichten over de zwaartekracht vergaard. Zo heeft men bijvoorbeeld ontdekt dat de kwantumvrijheidsgraden van supersymmetrische zwarte gaten kunnen worden beschreven via snaartheorie en via de zogenaamde holografie. Bovendien heeft men aangetoond dat stabiele vierdimensionale vacua ? in de vorm van Minkowksiruimtetijd of Anti-de Sitterruimtetijd (AdS) ? kunnen voorkomen in supersymmetrische configuraties in de snaartheorie. Het is een belangrijk vereiste voor snaartheorie om de realistische vierdimensionale wereld te beschrijven.

Een niet-supersymmetrische studie

Ondanks de kennis verkregen met behulp van supersymmetrie, begrijpen we nog steeds niet volledig de microscopische eigenschappen van realistische zwaartekrachtconfiguraties. Zo zijn zwarte gaten in ons universum van het type Kerr en die zijn totaal niet supersymmetrisch. Experimentele waarnemingen tonen ook een versnelde expansie van ons universum aan. Deze waarnemingen zijn een sterk bewijs voor de aanwezigheid van een kleine positieve kosmologische constante. Het vacum van de algemene relativiteitstheorie met deze waarde voor de kosmologische constante wordt beschreven door de Sitterruimtetijd. Omdat we verwachten dat de algemene relativiteitstheorie de effectieve beschrijving is op lage energien van de snaartheorie, is het belangrijk om binnen de snaartheorie een vierdimensionaal de Sittervacum (dat niet supersymmetrisch is) te construeren. Wanneer dat niet mogelijk is, wordt het lastig om contact te maken tussen snaartheoretische voorspellingen en gemaakte observaties in ons universum.

Over dit proefschrift

Dit proefschrift is gewijd aan de studie van zwaartekrachtoplossingen met gebroken supersymmetrie. Het gepresenteerde onderzoek wordt in twee hoofdonderdelen gepresenteerd. Elk onderdeel is voorzien van een aparte introductie en overzicht waarin het belang van het uitgevoerde onderzoek in een historische en state-of-the-art context wordt uitgelegd. Na de inleiding wordt een meer technische uiteenzetting gepresenteerd met relevante achtergrondkennis. Daarna volgt het onderzoek zelf, met de presentatie van de resultaten en een verdere discussie daaromtrent. We schetsen nu kort de hoofdpunten van dit proefschrift.

Niet-supersymmetrische zwarte gatenholografie

Deel II van dit proefschrift behandelt niet-extreme zwarte gaten die tegelijkertijd ook niet-supersymmetrisch zijn in de context van snaartheorie. Het gebrek aan supersymmetrie stelt ons niet in staat om dezelfde rekentechnieken toe te passen op zwarte gaten als op hun supersymmetrische tegenhangers. Hierdoor

is het moeilijk om een snaartheoretische configuratie of een holografische beschrijving van de microtoestanden van het zwarte gat te vinden. Daarom hebben we een nieuwe benaderingen nodig die inzichten kan geven over de microscopie van zulke zwarte gaten. Om die reden onderzoeken wij een methode die Subtracted Geometry heet. Subtracted Geometry stelt dat de relevante vrijheidsgraden kunnen worden beschreven door een tweedimensionale conforme veldentheorie (CFT2). Minimaal gekoppelde scalaire velden op deze resulterende achtergronden vertonen een exacte conformesymmetrie. Na het verheffen van deze achtergrond tot hogere dimensies, blijken ze lokaal het product van een AdS3 en een bol te zijn, waardoor een holografische beschrijving van hun microscopisch vrijheidsgraden mogelijk is via de zogenaamde AdS3 / CFT2 dualiteit. Deze en andere interessante kenmerken van Subtracted Geometry ondersteunen de toepassing van deze methode.Het gepresenteerde onderzoek vindt plaats voordat de achtergrond wordt verheven naar hogere dimensies. We testen of de duale theorie eigenschappen toont die kunnen worden toegeschreven aan een CFT2. Met dit als doel bestuderen we de quasinormale tonen van zulke achtergronden. We gebruiken deze quasinormale tonen als een holografisch kenmerk omdat we weten hoe ze zich moeten gedragen wanneer de duale beschrijving CFT2 is, d.w.z. het geval van het zogenaamde BTZ zwarte gat.

Niet-supersymmetrische metastabiele Vacua

Deel III is gewijd aan de studie van niet-supersymmetrische metastabiele toestanden in de snaartheorie. Deze metastabiele toestanden worden geconstrueerd met behulp van supersymmetriebrekende antibranen. De focus op antibranen is vanwege hun rol in de snaartheorie: ze worden doorgaans gebruikt in de snaartheorie om niet-supersymmetrisch configuraties te construeren. Met behulp van metastabiele toestanden van antibranen is aangetoond dat vierdimensionale de Sittervacua kunnen worden geconstrueerd binnen de snaartheorie. Niettemin is dit resultaat betwist omdat op dit moment het mechanisme alleen goed gedefinieerd is als de antibranen niet reageren op de achtergrond en materievelden. Sinds 2009 is het bekend dat de reactie van de antibranen op de achtergrond en materievelden (en vice versa) bij de eerste-orde-benadering onfysisch gedrag vertoont. Er wordt beweerd dat het onfysische gedrag een artefact is van de benadering die werd gebruikt om de onderlinge interactie van de antibranen, de achtergronden en de materievelden te benaderen. De verwachtingen zijn dat het volledig in acht nemen van de onderlinge interacties deze twist moet beslechten. Helaas is het volledig in acht nemen van de onderlinge interacties nog niet mogelijk omdat dit een enorme technische inspanning vereist. In dit proefschrift ontwikkelen een techniek waarmee we een de onderlinge interacties kunnen benaderen zonder gebruik te maken van de expliciete volledige oplossing. Met dit als uitgangspunt kunnen wij randvoorwaarden onderzoeken die een systeem zonder onfysisch gedrag toestaan. Deze aanpak is veelbelovend maar nog geen hard bewijs omdat we niet laten zien dat er een oplossing is die aan de gegeven randvoorwaarden voldoet. We doen dit voor tien- en elfdimensionale superzwaartekracht. De tiendimensionale antibraanconfiguratie is van bijzonder belang omdat het kan worden gebruikt om het vierdimensionale de Sittervacum te verkrijgen.

Vooruitzicht

We eindigen met Deel IV, het vooruitzicht (Prospect), waarin we een korte algemene discussie geven over het onderzoek dat wordt besproken in dit proefschrift en we bespreken de interessante vooruitzichten die de resultaten van dit onderzoek voor de toekomst biedt.

Contents

Part I

Summary

“Now, where was I?”

— Leonard Shelby, *Memento*

Chapter 1

Black Holes and Vacua in String Theory: A Non-supersymmetric Study

During the past few decades, an important part of the understanding of gravity in the context of string theory has relied on gravitational configurations that enjoy supersymmetry. Black holes, when supersymmetric, allow their quantum degrees of freedom to be described via string theory configurations or holography. Additionally, supersymmetric string theory configurations have been proven to give rise to stable four-dimensional vacua – in the shape of Minkowski or anti-de Sitter (AdS) spacetimes – fulfilling a critical requirement needed if string theory intends to describe a realistic four-dimensional spacetime.

A Non-supersymmetric Study

Despite the knowledge retrieved under supersymmetry, we still do not fully understand the microscopics of realistic gravitational configurations. Black holes in the Universe are of the Kerr type and enjoy no supersymmetry at all. Also, experimental observations demonstrated an accelerated expansion of our universe. These observations are strong evidence for the presence of a small positive cosmological constant. The vacuum of general relativity with this cosmological constant contribution is described by de Sitter spacetime. As we expect general relativity to be the low energy effective description of string theory, it is then desirable to construct four-dimensional de Sitter vacuum (which is non-supersymmetric) within string theory. If not, we are failing to make contact between string theory and current observations about the Universe.

About this Thesis

This thesis is devoted to the study of gravitational solutions with broken supersymmetry. The involved research separates into two main parts. Each part has its introduction and overview that puts in place the importance of the performed research in a historical and state-of-the-art context. A somewhat more technical discussion is given after this introduction, showing some relevant and useful background knowledge. After that comes the main research itself, with the presentation of the results and their further discussion. We now briefly outline the thesis.

Non-supersymmetric Black Holes Holography

Part II tackles non-extremal black holes, which are non-supersymmetric in string theory. For black holes, the lack of supersymmetry does not allow us to apply the same computational techniques as with their supersymmetric counterparts, making it hard to find a stringy configuration or a holographic description of the black hole's microstates. Therefore, we are in need of novel approaches that could give insights about their microscopics. We scrutinize one of these approaches, the so-called "subtracted geometry" program. The subtracted geometry program conjectures that by isolating the relevant degrees of freedom, via a procedure that is called subtraction, the microscopics of four- and five-dimensional asymptotically flat black holes (which includes the Kerr black hole) can be described by a two-dimensional conformal field theory (CFT_2). Minimally coupled scalars on these subtracted black hole backgrounds exhibit an exact conformal symmetry. After an uplift, these backgrounds are locally a product of an AdS_3 and a sphere, allowing a holographic description of their microscopic degrees of freedom via the AdS_3/CFT_2 duality. These and other interesting features of subtracted geometries support the conjecture. Our scrutiny happens at the non-uplifted level, where we test if the dual theory shows properties that could be attributed to a CFT_2. For this purpose, we study the quasinormal modes of static subtracted geometries. We use these quasinormal modes as a holographic benchmark because we know how they behave when the dual description of the black hole background is a CFT_2, i.e., the BTZ black hole.

Non-supersymmetric Metastable Vacua

Part III is dedicated to the study of non-supersymmetric metastable states in string theory. These metastable states are constructed using supersymmetry breaking antibranes. The focus on antibranes is due to their relevance: they are generally used in string theory to construct non-supersymmetric configurations. Using metastable states of antibranes, it has been shown that four-dimensional de Sitter vacua can be constructed within string theory. Nevertheless, this result has been contested, since for the moment this mechanism is well defined only when the antibranes do not back-react on the background. Since 2009, it has been known that the antibrane back-reaction at first order approximation exhibits unphysical behavior in the matter fields. It is argued that this issue is an artifact of the approximation used to include the back-reaction effects. The expectations are that full inclusion of back-reaction should be conclusive about the existence of the metastable state. Unfortunately, a fully back-reacted picture is unavailable and requires an enormous technical effort. We develop a technique that allows us to explore a fully back-reacted picture without the explicit full solution. From here, we can set the boundary conditions that allow for a system with no unphysical behavior. This resolution is suggestive but not yet conclusive since we do not prove the existence of a solution that satisfies these boundary conditions. We do this for ten- and eleven-dimensional supergravity. The ten-dimensional antibrane configuration is of particular importance since it can be used to obtain four-dimensional de Sitter vacuum.

Prospect

We end up with Part IV, the Prospect, where we give a short general discussion about this thesis' research and point out interesting prospects in relation to it.

Part II

Non-supersymmetric Black Holes Holography

"Look at the sky, that everything dwarfs. Our jobs, meetings, and careers: so futile. What a relieve."

— Gregory Cohen-Muñoz

Chapter 2

Black Holes Subtraction

Black Hole Entropy and Subtracted Geometries

The microscopic origins of the entropy of a black hole S_{BH} have been a fascinating puzzle since Bekenstein [6] and Hawking [7] proved during the 70's that black holes carry entropy. Since then, the study of S_{BH} has met two milestones discoveries:

- In [8], Brown and Henneaux set the starting point for the description of S_{BH} via a dual CFT$_2$ for black holes containing an AdS factor in their geometry. For example, the BTZ black hole which is asymptotically AdS$_3$ [9], or extremal black holes (i.e., zero Hawking temperature) whose near-horizon limit contains an AdS$_2$ factor.

- In [10], Strominger and Vafa demonstrated that the entropy of a supersymmetric five-dimensional charged black hole in the extremal limit is described by a microscopic string theory configuration. This result was later extended to other extremal [11] and near-extremal examples [12, 13].

These two results are not immediately generalized for black holes that do not have an AdS factor in their geometry or are non-extremal. For black holes non embedded in AdS, a dual field theory is not immediately evident, since the traditional AdS/CFT duality does not hold anymore. And for non-extremal black holes, a Strominger-Vafa approach is not possible. The reason is that non-extremal black holes are non-supersymmetric in string theory. With no supersymmetry, we cannot extrapolate some relevant observables from weak to strong coupling, which is a fundamental step in [10].

Black holes in astrophysical settings are expected to be finite-temperature Kerr black holes [14], so non-extremal, and generally with no AdS factor – besides the extremal and near-extremal limit[1]. Therefore, it is evident that a shortage of the understanding of black holes beyond extremality or without an AdS factor is equivalent to an incomplete comprehension of the universe.

[1]Near-extremal Kerr black holes are claimed to exist in our universe [15, 16, 17]. These black holes are interesting to study since it is likely that observations could confirm AdS/CFT predictions. Theoretically, extremal and near-extremal Kerr black holes have a near-horizon dynamics governed by an $SL(2,\mathbb{R})$ conformal symmetry [18, 19]. This symmetry constraints the gravitational radiation and orbits of in-falling objects within this region, and allows to solve for their orbits and resulting gravitational radiation [20, 21, 22, 23]. The frequency of this radiation is very characteristic for a near-extremal Kerr black hole [24, 25]. Therefore, it could be used for Kerr black holes detection. Further experimental confirmation of the near-horizon region conformal properties could also be possible.

However, there is evidence indicating that non-extremal black holes like Kerr might be dual to a CFT_2. The S_{BH} of general four- and five-dimensional asymptotically flat black holes can be recast as suggesting that a CFT_2 is responsible for it, i.e., S_{BH} for these black holes can be written resembling a left- and right-moving independent microscopic contributions [26]. Also, it was found in [27] that a massless scalar probe on a general Kerr background exhibits an approximate conformal symmetry. Even if approximate, this symmetry was enough to construct a Cardy entropy matching the S_{BH} of the Kerr black hole [27]. Also in [27], it was shown that scattering amplitudes (absorption probabilities) on the Kerr background are approximately the finite-temperature absorption cross-section of a CFT_2. The derived left and right temperatures of this cross section correspond precisely to the expected ones of a *hypothetical* CFT_2 dual to the general Kerr black hole [27][2]. It is tempting then to say that, somehow, a dual CFT_2 exists for these non-extremal black holes, although no AdS factor is found in their geometry.

An attempt to explain the origin of these suggestive features is the subtracted geometry program [28, 29, 30, 31, 32]. Subtracted geometries are black hole spacetimes obtained by modifying the warp factor in the geometry of four- and five-dimensional asymptotically flat black holes. These geometries are not embedded in AdS, so a dual CFT description is not immediately available. Nevertheless, subtracted geometries exhibit interesting features, among which:

- In a subtracted geometry spacetime, the approximate conformal symmetry of [27] for probe scalars becomes exact, supporting the conjecture that these spacetimes should be well described by a dual CFT.
- The black hole and its subtracted geometry have the same horizon quantities, such as temperature or entropy. This suggests that the black hole microscopics is unchanged after the subtraction procedure.

The interpretation here is that a subtracted geometry is a way to put a black hole in a box: it decouples away its asymptotic structure and isolates its relevant degrees of freedom. This interpretation is appealing since a black hole in a box is a system in thermodynamic equilibrium and with positive specific heat [28]. The last is desirable if we intend to describe the black hole via a dual CFT since all unitary CFTs have positive specific heat. Let us remind the reader that a subtracted geometry is not embedded in AdS; thus a dual CFT description remains as a conjecture.

The features mentioned above make subtracted geometries interesting for holographic studies. A holographic interpretation of these spacetimes is possible, but only after an uplift to one more dimension. The uplift spawns an AdS_3 factor in the line element of the subtracted geometry, where the four-dimensional subtracted geometry uplifts to $\text{AdS}_3 \times S^2$ [30] and the five-dimensional to $\text{AdS}_3 \times S^3$ [28]. Thus, using the $\text{AdS}_3/\text{CFT}_2$ duality, the S_{BH} of the uplifted subtracted geometry can be described via a CFT_2 dual.

The non-uplifted subtracted geometry has no obvious dual field theory description, despite all the mentioned evidence pointing to a CFT_2. This part of the thesis is devoted to advance in this direction.

[2]The last two results are the core of the "Hidden Conformal Symmetry of a Kerr Black Hole" [27] that we review at the beginning of chapter 2.

We scrutinize the non-uplifted subtracted geometry/CFT_2 conjecture, finding in chapter 5 evidence against it. We study the quasinormal modes of the subtracted geometry to build up this evidence. We describe now how these quasinormal modes can give insights about the dual field theory of a black hole background.

Quasinormal Modes and Holography

Quasinormal modes are the late-time solution of the wave equations describing linear perturbations on a given background. These wave equations have dissipative boundary conditions, and they can be written as the following eigenvalue problem [33],

$$\mathcal{P}(\partial_t, \partial_i)\psi(t, x^i) = 0, \tag{2.1}$$

where t is the time, x^i are the spatial dimensions, ψ is the field encoding the perturbations, and $\mathcal{P}$ is a second (first) order differential operator for integer $(1/2)$ spin. The quasinormal modes in (2.1) have complex spectrum (complex frequencies), characterizing then a dissipative phenomenon. Quasinormal modes differ from the traditional normal modes, which are non-dissipative and thus very long-lived; hence the prefix "quasi."

The eigenfrequencies of (2.1) are known to carry information about the background geometry. Maybe the most famous example in this regard is Kac's "hearing the shape of a drum" [34]. The study of the quasinormal modes of (2.1) allows for (limited) insights about the curved background where they propagate through. Let us take for example the Schwarzschild black hole. Solving for the quasinormal frequencies ω_ℓ in this background, where ℓ is the spherical harmonics multipolar momentum, allows the extraction of the mass M of the black hole [35] [3],

$$\omega_\ell \propto \frac{\ell}{M}, \tag{2.2}$$

where $\ell \gg 1$. In this case, M is the parameter characterizing the geometry, and its value can (approximately) be evaluated by knowing the quasinormal frequency and the multipolar momentum associated with it. It is good to remark that quasinormal modes, as a late-time solution, do not give information about the initial perturbation that originated (2.1).

Notice that an asymptotically flat black hole, like the Schwarzschild example above, is naturally a dissipative system. Modes are trapped and absorbed in the horizon of the black hole, while asymptotically they are escaping to infinity. This information is implemented via the boundary conditions[4] in (2.1), and it is crucial to describe quasinormal modes behavior when studying black holes.

In this thesis, we focus on the quasinormal modes of black holes. These quasinormal modes have been extensively investigated in astrophysical and theoretical settings (see [36, 37, 38, 39] for detailed reviews). With the detection of gravitational waves originated from the coalescence of compact binaries [40], the empirical relevance of these quasinormal modes in astrophysics has increased notably.

[3] This publication also happens to be the one where the term "quasinormal mode" was coined.

[4] For another asymptotical structure, like AdS, the correct choice of the asymptotic boundary condition is less obvious; we discuss this in section 4.

Quasinormal modes are providing the first tests of general relativity in its non-linear and dynamical strong-field regime since:

1. The gravitational waves emitted during the late-time of the ringdown[5] stage is expected to be well described by quasinormal modes [36, 37, 38, 39]. If general relativity holds within this regime, the quasinormal spectrum should depend only on the mass and angular momentum of the black hole.

2. The measurement of the frequency of the dominant mode – the lowest frequency mode –, allows retrieving the experimental mass and angular momentum values.

3. Further measurements for higher frequency modes permit to test the no-hair theorem [41, 42] since the whole spectrum should be characterized by the mass and angular momentum values, already fixed in step 2. The no-hair theorem is a proxy for the validity of general relativity.

Positive results in this regard [40, 43] are evidence that general relativity has passed its first strong-field regime tests. The existence of event horizons is a more subtle discussion, although it is expected to be confirmed by a more in-depth study of the late-time ringdown signal [44].

For our purposes, we focus on quasinormal modes of black holes in holography. They will be useful to scrutinize the dual field theory properties of subtracted geometries. More specifically, we use the BTZ black hole [9] as a benchmark, as this black hole is known to be dual to a CFT_2. Its quasinormal spectrum for scalar, fermionic and vectorial perturbations is dual to the poles of the retarded real-time correlation functions of the CFT_2 corresponding operators [45]. Thus, if a black hole background exhibits a quasinormal spectrum like the BTZ, it is evidence for the existence of a dual CFT_2 description. Likewise, the absence/departure from such spectrum is evidence against a dual CFT_2 description. In this last case, another dual field theory might be responsible for the description of the black hole microscopics. Using this logic, we test if subtracted geometries are dual to a CFT_2.

As an illustration of the last, let us advance one of our results of this part of the thesis. We will see later in section 5.4.2 that for the subtracted geometry of a Schwarzschild black hole – as a solution for an Einstein-Maxwell-Dilaton theory –, the quasinormal modes spectrum for vectorial perturbations[6] is

$$\frac{\omega}{4\pi T} = -i(\Delta_V^+ + n) \ , \qquad n = 0, 1, 2, \dots \ , \tag{2.3}$$

with

$$\Delta_V^+ = \left\{ \left(\frac{3}{2} + k_V^2 \pm \frac{1}{2}\sqrt{13 + 12k_V^2} \right)^{1/2} , 1 + \sqrt{2 + k_V^2} \right\} \ .$$

In the expression above, $k_V^2 = \ell(\ell+1) - 1$, with ℓ an integer greater or equal than 1, and T is the temperature of the "subtracted Schwarzschild." In (2.3) there are two towers of modes, and both of them are integer spaced and purely imaginary. These spectrum characteristics are qualitatively the

[5] The ringdown is the stage where the end-product of the coalescence is relaxing – as predicted by general relativity – towards a Kerr black hole.

[6] In this case, vectorial perturbations are the ones exciting the vectorial sector of the background Schwarzschild metric and the (zero-valued in this case) background gauge field.

same for a BTZ black hole. This similarity is evidence for the existence of a dual CFT_2.

When adding charge to the black hole above, the spectrum departs from the BTZ one: the quasinormal frequencies are not purely imaginary anymore – see figure 2.1. This departure is evidence against a dual CFT_2, at least in the charged static case. It can be argued that the study case in this thesis is a very particular one. Further research on subtracted geometry configurations is needed in order to come up with a more definitive statement about its dual nature – see section 5.1 for more specific comments on this.

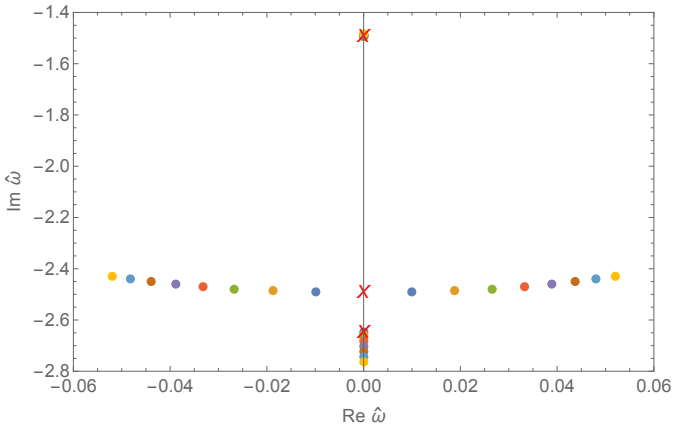

Figure 2.1: Extension of the spectrum (2.3) for a charged static subtracted geometry. Different colors correspond to different values of the charge. The red crosses correspond to the analytical values in (2.3). The first and third QNM remain on the imaginary axis, moving away from each other. The second QNM moves onto the complex plane, departing then from the BTZ black hole spectrum features.

Outline

We elaborate more, in technical and conceptual grounds, about subtracted geometries in chapter 3 and quasinormal modes in chapter 4. In chapter 5 we study the quasinormal modes spectrum of static subtracted geometries as solutions of the STU model and Einstein-Maxwell-Dilaton theory. Further comparison with the BTZ quasinormal spectrum reveals discrepancy, making unlikely the fact that subtracted geometries (at least the static case) have a CFT_2 as a dual description.

Chapter 3

Subtracted Geometries

The subtracted geometry program [28, 29, 46, 31, 30, 32, 47] attempts to understand general four- and five-dimensional asymptotically flat black holes. The main emphasis is placed on the microscopic origin of their Bekenstein-Hawking entropy, which is conjectured to be captured by an underlying dual CFT_2. We review in this section the origins of the program, its physical interpretation, methodology, and string theory and holographic description. Other interesting results about subtracted geometries, regarding their thermodynamics, holographic renormalization, minimally coupled scalars probes, and relation to the attractor mechanism can be found in [48, 49, 50, 51, 52, 53].

The subtracted geometry program began as an attempt to exploit the "hidden conformal symmetry" found in the Kerr black hole [27], in more general charged and rotating asymptotically flat black holes in four and five dimensions in string theory. As we shall see more in detail below, the key idea is to place these black holes into a "conical box." This induces an upgrade of the approximate (small frequency limit) conformal symmetry of the massless scalar wave equation in a Kerr background to an *exact* symmetry.

These geometries describing black holes inside a conical box were dubbed "subtracted geometries." They have a clear holographic interpretation once uplifted to one dimension more, since they become $\text{AdS}_3 \times S^2$ or $\text{AdS}_3 \times S^3$ locally, albeit its non-uplifted version still lacks a dual description. The holographic dual properties of the non-uplifted subtracted geometries are our main concern in this part of the thesis. We now review the basics of the program.

We start by recalling the hidden conformal symmetry of a Kerr black hole, noted first in [27]. The story starts with the realization that the massless scalar wave equation probing a Kerr background exhibits a conformal symmetry at distances small compared with the inverse frequency. More concretely, we write the massless wave equation as

$$\frac{1}{\sqrt{-g}}\partial_\mu(\sqrt{-g}g^{\mu\nu}\partial_\nu\Phi) = 0, \tag{3.1}$$

on the background of a Kerr background (in Boyer-Lindquist coordinates),

$$\begin{aligned} ds^2 &= \frac{\rho^2}{\Delta}dr^2 - \frac{\Delta}{\rho^2}(dt - a\sin^2\theta d\phi)^2 + \rho^2 d\theta^2 + \frac{\sin^2\theta}{\rho^2}((r^2+a^2)d\phi - a\,dt)^2, \\ \Delta &\equiv r^2 + a^2 - 2Mr, \quad \rho^2 \equiv r^2 + a^2\cos^2\theta, \end{aligned} \tag{3.2}$$

with mass M and angular momentum $J = Ma$. The wave equation on this background is separable [54], so we can write down an ansatz of the form

$$\Phi(t, r, \theta, \phi) = e^{-i\omega t + im\phi} R(r) S(\theta). \tag{3.3}$$

It can be seen explicitly [27] that the wave equation exhibits a conformal symmetry for $r \ll \frac{1}{\omega}$. This region was termed in [27] as the "near region." Note that this is not to be confused with the near horizon region since, for small values of ω, the near region can be arbitrarily large. This conformal symmetry is described by local $SL(2,R)_L \times SL(2,R)_R$ generators, that globally break down to $U(1)_L \times U(1)_R$ ones, due to the identification of the azimuthal angle $\phi \sim \phi + 2\pi$.

The presence of this approximate symmetry suggests that we can attempt to describe the near region dynamics of the black hole in terms of a dual CFT$_2$. Following [55], the azimuthal angle identification mentioned above gives rise to left- and right-sector temperatures T_L and T_R given by the Hawking temperatures at the outer and inner horizons by [27]

$$T_R = \frac{r_+ - r_-}{4\pi a}, \quad T_L = \frac{r_+ + r_-}{4\pi a}, \tag{3.4}$$

where $r_\pm = M \pm \sqrt{M^2 - a^2}$ are the outer and inner horizon of the Kerr black hole.

Following our assumption that the near region can be described by a dual CFT$_2$, we would expect the Cardy formula,

$$S_{\text{Cardy}} = \frac{\pi^2}{3}(c_L T_L + c_R T_R), \tag{3.5}$$

to match the Bekenstein-Hawking entropy of the black hole. For this purpose, we need the values of the central charges c_L and c_R. These central charges were computed in the case of the *extremal* Kerr solution in [18, 56, 19], and turn out to be

$$c_R = c_L = 12J. \tag{3.6}$$

Assuming that the conformal symmetry found in the extremal Kerr case connects smoothly with the hidden conformal symmetry for Kerr, we can use the values in (3.6) for our computations. These central charge values, in addition to the temperatures T_L and T_R in (3.4), give us all the ingredients to fill up the Cardy formula of the supposed dual CFT$_2$, obtaining then

$$\begin{aligned} S_{\text{Cardy}} &= \frac{\pi^2}{3}(c_L T_L + c_R T_R) \\ &= 2\pi M r_+ \\ &= \frac{A_H}{4}, \end{aligned} \tag{3.7}$$

where A_H is the area of the Kerr black hole's horizon. To everyone's surprise, the Cardy entropy *agrees on the nose* with the Bekenstein-Hawking entropy of the Kerr black hole [27]. What is surprising is the fact that there is no conformal symmetry in the geometry of the near region Kerr spacetime, the usual smoking gun of a dual CFT description [57]. Comparison of absorption probabilities in the black hole's near-region to absorption cross-sections of a thermal CFT_2 at temperatures T_L and T_R reveals further agreement [27]. Thus, there is evidence pointing to the conclusion that, somehow, a general Kerr black hole is dual to a CFT_2.

Although insightful, this evidence is still rudimentary. As the authors of [27] pointed out, a systematic way of conjecturing such a duality usually is undertaken by constructing the asymptotic symmetry group [8, 57] of the geometry, or by the black hole description via a brane configuration [10] – neither of which have been implemented in the case above [27]. Moreover, as soon as we leave the near-region regime, any trace of symmetry disappears, dragging all the collected evidence with it. Willing to understand the Kerr/CFT conjecture in a more robust framework is when subtracted geometries come in.

Subtracted geometries made their first appearance in [28, 29]. Therein, it was noticed that asymptotically flat black holes, solutions of four-dimensional $\mathcal{N}=4$ [29] and five-dimensional $\mathcal{N}=4,8$ [28] supergravities, can be modified in order to promote the approximate conformal symmetry of [27] to an exact symmetry of the full spacetime. The modified geometry was termed "subtracted geometry." The origin of this name is due to the modification (performed in the warp factor of the black hole) that is needed to obtain its subtracted version. This modification is effectively a "subtraction" of the black hole's asymptotics.

As an example of a subtraction procedure, it suffices to consider the metric of a four-dimensional rotating black hole with two electric and two magnetic $U(1)$ charges [29] – the full solution can be found in [58]. Its asymptotic charges (mass, charges and angular momentum) are parametrized by

$$M=\frac{1}{4}m\sum_{I=0}^{3}\cosh 2\delta_I,\quad Q_I=\frac{1}{4}m\sinh 2\delta_I,\quad J=ma(\Pi_c-\Pi_s), \tag{3.8}$$

where

$$\Pi_c\equiv\prod_{I=0}^{3}\cosh\delta_I,\quad \Pi_s\equiv\prod_{I=0}^{3}\sinh\delta_I, \tag{3.9}$$

with m, a, δ_I constants, and $I=0,1,2,3$ labels the four $U(1)$ charges.

The geometry of the black hole is

$$ds_4^2 = -\frac{G}{\sqrt{\Delta_0}}(dt+\mathcal{A})^2+\frac{\sqrt{\Delta}_0}{X}dr^2+\sqrt{\Delta_0}\left(d\theta^2+\frac{X}{G}\sin^2\theta d\phi^2\right), \tag{3.10}$$

with

$$\begin{aligned} X &= r^2-2mr+a^2,\quad G=r^2-2mr+a^2\cos^2\theta, \\ \mathcal{A} &= \frac{2ma\sin^2\theta}{G}[(\Pi_c-\Pi_s)r+2m\Pi_s]d\phi, \end{aligned} \tag{3.11}$$

$$\begin{aligned}\Delta_0 &= \prod_{I=0}^{3}(r+2m\sinh^2\delta_I)+2a^2\cos^2\theta\left[r^2+mr\sum_{I=0}^{3}\sinh^2\delta_I+4m^2(\Pi_c-\Pi_s)\Pi_s\right.\\ &- \left.2m^2\sum_{I<J<K}\sinh^2\delta_I\sinh^2\delta_J\sinh^2\delta_K\right]+a^4\cos^4\theta, \end{aligned} \tag{3.12}$$

where $m,\ a,\ \delta_I$ are constants. The subtraction procedure takes place at the warp factor in the following way,

$$\Delta_0 \to \Delta = (2m)^3 r(\Pi_c^2-\Pi_s^2)+(2m)^4\Pi_s^2-(2m)^2(\Pi_c-\Pi_s)^2a^2\cos^2\theta. \tag{3.13}$$

This changes the warp factor and asymptotics of the black hole geometry. When probing the massless scalar in this new subtracted background, its wave equation shows exact conformal symmetry [28, 29], i.e. the solutions are hypergeometric functions – an explicit example of this behavior can be found in section 5.4.1 with a Reissner-Nordstrom subtracted geometry.

The warp factor modification (3.13) achieves this enlargement of conformal symmetry [28]. However, the remaining matter fields have been kept intact. This configuration no longer satisfies the equations of motion [29]. This can be solved by constructing the subtracted geometries via a scaling limit or solution generating techniques. We will review both procedures later on in this chapter, after discussing the physical interpretation of a subtracted geometry. As a last remark, notice that a Kerr black hole is the uncharged case of the background (3.10)-(3.12), so it is fitted for a subtraction procedure.

The physical interpretation of the subtraction procedure is the decoupling of the black hole from its asymptotics by enclosing it in a "conical box" [46]. This can be seen from the confinement properties of subtracted geometries. Four-dimensional charged and rotating subtracted geometries, originated from black holes as in (3.10), at spatial infinity are asymptotically conical spacetimes [46], generically described by

$$ds^2=-\left(\frac{R}{R_0}\right)^{2p}dt^2+B^2dR^2+R^2(d\theta^2+\sin^2\theta d\phi^2), \tag{3.14}$$

with R_0, p, B constants, and R being the radial distance to the origin. In particular, the spatial asymptotic of the subtracted geometries of charged and rotating black holes (3.10),

$$\begin{aligned}ds^2_{4,r\to\infty} &= -\frac{r^{3/2}}{\sqrt{(2m)^3(\Pi_c^2-\Pi_s^2)}}dt^2+\frac{\sqrt{(2m)^3(\Pi_c^2-\Pi_s^2)}}{r^{3/2}}dr^2\\ &+ r^{1/2}\sqrt{(2m)^3(\Pi_c^2-\Pi_s^2)}(d\theta^2+\sin^2\theta d\phi^2),\end{aligned} \tag{3.15}$$

is a conical geometry of the form (3.14) with

$$R^2=r^{1/2}\sqrt{(2m)^3(\Pi_c^2-\Pi_s^2)},\quad B^2=16,\quad R_0=(2m)(\Pi_c^2-\Pi_s^2)^{1/3}. \tag{3.16}$$

These conical geometries endorse confining properties qualitatively equal to anti-de Sitter spacetimes.

This can be seen in the way that the Ehrenfest-Tolman temperature[1] falls [46],

$$T \propto \frac{1}{\sqrt{g_{00}}} \propto R^{-p}, \tag{3.17}$$

thus, for $p > 1$, the total energy and entropy are finite (for subtracted geometries, $p = 3$, so this inequality is always satisfied [46]). This adds evidence to the claim that the subtracted black hole system may have a dual CFT description. Inside the box, the black hole is in thermodynamical equilibrium and has positive specific heat, like all unitary CFTs. Moreover, the horizon area, angular and (Euclidean) time periodicity remain unchanged after the subtraction procedure [28]. This property suggests that the microscopic system behind the thermodynamics of a black hole remains the same after the subtraction procedure.

We have seen that the subtracted geometry shows compelling evidence of being dual to a CFT_2. Moreover, the Bekenstein-Hawking and Cardy entropy of a subtracted black hole, after a calculation in the same lines of [27], can be shown to match [29]. However, a subtracted black hole does not realize a conformal symmetry at spacetime level. Thus, a formal explanation in the fashion of [8, 57, 10] for this matching is still lacking, just like the case of the hidden conformal symmetry of the Kerr black hole [27]. In this regard, the program has not given a satisfactory answer.

When the subtraction procedure was first proposed, the subtracted end-products were not solutions of the original supergravity theory [28, 29]. Later was found that subtracted geometries were solutions of the STU model ($\mathcal{N} = 2$ $4d$) and its five-dimensional uplift ($\mathcal{N} = 2$ $5d$ supergravity) [31, 32, 30]. Methods to build these solutions from asymptotically flat black holes were also developed: (1) via a scaling limit [46] and (2) via solution generating techniques called *Harrison transformations* and *STU transformations* [30, 31, 32].

The scaling limit method subtracts an asymptotically flat black hole through a particular transformation of its geometry and matter fields. This transformation is controlled by a parameter subject further to a limiting procedure. We give now an example, following [46]. Consider a four-dimensional charged rotating black hole, solution of the STU model. We have already written down the geometry for this black hole in (3.10), (3.11) and (3.12). This black hole has four $U(1)$ charges. For simplicity, we will take three charges equal $\delta_1 = \delta_2 = \delta_3 = \delta$ and $\delta_4 = \delta_0$. The gauge fields $A_{1,2,3}$ will be sourced by δ and A_0 by δ_0.

The matter supporting the geometry is given by three dilatons $\eta_1,\ \eta_2,\ \eta_3$ and axions $\chi_1,\ \chi_2,\ \chi_3$,

$$\begin{aligned} e^{\eta_1} = e^{\eta_2} = e^{\eta_3} &= \frac{(r + 2m\sinh^2\delta)^2 + a^2\cos^2\theta}{\sqrt{\Delta_0}}, \\ \chi_1 = \chi_2 = \chi_3 &= \frac{2m\,a\cos\theta\cosh\delta\sinh\delta(\cosh\delta\sinh\delta_0 - \sinh\delta\cosh\delta_0)}{(r + 2m\sinh^2\delta)^2 + a^2\cos^2\theta}. \end{aligned} \tag{3.18}$$

[1]The Ehrenfest-Tolman temperature [59] is the temperature measured by a local observer who follows an orbit described by a Killing vector normal to the horizon. This temperature diverges at the horizon and reduces to the Hawking temperature at infinity, just as expected [60].

The gauge fields are explicitly

$$\begin{aligned} A_I &= \frac{2m}{\Delta_0}([(r+2m\sinh^2\delta)^2(r+2m\sinh^2\delta_0)+ra^2\cos^2\theta] \\ &\times [\cosh\delta\sinh\delta\,dt - a\sin^2\theta\cosh\delta\sinh\delta(\cosh\delta\cosh\delta_0-\sinh\delta\sinh\delta_0)d\phi] \\ &+ 2m\,a^2\cos^2\theta[e\,dt - a\,\sin^2\theta\sinh^2\delta\cosh\delta\sinh\delta_0 d\phi]), \qquad (3.19) \\ A_0 &= \frac{2m}{\Delta_0}([(r+2m\sinh^2\delta_0)^3+ra^2\cos^2\theta] \\ &\times [\cosh\delta_0\sinh\delta_0\,dt - a\sin^2\theta(\cosh^3\delta\sinh\delta_0-\sinh^3\delta_0\cosh\delta_0)d\phi] \\ &+ 2m\,a^2\cos^2\theta[e_0\,dt - a\,\sin^2\theta\sinh^3\delta\cosh\delta_0 d\phi]), \qquad (3.20) \end{aligned}$$

with

$$\begin{aligned} e &= \sinh^2\delta\cosh^2\delta\cosh\delta_0\sinh\delta_0(\cosh^2\delta+\sinh^2\delta) \\ &- \sinh^3\delta\cosh\delta(\sinh^2\delta+2\sinh^2\delta_0+2\sinh^2\delta\sinh^2\delta_0), \qquad (3.21) \\ e_0 &= \sinh^3\delta\cosh^3\delta(\cosh^2\delta_0+\sinh^2\delta_0)-\sinh\delta_0\cosh\delta_0(3\sinh^4\delta+2\sinh^6\delta), \end{aligned}$$

where $I=1,2,3$. The scaling limit is performed by first doing the following transformations,

$$\begin{aligned} r &\to r\epsilon,\;\; t\to r\epsilon^{-1},\;\; m\to m\,\epsilon,\;\; a\to a\,\epsilon, \\ 2m\sinh^2\delta &\to 2m\epsilon^{-1/3}(\Pi_c^2-\Pi_s^2)^{1/3},\;\; \sinh^2\delta_0\to\frac{\epsilon\,\Pi_s^2}{\Pi_c^2-\Pi_s^2}, \end{aligned} \qquad (3.22)$$

and then taking the limit $\epsilon\to 0$. Once this limit has been performed, the matter fields are formally infinite. However, the divergences can be removed by a gauge transformation in the scalar and gauge fields [46, 48]. After this has been done, we arrive at the subtracted version of the black hole,

$$\begin{aligned} \Delta &= (2m)^3 r(\Pi_c^2-\Pi_s^2)+(2m)^4\Pi_s^2-(2m)^2a^2(\Pi_c-\Pi_s)^2\cos^2\theta, \\ \chi_{1,2,3} &= -\frac{2ma(\Pi_c-\Pi_s)\cos\theta}{2m}, \\ e^{\eta_{1,2,3}} &= \frac{(2m)^2}{\Delta^{1/2}}, \\ A &= -\frac{r}{2m}dt+\frac{(2m)a^2[2m\Pi_s^2-r(\Pi_s-\Pi_s)^2]\cos^2\theta}{\Delta}dt, \\ A_0 &= \frac{(2m)^4\Pi_c\Pi_s+(2m)^2a^2(\Pi_c-\Pi_s)^2\cos^2\theta}{(\Pi_c^2-\Pi_s^2)\Delta}dt \\ &+ \frac{(2m)^4a(\Pi_c-\Pi_s)\sin^2\theta}{\Delta}d\phi, \qquad (3.23) \end{aligned}$$

where we have recovered the warp factor (3.13), plus having explicitly found the fields that sustain the box surrounding the black hole.

It is worth emphasizing that the scaling limit for a subtracted geometry is different from the near-horizon limit [29]. In order to see this, let us set the charges to zero in the warp factor (3.12), namely $\Pi_c=1,\;\Pi_s=0,\delta_I=0$. For these charge values, the geometry (3.10) describes a Kerr black hole,

although not in the common Boyer-Lindquist coordinates [29]. The NHEK limit is obtained by the following transformation [61],

$$r \to m + \lambda r, \;\; a^2 \to m^2, \tag{3.24}$$

and then taking the limit $\lambda \to 0$. The warp factor (3.12) then becomes

$$\sqrt{\Delta_{0,\text{NHEK}}} = 2m^2 \frac{1}{2}(1 + \cos^2\theta). \tag{3.25}$$

The NHEK limit in the subtracted warp factor (3.12) bring us to

$$\sqrt{\Delta_{\text{NHEK}}} = 2m^2\sqrt{1 + \sin^2\theta}. \tag{3.26}$$

It is clear from here that the NHEK and subtracted limits are different. This difference is a curious feature since both scaling limits share the property that a hypergeometric function on these backgrounds solves the scalar wave equation. This suggests that two different CFT descriptions of extremal rotating black holes might be available [29], one related to the NHEK [18] and the other to the subtracted geometry. Finding the relation between both limits could teach us further about what the subtracted geometry dual description is.

As already mentioned, the construction of subtracted geometries can be undertaken by solution generating techniques, namely Harrison transformations and STU transformations [30]. These connect black holes to their subtracted version. The existence of these transformations confirms that the subtracted black holes are also solutions of the relevant supergravity theory. Moreover, physical properties of the original black hole which are invariant under these transformations remain the same for the subtracted black hole. It is worth noting that, besides the notable exception of the Kerr black hole, the black hole entropy *is not* invariant under a general Harrison or STU transformation; however, the parameters controlling the transformations can be adjusted for this purpose [46]. As an illustration of how these solution generating methods work, let us subtract the Schwarzschild black hole case through a Harrison transformation. We follow section 2.3 of [46].

The Schwarzschild STU model solution is effectively described by the $4d$ Einstein-Dilaton-Maxwell theory,

$$\mathcal{L}_4 = \sqrt{-g}\left(\frac{1}{4}R - \frac{1}{2}(\partial\phi)^2 - \frac{1}{4}e^{-2\alpha\phi}F^2\right), \tag{3.27}$$

which is a consistent truncation of the STU model with the axions set to $\chi_i = 0$, the dilatons to $\eta_i = -\frac{2}{\sqrt{3}}\phi$, only one Maxwell field F is present, $\alpha = \frac{1}{\sqrt{3}}$, and the metric is given by the ansatz

$$\begin{aligned} ds_4^2 &= -\frac{X}{\sqrt{\Delta_0}}dt^2 + \frac{\sqrt{\Delta_0}}{X}dr^2 + \sqrt{\Delta_0}\left(d\theta^2 + \sin^2\theta d\phi^2\right), \\ X &= r^2 - 2mr, \end{aligned} \tag{3.28}$$

where Δ_0 is a function of r and m is a constant. To perform the Harrison transformation, we first reduce to a three-dimensional theory in the time-like direction using the following ansatz,

$$ds^2 = -e^{2U}dt^2 + e^{-2U}\gamma_{ij}dx^i dx^j, \;\; F_{i0} = \partial_i\psi, \tag{3.29}$$

where U and ψ depend in the x^i coordinates.

The three-dimensional action becomes

$$\mathcal{L}_3 = \sqrt{\gamma}\left(R(\gamma_{ij}) - 2\gamma^{ij}(\partial_i x\partial_j x + \partial_i y\partial_j y - e^{-2\sqrt{1+\alpha^2}x}\partial_i\psi\partial_j\psi)\right), \tag{3.30}$$

with $x \equiv \frac{U+\alpha\phi}{\sqrt{1+\alpha^2}}$, $y \equiv \frac{-\alpha U+\phi}{\sqrt{1+\alpha^2}}$. The action can be recast in the following form,

$$\mathcal{L}_3 = \sqrt{\gamma}\left(R(\gamma_{ij}) + \frac{1}{1+\alpha^2}\gamma^{ij}\text{Tr}(\partial_i P\partial_j P^{-1})\right), \tag{3.31}$$

with

$$P = e^{-\sqrt{1+\alpha^2}(x+y)}\begin{pmatrix} e^{2\sqrt{1+\alpha^2}x} - (1+\alpha^2)\psi^2 & -\sqrt{1+\alpha^2}\psi \\ -\sqrt{1+\alpha^2}\psi & -1 \end{pmatrix}, \tag{3.32}$$

with $P = P^T$ and det$P = -e^{-2\sqrt{1+\alpha^2}y}$.

Having collected these results, we can perform the Harrison transformation, given explicitly by

$$P \to H\,P\,H^T, \quad H \equiv \begin{pmatrix} 1 & 0 \\ \beta & 1 \end{pmatrix}, \tag{3.33}$$

where $H \in SO(1,1)$. The properties $P = P^T$ and det$P = -e^{-2\sqrt{1+\alpha^2}y}$ are invariant under the Harrison transformation, and so is the action (3.31), while the matter configuration will change – thus, the end-product of the transformation is another solution of the theory. The transformation at the level of the matter configuration is,

$$\begin{aligned} y' &= y, \quad e^{\sqrt{1+\alpha^2}x'} = \Lambda^{-1}e^{\sqrt{1+\alpha^2}x}, \\ \psi' &= \Lambda^{-1}\left[\psi + \frac{\beta}{\sqrt{1+\alpha^2}}\left(e^{2\sqrt{1+\alpha^2}x} - (1+\alpha^2)\psi^2\right)\right] \\ \Lambda &\equiv (\beta\psi+1)^2 - \beta^2 e^{2\sqrt{1+\alpha^2}x}. \end{aligned} \tag{3.34}$$

The Schwarzschild case is described by $e^{2U} = 1 - \frac{2m}{r}$ (this effectively sets $\Delta_0 = r^4$ in (3.29)), $\phi = 0$, and $\psi = 0$. In the infinite boost limit $\beta \to 1$ [46], we have that $\Lambda \to \frac{2m}{r}$, and the warp factor and matter configuration changes to

$$\Delta_{\text{subtracted}} = (2m)^3 r, \quad e^{-2\phi/\sqrt{3}} = \sqrt{\frac{2m}{r}}, \quad \sqrt{\frac{2}{3}}F_{tr} = \frac{1}{2m}, \tag{3.35}$$

which is the same warp factor of (3.23) for the uncharged non-rotating case [2], i.e., $\Pi_c = 1$ and $\Pi_s = 0$. This Harrison transformations result extends to four-dimensional, four $U(1)$ charges rotating black hole [30, 31] and to five-dimensional multi-charged rotating non-extremal black holes [32] – in the later, the subtraction procedure can also be undertaken via the STU transformations [30].

[2]The field strength shows a $\sqrt{2/3}$ factor difference. This is simply just a definition issue between the truncated and the full STU model field strength [46].

These solution generating techniques open the door to a possible description of four- and five-dimensional asymptotically flat black holes via brane configurations. As already noticed, when four-dimensional subtracted geometries are uplifted by one dimension, their geometry becomes locally $AdS_3 \times S^2$ [29] supported by three magnetic fluxes threading the S^2. This configuration corresponds to the near-horizon of the D0-D4 system in type IIA, or the near-horizon of a set of intersecting M5 branes in M-theory [62, 63], each one wrapping a different four-cycle on an internal six-torus T^6. In M-theory, the Harrison transformations are equivalent to a set of T-dualities and timelike Melvin twists [30]. Since the intersecting M5s microscopics is known to be described by the dual MSW CFT [64], the understanding of the dual theory description of four-dimensional asymptotically flat black holes is reduced to the understanding of the dual versions of these timelike Melvin twists and T-dualities on the MSW system [30].

The methodology mentioned above can be extended to five-dimensional asymptotically flat black holes. Its subtracted geometry uplifts to an $AdS_3 \times S^3$ geometry [28], the near-horizon limit of the D1-D5 system [65]. The D1-D5 system is two T-dualities away from the D0-D4 configuration – so we only need to add these T-dualities to the already existing set of T-dualities and timelike Melvin twist for the D0-D4 case. A depiction of this whole procedure can be found in figure 3.1.

Insights about the dual theory for a subtracted geometry can also be obtained by the study of its uplift via AdS_3/CFT_2. For example, In [47], an explicit family of solutions was constructed that interpolates between a Reissner-Nordstrom black hole geometry and its subtracted version. These solutions are helpful for the identifications of which linear perturbations on the subtracted Reissner-Nordstrom are responsible for initiating the flow towards the original Reissner-Nordstrom. After uplifting the subtracted black hole and performing a reduction on the S^2, these perturbations are identified with irrelevant perturbations in the dual CFT_2 [47]. This is the expected result if we think of the subtracted geometry as an IR limit of the original asymptotically flat geometry [47].

Even though a holographic dual of a subtracted geometry is available after its uplift, it is desirable to test to which extent a CFT_2 description is present in the non-uplifted version. After all, in the hidden conformal symmetry of the Kerr black hole, the near region (which is the region described by the Kerr subtracted geometry) is the one that is conjectured to be dual to a CFT_2. Therefore, and despite all the evidence as mentioned earlier supporting a dual CFT_2, we need to test further if conjectured duality is well-based. A step would be to construct the asymptotic symmetry group [8] of the non-uplifted subtracted geometry. However, other methods can also tell us very useful insights about the dual theory. The study of subtracted black hole quasinormal modes is one of them. This is the chosen approach in this thesis, and that we present in the following section.

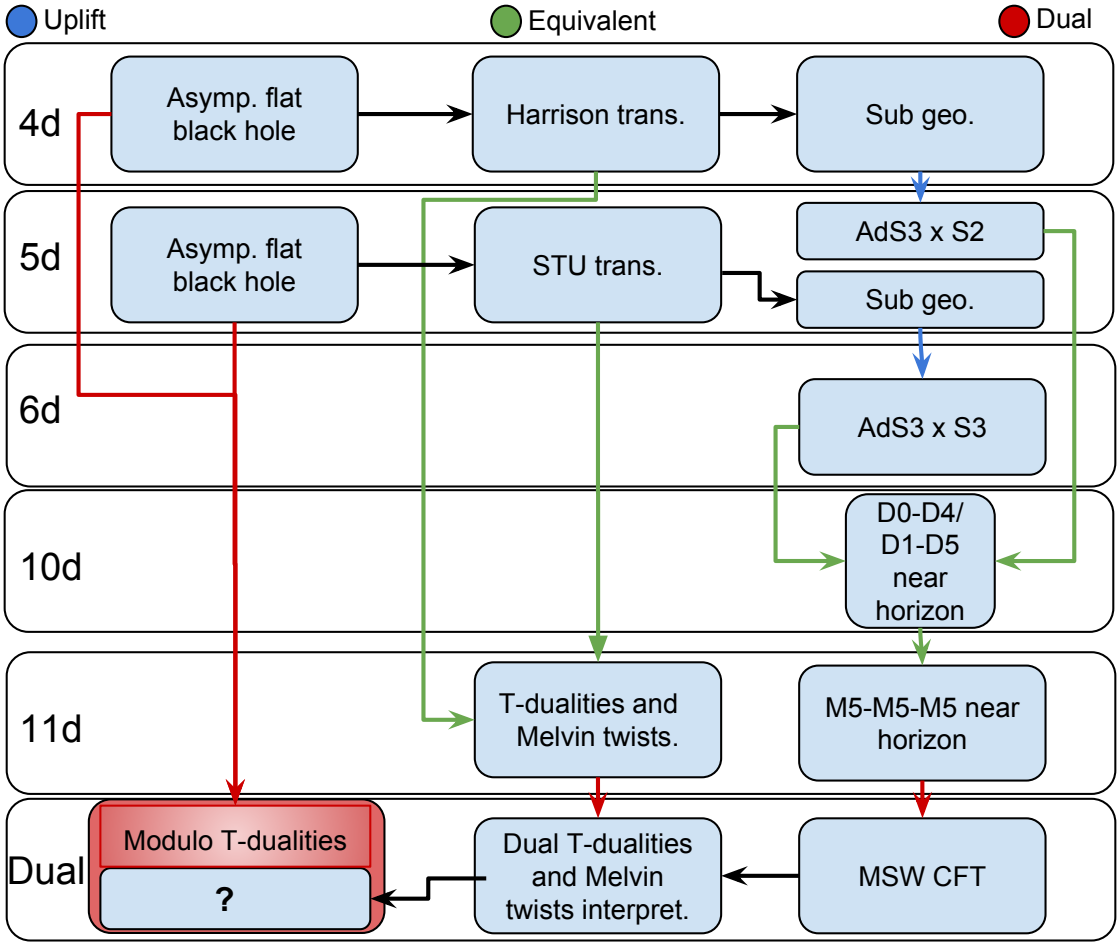

Figure 3.1: Description of how the subtracted geometry program allows for a four- and five-dimensional general asymptotically flat black holes dual description via (dual) T-dualities and Melvin twists on the MSW CFT.

Chapter 4

Linear Perturbations and Quasinormal Modes

In this thesis, we use quasinormal modes with the purpose of finding evidence that supports (or disfavors) the conjecture of a subtracted geometry being dual to a CFT$_2$. In order to obtain the quasinormal modes of a given background, firstly we need to study its linearized perturbations. A proper study of the linearized perturbations requires to disentangle their "raw" equations of motion to clean-cut wave equations of the form (2.1). For this purpose, we follow [66], where Kodama and Ishibashi formulated a systematic disentangling procedure for tensorial, vectorial, and scalar linear perturbations for $d \geq 4$ dimensional black holes in Einstein-Maxwell theory. A subtracted geometry does not fit in the study cases of [66], although an extension of method therein will allow for the disentangling of its linear perturbations to wave equations. However, these wave equations do not describe quasinormal modes yet; a sensible choice of boundary conditions is needed. We elaborate on these topics in this chapter.

Let us outline the Kodama-Ishibashi method for vectorial perturbations[1] on a Reissner-Nordstrom background, where we can see vividly how the disentangling process takes place. The Reissner-Nordstrom black hole is given by

$$\begin{aligned} ds^2 &= -f(r)dt^2 + \frac{dr^2}{f(r)} + r^2 d\Omega_2^2, \\ f &= 1 - \frac{2M}{r} + \frac{Q^2}{r^2}, \quad \mathcal{F} = \frac{Q}{r^2} dt dr, \end{aligned} \tag{4.1}$$

where $\mathcal{F}$ is our accustomed electrically sourced field strength, and the constants M and Q are the mass and electrical charge of the black hole. We separate the coordinates as $(t, r) = (a, b)$ and $(\theta, \phi) = (i, j)$, D_a and $\hat{D}_i$ are the respective covariant derivatives, and ϵ^{ab} and ϵ^{ij} the respective Levi-Civita tensors. This background is a solution of Einstein-Maxwell theory, so it satisfies the equations of motion

$$\begin{aligned} R_{\mu\nu} &= \kappa^2 \left(T_{\mu\nu} - \frac{1}{2} T g_{\mu\nu} \right), \\ d\mathcal{F} &= 0, \;\; d \star \mathcal{F} = 0. \end{aligned} \tag{4.2}$$

[1] In the literature, vectorial perturbations are also called Regge-Wheeler type or odd-parity type [38].

We are taking for the rest of the chapter the value $\kappa^2 = 2$. This choice does not influence at all in the method and makes for a cleaner computation.

We define a perturbed field Ψ as

$$\Psi = \bar{\Psi} + \delta\Psi, \quad \mathcal{O}\left(\delta\Psi^2\right) \sim 0, \tag{4.3}$$

where $\bar{\Psi}$ is the background field value and $\delta\Psi$ its perturbation. Ψ must satisfy the equations of motion (4.2). This restriction implies that the dynamics of $\delta\Psi$ will be dictated by (4.2) at the linear level.

The background geometry (4.1) is a product between a two-dimensional spacetime and a maximally symmetric space of dimension two – namely, the two-sphere S^2. The isometries of this maximally symmetric space are used to expand the linear perturbations in terms of according harmonics [67]. For the S^2, these are spherical harmonics. Thus, a perturbation to the metric, $\delta g_{\mu\nu}$, can be decomposed as [68]

$$\begin{aligned} \delta g_{\mu\nu}dx^\mu dx^\nu &= \delta g_{ab}dx^a dx^b + \delta g_{ai}dx^a dx^i + \delta g_{ij}dx^i dx^j \\ &= h_{ab}\mathbb{S}\,dx^a dx^b + (h_{(T),a}\mathbb{V}_i + h_{(L),a}\hat{D}_i\mathbb{S})dx^a dx^i \\ &+ \left(h_{(T)}\mathbb{T}_{ij} + h_{(LT)}\hat{D}_{(i}\mathbb{V}_{j)} + h_{(LL)}(2\hat{D}_i\hat{D}_j + k_V^2\Omega_{ij})\mathbb{S} + h_{(Y)}\Omega_{ij}\mathbb{S}\right)dx^i x^j, \end{aligned} \tag{4.4}$$

where the $h_{...}$ functions[2] depend on the x^a coordinates only, Ω_{ij} is the S^2 metric, and $\mathbb{S}(\theta,\phi)$, $\mathbb{V}_i(\theta,\phi)$, $\mathbb{T}_{ij}(\theta,\phi)$ are scalar, transverse vectorial, and tensorial spherical harmonics respectively. Inspecting (4.4), and using orthogonality arguments between different kind of harmonics, we classify the perturbations in three different sets [68],

$$\begin{aligned} \{h_{ab},\ \ h_{(L),a},\ \ h_{(LL)},\ \ h_{(Y)}\} &= \text{scalar perturbations}, \\ \{h_{(T),a},\ \ h_{(LT)}\} &= \text{vector perturbations}, \\ \{h_{(T)}\} &= \text{tensor perturbations}. \end{aligned} \tag{4.5}$$

For S^2, tensorial harmonics do not exist [69], so we will not consider them further, i.e., $h_{(T)} = 0$. We classify now the perturbations of the electromagnetic field. Let us notice first that the equation of motion

$$d\mathcal{F} = 0 \tag{4.6}$$

implies $\delta\mathcal{F} = d(\delta\mathcal{A})$, meaning that a vector potential can describe the electromagnetic perturbations. Expanding as before,

$$\delta A_\mu dx^\mu = a_a\mathbb{S}dx^a + (b_T\mathbb{V}_i + b_L\hat{D}_i\mathbb{S})dx^i, \tag{4.7}$$

where a_a, b_T, and b_L depend on the x^a coordinates. Again, we can group up the perturbations as

$$\{a_a,\ \ b_L\} = \text{scalar perturbations}, \tag{4.8}$$

$$\{b_T\} = \text{vector perturbations}. \tag{4.9}$$

[2]The subindices T and L hold for "transverse" and "longitudinal" harmonics, see the appendix in [68].

Then, the perturbations in the Reissner-Nordstrom background (4.1) can qualitatively be described as

$$\delta\Psi = \delta\Psi^{(V)} + \delta\Psi^{(S)}, \tag{4.10}$$

where the superscripts represent to which modes do they belong (vector or scalar).

As our goal is to find the quasinormal modes of the background (4.1), we take the time dependence to be $e^{-i\omega t}$ for all perturbations, i.e.,

$$\delta\Psi(t,r) = e^{-i\omega t}\delta\Psi(r), \tag{4.11}$$

where the frequency ω will become the quasinormal frequency. This time dependence reflects that the system under study is in a stationary stage, which is the expected late-time behavior [33]. Hence, the time dependence (4.11) fits well if we want to study the quasinormal character of the linear perturbations.

We have already parametrized the perturbations in terms of time, radial, and angular dependence. Now, we want to know the dynamics of the perturbations. For this purpose, we insert the perturbed $g_{\mu\nu}$ and $\mathcal{F}$ – in the shape of (4.3) – in the equations of motion (4.2). This will give us the "raw" equations of motion for the perturbations, that we will further disentangle obtaining wave equations for the perturbations.

We start by studying the Maxwell equations in (4.2). As already discussed around (4.6), the left side Maxwell equation in (4.2) implies that a vector potential can describe the perturbation of the field strength,

$$\delta\mathcal{F} = d\,(\delta\mathcal{A}). \tag{4.12}$$

The right side Maxwell equation in (4.2) gives the following equations of motion for the field strength perturbations,

$$\frac{1}{r^2}D_b(r^2\delta\mathcal{F}^{ab}) + \hat{D}_i\delta\mathcal{F}^{ai} + \frac{Q}{r^2}\epsilon^{ab}\left(\frac{1}{2}D_b(\delta g^i_i - \delta g^c_c) - \hat{D}_i\delta g^i_b\right) = 0 \tag{4.13}$$

$$D_a\left(\delta\mathcal{F}^a_i + \frac{Q}{r^2}\epsilon^{ab}\delta g_{ib}\right) + \hat{D}_j\delta\mathcal{F}^j_i = 0. \tag{4.14}$$

Now we want to do the same for the Einstein equations. Unfortunately, these are too lengthy to write for general $\delta g_{\mu\nu}$ and $\delta\mathcal{F}$ perturbations. Here we are working out the quasinormal modes for vectorial perturbations. Thus, it suffices to write out only the vectorial perturbations of the Einstein equations. Before writing down these explicitly, we need to elaborate further about vectorial perturbations and the construction of gauge invariant quantities involving the perturbations. This will allow us to write out the Einstein equations for the perturbations in a compact way.

We parametrize our vectorial perturbation as [66]

$$\begin{aligned} \delta g_{ab} &= 0,\ \delta g_{ai} = r f_a \mathbb{V}_i,\ \delta g_{ij} = 2r^2 H_T \mathbb{V}_{ij}, \\ \delta\mathcal{F}_{ab} &= 0,\ \ \delta\mathcal{F}_{ai} = D_a\mathcal{A}\mathbb{V}_i,\ \ \delta\mathcal{F}_{ij} = \mathcal{A}(\hat{D}_i\mathbb{V}_j - \hat{D}_j\mathbb{V}_i), \end{aligned} \tag{4.15}$$

where $f_a, H_T, \mathcal{A}$, are functions of (t, r). The transverse vector harmonics $\mathbb{V}_i$ can be described in terms of scalar harmonics $\mathbb{S}$ as

$$\mathbb{V}_i = \epsilon^{ij}\hat{D}_j\mathbb{S}, \tag{4.16}$$

satisfying the following properties,

$$\begin{aligned}(\hat{D}_j\hat{D}^j + k_V^2)\mathbb{V}_i &= 0, &(4.17)\\ \hat{D}^i\mathbb{V}_i &= 0, &(4.18)\\ \mathbb{V}_{ij} &= -\frac{1}{k_V}\hat{D}_{(i}\mathbb{V}_{j)}, &(4.19)\end{aligned}$$

where $k_V^2 = \ell(\ell+1) - 1$, with ℓ an integer greater or equal to 1. These expressions are convenient in the context of the disentangling process. They allow for factoring out the angular (θ, ϕ) dependence of the equations of motion for the linear perturbations. Thus, from now on, we focus only on the (t, r) dependence of these equations of motion. We could also Fourier transform the perturbations by now, i.e., use (4.11). However, we prefer to refrain from doing this until the quasinormal modes analysis. Thus, we are keeping the t dependence on the functions parametrizing the perturbations.

The wave equations for the linear perturbations should capture only the relevant/physical degrees of freedom. Therefore, we would like to rewrite the equations of motion for the linear perturbations using gauge invariant quantities. This step is part of the disentangling process. We perform this step systematically by studying the diffeomorphisms at the level of the linear perturbations. For $\delta g_{\mu\nu}$, we have [67]

$$\delta g_{\mu\nu} \to \delta g_{\mu\nu} - \pounds_\xi g_{\mu\nu} = \delta g_{\mu\nu} - \nabla^{\rm bg}_\mu \xi_\nu - \nabla^{\rm bg}_\nu \xi_\mu, \tag{4.20}$$

where the superscript "bg" stands for background, ξ_μ is an arbitrary vector field, and $\nabla^{\rm bg}_\mu$ is the covariant derivative acting in the background four-dimensional spacetime. This implies that [67]

$$\begin{aligned}\delta g_{ab} &\to \delta g_{ab} - D_a\xi_b - D_b\xi_a, &(4.21)\\ \delta g_{ai} &\to \delta g_{ai} - r^2 D_a\left(\frac{\xi_i}{r^2}\right) - \hat{D}_i\xi_a,\\ \delta g_{ij} &\to \delta g_{ij} - \hat{D}_i\xi_j - \hat{D}_j\xi_i - 2rD^a r\xi_a\gamma_{ij}.\end{aligned}$$

From (4.21), we can construct gauge invariant quantities. Let us see how. Just as we did in (4.4) and (4.7), we expand the vector field ξ_μ as [68]

$$\xi_\mu = \xi_a\mathbb{S}dx^a + (\xi^{(T)}\mathbb{V}_i + \xi^{(L)}\hat{D}_i\mathbb{S})dx^i, \tag{4.22}$$

where $\xi_a, \quad \xi^{(T)}, \quad \xi^{(L)}$ are functions of x^a. The expansion (4.22) allow us to separate in scalar and vector sectors the equations (4.21). Since we are studying vectorial perturbations, we parametrize ξ_μ as [67]

$$\xi^{(S)}_a = 0, \;\; \xi^{(T)} = rL(t, r), \;\; \xi^{(L)} = 0, \tag{4.23}$$

where $L(t,r)$ is an arbitrary function. Using the expression above in the second and third equation of (4.21) we obtain

$$f_a \rightarrow f_a - rD_a\left(\frac{L(t,r)}{r}\right), \tag{4.24}$$

$$H_T \rightarrow H_T + \frac{k_V}{r}L(t,r), \tag{4.25}$$

from which we can construct the gauge invariant [67],

$$F_a \equiv f_a + rD_a\left(\frac{H_T}{k_V}\right). \tag{4.26}$$

This gauge invariant will help to disentangle the equations of motion for the vector perturbations. For a vector perturbation, the $\mathcal{A}$ perturbation potential in (4.15) is already a gauge invariant[3]. The last can be confirmed by following the same steps as in the metric perturbation case.

Using the parametrization (4.15) and the gauge invariants F_a and $\mathcal{A}$, we can finally write down the Einstein equations for the vectorial perturbations [66],

$$D_a\left(r^3F^{(1)}\right) - m_V r\epsilon_{ab}F^b = -4r^3\epsilon_{ab}\tau^b, \tag{4.27}$$

$$k_V D_a(rF^a) = 0, \tag{4.28}$$

where $m_V \equiv k_V^2 - 1$, and we have defined the (gauge invariant) F_a-derived quantity

$$F^{(1)} \equiv \epsilon^{ab}rD_a\left(\frac{F_b}{r}\right), \tag{4.29}$$

with $r\tau_a = -\frac{Q}{r^2}\epsilon_{ab}D^b\mathcal{A}$. Of course, with the set of Einstein equations, an energy-momentum conservation law comes along,

$$D_a(r^3\tau^a) = 0. \tag{4.30}$$

We rewrite now the Maxwell equations (4.13) and (4.14) for the vectorial perturbations case, using (4.15) and the gauge invariants F_a and $\mathcal{A}$. Only (4.14) is non-trivial in this case,

$$D_aD^a\mathcal{A} - \frac{k_V^2+1}{r^2}\mathcal{A} = \frac{Q}{r^2}\,rF^{(1)}. \tag{4.31}$$

Now we are all set to disentangle the equations of motions for the perturbations. Using the energy-momentum tensor conservation law (4.30) together with (4.28), we can build up a potential quantity Ω that encodes both expressions, given that

$$D_a\left(rF^a - \frac{8}{m_V}r^3\tau^a\right) = 0, \tag{4.32}$$

which in turn implies

$$rF^a - \frac{8}{m_V}r^3\tau^a = \epsilon^{ab}D_b\Omega, \tag{4.33}$$

[3]If the perturbation were scalar, this would not be the case, and another gauge invariant quantity needs to be built.

The chosen pre-factor $8/m_V$ is just convenient for the calculation. Inserting this equation into (4.27), we obtain

$$r^2 D_a\left(\frac{1}{r^2}D^a\Omega\right) - \frac{m_V}{r^2}\Omega = -\frac{4}{m_V}r^2\epsilon^{ab}D_a(r\tau_b). \tag{4.34}$$

Defining another potential Θ,

$$\Theta = \Omega - \frac{8Q}{m_V}\mathcal{A}, \tag{4.35}$$

we can write (4.34) as

$$r^2 D_a\left(\frac{1}{r^2}D^a\Theta\right) - \frac{m_V}{r^2}\Theta = \frac{8Q}{r^2}\mathcal{A}. \tag{4.36}$$

Now we turn to the Maxwell equation (4.31). Using the last equation (4.36) and rewriting F^a in the new potential Θ defined in (4.35),

$$rF^a = \epsilon^{ab}D_b\Theta, \tag{4.37}$$

(4.31) can be written as

$$D_aD^a\mathcal{A} - \frac{1}{r^2}\left(k_V^2 + 1 + \frac{4Q^2}{r^2}\right)\mathcal{A} = \frac{Q\,m_V}{r^4}\Theta. \tag{4.38}$$

We have disentangled all the equations of motion for the perturbations to two coupled wave equations,

$$r^2 D_a\left(\frac{1}{r^2}D^a\Theta\right) - \frac{m_V}{r^2}\Theta = \frac{8Q}{r^2}\mathcal{A}, \tag{4.39}$$

$$D_aD^a\mathcal{A} - \frac{1}{r^2}\left(k_V^2 + 1 + \frac{4Q^2}{r^2}\right)\mathcal{A} = \frac{Q\,m_V}{r^4}\Theta. \tag{4.40}$$

These wave equations can be decoupled. Define

$$\Phi_\pm = a_\pm r^{-1}\Theta + b_\pm\mathcal{A}, \tag{4.41}$$

with

$$a_+ = \frac{Q\,m_V}{3M + \sqrt{9M^2 + 4m_VQ^2}}, \quad a_- = 1, \tag{4.42}$$

$$b_- = -\frac{4Q}{3M + \sqrt{9M^2 + 4m_VQ^2}}, \quad b_+ = 1. \tag{4.43}$$

Replacing Θ and $\mathcal{A}$ in terms of $\Phi_\pm$ and further replacing in (4.39), we obtain two decoupled wave equations,

$$D_aD^a\Phi_\pm - \frac{1}{f}V_\pm^{(V)}\Phi_\pm = 0, \tag{4.44}$$

with

$$V_\pm^{(V)} = \frac{f}{r^2}\left(k_V^2 + 1 + \frac{4Q^2}{r^2} + \frac{1}{r}(-3M \pm \sqrt{9M^2 + 4m_VQ^2})\right). \tag{4.45}$$

The superscript (V) denotes the fact that this is the potential for vectorial perturbations. In the case of tensor and scalar perturbations on a Reissner-Nordstrom background – tensor perturbations are non-trivial for higher dimensions –, the equations of motion for the linear perturbations can also be disentangled to wave equations [66].

The decoupling (4.41) is not necessarily possible for every system: we will see in chapter 5 that in the static subtracted geometry case this is not possible. We will have to be content with studying the coupled wave equations that describe the perturbations.

Quasinormal Modes

Let us now study further (4.44). This equation can be written as

$$(g^{tt}\partial_t^2 + \partial_r g^{rr}\partial_r)\Phi_\pm - \frac{1}{f}V_\pm^{(V)}\Phi_\pm \quad = \quad 0. \tag{4.46}$$

We apply (4.11) in order to Fourier transform this equation into

$$f(f\Phi_\pm')' + (\omega^2 - V_\pm^{(V)})\Phi_\pm = 0. \tag{4.47}$$

This equation can be recast in a different way that is useful to examine its boundary conditions. For this purpose, we define "tortoise coordinates,"

$$\frac{dr_*}{dr} = \frac{1}{f}, \tag{4.48}$$

where

$$r_{\text{horizon}} = r_* \to -\infty, \quad r_\infty = r_* \to \infty. \tag{4.49}$$

In these coordinates, (4.47) transforms to a Schrödinger equation,

$$\frac{d^2}{dr_*^2}\Phi_\pm + (\omega^2 - V_\pm^{(V)})\Phi_\pm = 0. \tag{4.50}$$

Now, as already mentioned in chapter 2, to study the quasinormal modes of (4.47), or (4.50), we need to set suitable boundary conditions. Notice that these wave equations encode more physics than the quasinormal modes. For example, studying the expectation value of the $\mathcal{O}$ operator defined by (4.50) as

$$\mathcal{O}\Phi_\pm \equiv \left(-\frac{d^2}{dr_*^2} + V_\pm^{(V)}\right)\Phi_\pm = \omega^2\Phi_\pm, \tag{4.51}$$

tells us about the stability of the black hole. If always non-negative, then its eigenvalues ω^2 are non-negative as well, implying that the perturbations do not grow exponentially in time. If this is the case, we can state that the black hole is perturbatively stable [66].

Let us go back to the discussion on the boundary conditions for quasinormal modes. The boundary conditions at the horizon of the black hole are virtually the same for every background, yet some subtleties are found regarding the asymptotic boundary conditions [38, 39]. We elaborate on this now.

As nothing should (classically) leave the horizon, we assume that at the horizon there are no outgoing modes. These are *ingoing boundary conditions*, and they characterize the existence of a horizon. On the other hand, when imposing asymptotic boundary conditions at spatial infinity, the discussion is a bit more subtle: in an astrophysical setting, namely four-dimensional asymptotically flat black holes, it makes sense to choose *outgoing boundary conditions*. These boundary conditions mean that there are not ingoing modes from infinity that might be regarded as unphysical. However, if we are interested in holography, we might want to set other boundary conditions at spatial infinity. For example, for an asymptotically AdS spacetime, it suits better to impose regularity on the fields at infinity – effectively Dirichlet boundary conditions. We come back to this point in a few more paragraphs.

We apply now the above discussion on boundary conditions to our Reissner-Nordstrom black hole study case. Inspecting equation (4.45) and (4.50), we see that the potential $V_{\pm}^{(V)}$ behavior at the horizon and spatial infinity is

$$V_{\pm}^{(V)} \sim 0, \tag{4.52}$$

so both at the horizon and spatial infinity we expect the solution to behave as $\Phi_{\pm} \sim e^{-i\omega(t\pm r_*)}$ [38]. Ingoing boundary conditions at the horizon and outgoing boundary conditions at spatial infinity explicitly means

$$\Phi_{\pm,\text{Horizon}} \sim e^{-i\omega(t+r_*)}, \quad \Phi_{\pm,\infty} \sim e^{-i\omega(t-r_*)}. \tag{4.53}$$

By solving the problem with these boundary conditions, we obtain the quasinormal frequencies. The quasinormal frequencies will be complex, and they depend on the mass M, the charge Q, the harmonic angular index ℓ, and the overtone[4] n. Unfortunately, for the Reissner-Nordstrom case solving for the quasinormal frequencies is not straightforward. It is technically challenging, and usually approximations or numerical techniques are needed[5] – see [70, 71, 72, 73, 74, 75, 76, 77] for studies related to numerical and approximate analytical values for Reisner-Nordstrom quasinormal modes.

Let us come back to the boundary conditions for spatial infinity, specifically for asymptotically AdS background spacetimes. For exemplifying this point, we switch to a four-dimensional Schwarzschild-AdS black hole,

$$\begin{aligned} ds^2 &= -f dt^2 + f^{-1} dr^2 + r^2 d\Omega^2, \\ f &= 1 + \frac{r^2}{L^2} - \frac{2M}{r}, \end{aligned} \tag{4.54}$$

where L is the AdS curvature radius. For a massless scalar perturbation Φ, the wave equation can be written as [38]

$$\frac{d^2\Phi}{dr_*^2} + (\omega^2 - V)\Phi = 0, \tag{4.55}$$

with

$$V = f\left(\frac{\ell(\ell+1)}{r^2} + \frac{2M}{r^3} + \frac{2}{L^2}\right). \tag{4.56}$$

[4]The overtone n measures how damped the mode is. As n increases, the mode gets more damped.

[5]An analytic example of the obtention of the quasinormal frequencies can be found in section 5.4.1, where we analize a minimally coupled scalar on a subtracted geometry background.

In this case, the solution at spatial infinity $r \to \infty$ will be [38]

$$\Phi \sim \frac{A}{r^2} + Br, \tag{4.57}$$

with A, B constant. In contrast with the asymptotically flat case, where outgoing boundary conditions are the most reasonable choice, in asymptotically anti-de Sitter space is not obvious which boundary conditions fit for our purposes – see section 3.1 of [38] and references therein. In our work with subtracted geometries, we take Dirichlet boundary conditions. This means that Φ takes a finite value at the boundary of AdS, so $B = 0$ in (4.57). Even though subtracted geometries are not asymptotically AdS – they are asymptotically conical –, they still show qualitatively the same confining properties of AdS, as we already discussed in section 3. Moreover, recall that we want to compare the quasinormal modes spectrum of the subtracted geometries with the BTZ black hole spectrum. The BTZ is asymptotically AdS, and its quasinormal spectrum was obtained using Dirichlet boundary conditions at spatial infinity [45]. In short: using the BTZ as a benchmark for the analysis of the subtracted geometry quasinormal spectrum only make sense when both spectra are derived with equivalent boundary conditions.

Chapter 5

The Spectrum of Static Subtracted Geometries

This chapter is based on [1].

Subtracted geometries are black hole solutions of the four dimensional STU model with rather interesting ties to asymptotically flat black holes. A peculiar feature is that the solutions to the Klein-Gordon equation on this subtracted background can be organized according to representations of the conformal group $SO(2,2)$. We test if this behavior persists for the linearized fluctuations of gravitational and matter fields on static, electrically charged backgrounds of this kind. We find that there is a subsector of the modes that do display conformal symmetry, while some modes do not. We also discuss two different effective actions that describe these subtracted geometries and how the spectrum of quasinormal modes is dramatically different depending upon the action used.

5.1 Introduction

Our understanding of microscopic properties of extremal and supersymmetric black holes are far superior to our understanding of their non-extremal counterparts. The advantage of the extremal solution is that we can decouple the near horizon geometry [78, 79, 80], i.e. we can place an extremal black hole in a box. This box not only isolates the horizon, but it as well enhances the symmetries of the geometry suggesting a dual description in terms of a CFT_2. This is the core of the Kerr/CFT correspondence [18], which is a proposal for the microscopic dual of the extreme Kerr solution.

Stretching the proposal of Kerr/CFT a step further, it is tempting to think of the non-extremal black hole as a finite temperature excitation of the CFT describing the extremal solution. In an attempt to realize this idea, it was noticed in [27] that, at low frequencies, linearized fluctuations around the Kerr black hole display a hidden conformal symmetry. More concretely, the solutions to the wave equation organize themselves in representations of the $SO(2,2)$ group in the same fashion as the three dimensional BTZ black hole [55, 81]. Despite the fact that the symmetry is only manifest in a low energy limit, it was robust enough to express the Bekenstein-Hawking entropy of the Kerr solution as the sta-

tistical entropy of a CFT_2 at high temperature [27, 82, 83, 84]. That is, one could express universally the area law as a Cardy formula, giving support to the Kerr/CFT proposal.

The drawback of this proposal is that the conformal features of the fluctuations is too fragile: as we move away from the low energy regime there is very little evidence that exploiting the $SO(2,2)$ symmetry is the correct way to describe the black hole [85]. A rather interesting way to overcome this obstacle was proposed in [28, 29]. The authors there suggested a concrete way to put a non-extremal black hole in a box. Remarkably, this idea realizes the hidden conformal symmetry in [27] for probe scalars without relying on a low frequency limit. The important feature of this box is that it doesn't tamper with the horizon of the original configuration: this suggests that the microscopic model that accounts for the entropy is unchanged after placing the box.

The solutions in [28, 29] are known as *subtracted geometries*: the box is constructed by subtracting certain metric factors from the asymptotically flat black hole solution. We recall now some points discussed in chapter 3. The subtracted geometry is a solution to $\mathcal{N}=2$ supergravity, and this allows to build these geometries in a variety of ways. For instance, they can be obtained by using solution generating techniques [31, 32, 30] or scaling limits [46]. It is possible as well to build interpolating solutions between the asymptotically flat black hole and the subtracted one [47]. Various properties of the subtracted geometries have been analysed in the literature. For instance, the thermodynamical properties of the solutions [49, 51] and holographic renormalization [51] have been worked out. In addition, the behaviour of minimally coupled scalars on this background has been considered in [48, 50]. See as well [52, 53] for a discussion on the attractor mechanism for subtracted geometries.

Our goal here is to understand dynamical properties of static subtracted geometries. In particular, we will study linearized fluctuations of the gravitational and matter modes that support the subtracted black hole. Along the way, we will report the scaling dimensions of the fluctuations and their quasinormal frequencies. The general subtracted geometry can carry angular momentum, electric and magnetic charges, in addition to mass. We will not include angular momentum in the backgrounds considered here: cases that are only electrically charged will have enough structure to illustrate intricate properties of the fluctuations. Nevertheless, it would be interesting to add rotation and see which features we find here persist.

These fluctuations will test if the hidden conformal symmetry persists for perturbations that are not necessarily minimally coupled. Unfortunately, we will see that this symmetry is only present in certain sectors. More broadly, a complete understanding of the fluctuations can provide useful information about a potential holographic dual. Given that our analysis can be performed analytically to a large extent, it would be very interesting to understand properties of the dual theory. One reason to do so is that some features of the subtracted geometries are also present in other holographic setups, such as those in Schrodinger spacetimes with $z=2$ [86] and hyperscaling violating solutions [87]. Here we will only present the bulk analysis of the fluctuations and highlight certain features of the fluctuations; we leave a more holographic analysis for future work.

5.1.1 Summary of results

The main portion of our work involves rather technical analysis of linearized fluctuations. Here we will summarize the key points of our method and highlights of our results. We will also comment briefly on future directions.

We will build the linearized fluctuations around static subtracted geometries; these geometries are described in Section 5.2. To construct the master fields and their equations we will use the technique – discussed previously in chapter 4) – developed by Kodama-Ishibashi [88, 66]; this analysis is done in Section 5.4. The strength of this method is that it exploits in a clever manner gauge invariance and isometries to get decoupled ODEs for the physical modes. The drawback is that spherical symmetry is crucial: for this reason we will only analyze static solutions that carry only electric charge. The modes will be decomposed in vector and scalar modes with respect to spherical harmonic decomposition. Our emphasis will be on finding solutions to the master field equations and the QNM frequencies.

We will work with two different actions that contain a static subtracted geometry as a solution: the STU model and an Einstein-Maxwell-Dilaton (EMD) model. At the level of matter fields, the difference between the two theories is that STU contains an axion field, χ, whereas EMD does not. Throughout our analysis we will compare the results for each theory: even though they are very closely related at the level of the action, the structure of the fluctuations will be rather different.

The quick summary of our results is:

Vector Sector. Here is where we find the most striking difference between the STU model and EMD. Due to a constraint arising from the equation of motion for the axion field, the STU model has no vector excitations. On the other hand, for EMD this sector is non-trivial and the coupled set of ODEs is given in (5.38). We have solved for the quasinormal frequencies of this system numerically and the results are in Fig. 5.1. The frequencies have both a real and imaginary part.

Scalar Sector. For the STU model we can consistently take $\delta\chi = 0$; here both the STU and EMD model will give the same results. When $\delta\chi = 0$ there are eight non-trivial branches of solutions for the modes. For four of these branches the solutions are hypergeometric functions and hence the quasinormal frequencies are integer spaced (and purely imaginary); see (5.74) and (5.76). For the other four branches, the modes are Heun functions, but rather surprisingly the quasinormal frequencies are still integer spaced and purely imaginary (5.85). For $\delta\chi \neq 0$, which only applies for the STU model, the modes are again Heun functions. However the quasinormal modes are not integer spaced; see Fig. 5.2.

It is important to emphasize that for one scalar subsector the fluctuations are appropriately weighted hypergeometric functions: this indicates that $SO(2,2)$ is the natural symmetry to organize this portion of the spectrum. Since the geometries in consideration have no obvious conformal isometries, it is highly non-trivial that this is occurring. However, there are modes that deviate significantly from this conformal pattern: the solutions in this case are Heun functions instead of hypergeometric functions. We don't have an alternative holographic interpretation of this sector at the moment; we just know it does not smell like a CFT and it does not mimic the fluctuations of BTZ black hole [45] in the way it does for minimally coupled scalars. It would be interesting to study further what are the basic features

of the dual theory based on our results and complement them with the analysis in [89]. In particular, some of the non-conformal modes are in the gravitational sector and they would contribute to the energy-density correlation functions. It would be interesting to analysis two-point functions of the stress tensor on this background.

It is possible to uplift a subtracted geometry from four to five dimensions. Rather interestingly, in five dimension the solution is locally $\text{AdS}_3 \times S^2$ [29]. This suggests that the modes should be organized using the conformal symmetry of AdS_3, but we do not find evidence of this from the four dimensional point of view. However the uplift is done in the magnetic frame, whereas we are always working in the electric frame, and this might obscure certain properties. For instance, there could be a non-trivial arrangement of the couplings as we uplift that restores the conformal features in the five dimensional geometry, but this is highly speculative. In this work we only discuss four dimensional properties of the solution.

5.2 The theory and the solution

In this section we will lay down the main features of the theory we will analyze, and more importantly, the solutions we will focus on. Our conventions mostly follow those in [47, 51]. Our theory will be a truncation of the STU model [90, 91], for which the matter content involves two gauge fields, a scalar and axion field. The action for this truncation is

$$\begin{aligned} I =& \frac{1}{16\pi G}\int d^4x\sqrt{g}\Big(R - \frac{3}{2}\partial_\mu\eta\partial^\mu\eta - \frac{3}{2}e^{2\eta}\partial_\mu\chi\partial^\mu\chi - \frac{1}{4}e^{-3\eta}(F^0)^2 \\ & - \frac{3}{4}\frac{e^{-\eta}}{(4\chi^2+e^{-2\eta})}(\tilde{F}-\chi^2F^0)^2 - \frac{\chi}{(4\chi^2+e^{-2\eta})}\Big[3\tilde{F}\wedge\tilde{F} + 3(2\chi^2+e^{-2\eta})\tilde{F}\wedge F^0 \\ & -\chi^2(\chi^2+e^{-2\eta})F^0\wedge F^0\Big]\Big)\,. \end{aligned} \tag{5.1}$$

This is known as the *electric frame* action; equations of motion and some conventions are presented in Appendix 5.A.1. The most commonly known version of this model is usually written in the *magnetic frame*, in which it reads

$$\begin{aligned} I =& \frac{1}{16\pi G}\int d^4x\sqrt{g}\Big(R - \frac{3}{2}\partial_\mu\eta\partial^\mu\eta - \frac{3}{2}e^{2\eta}\partial_\mu\chi\partial^\mu\chi - \frac{1}{4}e^{-3\eta}(F^0)^2 - \frac{3}{4}e^{-\eta}(F+\chi^2F^0)^2 \\ & + 3\chi F\wedge F + 3\chi^2F\wedge F^0 + \chi^3F^0\wedge F^0\Big)\,. \end{aligned} \tag{5.2}$$

The relation between both of them is given by

$$F_{\mu\nu} = -(4\chi^2+e^{-2\eta})^{-1}\left(\frac{1}{2}\varepsilon_{\mu\nu\rho\sigma}e^{-\eta}(\tilde{F}-\chi^2F^0)^{\rho\sigma} + 2\chi\,\tilde{F}_{\mu\nu} + \chi(2\chi^2+e^{-2\eta})F^0_{\mu\nu}\right)\,. \tag{5.3}$$

Here we will mostly use the electric frame: the reason simply being that the matter content will respect the spherical symmetry of the background solutions we will consider – in the magnetic frame, the background gauge field (5.13) explicitly breaks this symmetry with its $\cos\theta$ dependence.

The backgrounds that we will present below will all have $\chi = 0$. This is not a consistent truncation of the STU model (in either frame), since setting $\chi = 0$ in the equation of motion gives a constraint between the remaining fields:

$$\tilde{F}\wedge\tilde{F} - e^{-2\eta}F^0\wedge\tilde{F} = 0\,. \tag{5.4}$$

However, it is interesting to note that for configurations with $\chi = 0$, the equations of motion for the remaining fields can be obtained from the following action

$$I_{\text{eff}} = \frac{1}{16\pi G}\int \sqrt{g}\left[R - \frac{3}{2}\partial_\mu\eta\partial^\mu\eta - \frac{e^{-3\eta}}{4}(F^0)^2 - \frac{e^\eta}{4}\tilde{F}^2\right] . \tag{5.5}$$

We will refer to this theory as EMD: Einstein-Maxwell-Dilaton theory. Throughout our analysis, we will contrast the results obtained from using (5.1) versus (5.5).

5.3 Static Subtracted Geometries

The focus of our work is to study dynamical properties of a specific class of solutions to (5.1): electrically charged black holes which are asymptotically conical. These solutions are known as subtracted Reissner-Nordstrom (subRN) geometries, since they were first constructed by subtracting certain metric factors from the asymptotically flat Reissner-Nordstrom solution [28, 29]. More generally, these solutions can be obtained using solution generating techniques [31, 32, 30], scaling limits [46] or interpolating solutions [47]. In the following we will summarize some basic properties of subRN background.

The asymptotically flat Reissner-Nordstrom with electric and magnetic sources is given by

$$\begin{aligned} ds^2 &= \frac{\sqrt{\Delta_{\text{RN}}}}{X}dr^2 - \frac{X}{\sqrt{\Delta_{\text{RN}}}}dt^2 + \sqrt{\Delta_{\text{RN}}}d\Omega_2^2 , \qquad e^\eta = \sqrt{\frac{p(r)}{p_0(r)}} \\ \chi &= 0 , \qquad A^0 = \frac{m\sinh(2\delta_0)}{p_0(r)}dt , \qquad A = m\sinh(2\delta)\cos\theta d\phi , \end{aligned} \tag{5.6}$$

where

$$\begin{aligned} &\Delta_{\text{RN}}(r) = p(r)^3 p_0(r) , \quad X(r) = r^2 - 2mr , \\ &p(r) = r + 2m\sinh^2\delta , \quad p_0(r) = r + 2m\sinh^2\delta_0 . \end{aligned} \tag{5.7}$$

Here m, δ and δ_0 are constants. This solution asymptotes to $\mathbb{R}^{3,1}$ and has an inner and outer horizon located at the zeroes of $X(r)$. The conserved charges of this black hole, i.e. mass, electric and magnetic charge, are

$$M = \frac{m}{4G}(\cosh(2\delta_0) + 3\cosh(2\delta)) , \quad Q_{\text{elec}} = \frac{m}{4G}\sinh(2\delta_0) , \quad Q_{\text{mag}} = \frac{3m}{4G}\sinh(2\delta) . \tag{5.8}$$

The Hawking temperature reads

$$T = \frac{1}{8\pi m}(\cosh\delta_0\cosh^3\delta)^{-1} , \tag{5.9}$$

and the entropy is given by

$$S_{\text{BH}} = \frac{A_H}{4G} = \frac{4\pi m^2}{G}\cosh\delta_0\cosh^3\delta . \tag{5.10}$$

A so-called subtracted version of (5.6) is given as follows. In the magnetic frame, the subtracted solution takes the form

$$\begin{aligned} ds^2 &= \frac{\sqrt{\Delta}}{X}dr^2 - \frac{X}{\sqrt{\Delta}}dt^2 + \sqrt{\Delta}d\Omega_2^2 , \\ e^\eta &= \frac{B^2}{\sqrt{\Delta}} , \qquad \chi = 0 , \qquad A^0 = \frac{2mB^3\Pi_s\Pi_c}{(\Pi_c^2 - \Pi_s^2)}\Delta^{-1}dt , \qquad A = B\cos\theta d\phi , \end{aligned} \tag{5.11}$$

with $X(r)$ as in (5.7) and

$$\Delta(r) = (2m)^3(\Pi_c^2 - \Pi_s^2)r + (2m)^4\Pi_s^2 \,. \tag{5.12}$$

The parameters $\Pi_{c,s}$, m and B are constant. The horizons of this solution are again given by the zeroes of $X(r)$. Note that this solution, as $r \to \infty$, takes the form

$$\begin{aligned} ds^2 &= \sqrt{r}\left(\ell^2\frac{dr^2}{r^2} - \frac{r}{\ell^2}dt^2 + \ell^2 d\Omega_2^2\right) \,, \qquad \ell^2 = \sqrt{(2m)^3(\Pi_c^2 - \Pi_s^2)} \,, \\ e^\eta &= \frac{B^2}{\ell^2\sqrt{r}} \,, \qquad \chi = 0 \,, \qquad A^0 = 0 \,, \qquad A = B\cos\theta d\phi \,, \end{aligned} \tag{5.13}$$

which we would identify as a "vacuum solution" to (5.11) and as such it gives a reference point to quantify observables [51]. This solution has interesting scaling properties, which mimics those in hyperscaling violating geometries [92, 93]. However, it is a singular solution to the system and hence it is only used as an asymptotic solution.

As we mentioned above, (5.6) has an intimate relation to (5.11) via solution generating techniques, scalings, or explicit subtractions. This relates the parameters in the solutions as

$$\Pi_s = \sinh\delta_0 \sinh^3\delta \,, \qquad \Pi_c = \cosh\delta_0\cosh^3\delta \,, \qquad B = 2m\sinh\delta \,. \tag{5.14}$$

This relation in particular assures that the entropy of both black holes is exactly the same and given by (5.10). Furthermore, the surface gravities of both black holes are as well the same (provided the same Killing vector is used for both solutions). However, the subRN solution has its own conserved charges: using canonical definitions within the framework of holographic renormalization, the physical quantities associated to (5.16) are [51]

$$M = \frac{(2m)^4}{8G\ell^4}(\Pi_c^2 + \Pi_s^2) \,, \quad Q_{\rm elec} = \frac{(2m)^2\Pi_c\Pi_s}{4GB^3} \,, \quad Q_{\rm mag} = \frac{3B}{4G} \,. \tag{5.15}$$

For the purpose of studying the fluctuations around subRN, it is more convenient to have a electrically charged solution. The subtracted version of (5.11) in the electric frame is given by

$$\begin{aligned} ds^2 &= \frac{\sqrt{\Delta}}{X}dr^2 - \frac{X}{\sqrt{\Delta}}dt^2 + \sqrt{\Delta}d\Omega_2^2 \,, \qquad e^\eta = \frac{B^2}{\sqrt{\Delta}} \\ \chi &= 0 \,, \qquad A^0 = \frac{2mB^3\Pi_s\Pi_c}{(\Pi_c^2 - \Pi_s^2)}\Delta^{-1}dt \,, \qquad \tilde{A} = -\frac{1}{B}(r-2m)dt \,, \end{aligned} \tag{5.16}$$

which is a solution to both (5.1) and (5.5). This will be the solution we will use throughout our analysis in the following section, and we emphasize that we will not use (5.14): the parameters in (5.16) should be thought to be independent. Finally, for sake of simplicity, in Section 5.4 we will set $B = 2m$. Shifting the value of B can be acomplished by shifting η by a constant and rescaling the field strengths appropriately, i.e.

$$\eta \to \eta + \eta_0 \,, \qquad \tilde{F} \to e^{-\eta_0/2}\tilde{F} \,, \qquad F^0 \to e^{3\eta_0/2}F^0 \,, \tag{5.17}$$

with η_0 constant. This is a symmetry of the equations of motion (for $\chi = 0$) and hence qualitative aspects of our results are not impacted by making the choice $B = 2m$.

When $\Pi_s = 0$, $\Pi_c = 1$ and $B = 2m$ we obtain a version of subtracted Schwarzschild [94]. The solution is conformal to $AdS_2 \times \mathbb{R}^2$ as can be checked explicitly from the above expressions. As we study the fluctuations we will consider this a limit case, and due to the explicit symmetry of the background all perturbations can be solved for exactly in terms of Hypergeometric functions. See [95, 96, 97] for related examples.

5.4 Linearized fluctuations

In this section we study the linearized fluctuations of the metric and matter fields of subRN in the electric frame of the STU model and the EMD theory described section 5.2. The background solution we will always consider is (5.16).

5.4.1 Warm-up: minimally coupled scalars

Before proceeding, it is instructive to review the key property that initially motivated the construction of the subtracted geometries: the dynamics of a probe scalar field. Prior analysis similar to the one below are given in [29, 48]. The behavior of this field should be contrasted with the modes in (5.27) which we will derive in the following section. Consider a massless and neutral scalar field; its Klein Gordon equation is

$$\frac{1}{\sqrt{-g}}\partial_\mu\left(\sqrt{-g}g^{\mu\nu}\partial_\nu\Psi\right)=0\ . \tag{5.18}$$

Expanding in eigenmodes and using separability

$$\Psi(x^\mu)=e^{-i\omega t}\mathbb{S}(\theta,\phi)R(r)\ , \tag{5.19}$$

gives that (5.18) reduces to

$$R''+\frac{X'}{X}R'+\left(-\frac{\ell(\ell+1)}{X}+\frac{\omega^2\Delta}{X^2}\right)R=0\ . \tag{5.20}$$

Here primes denote derivatives with respect to r, $\mathbb{S}$ are the usual spherical harmonics on S^2 defined by

$$(\hat{\nabla}^2+\ell(\ell+1))\mathbb{S}=0\ , \tag{5.21}$$

with $\hat{\nabla}^2$ the Laplacian on S^2 and $l\in\mathbb{Z}^+$. Introducing

$$y=\frac{2m}{r}\ ,\qquad \hat{\omega}=\frac{\omega}{4\pi T}\ , \tag{5.22}$$

where the Hawking temperature for subRN is given by $T=(8\pi m\Pi_c)^{-1}$, we verify that (5.20) depends on the charges only via

$$\epsilon\equiv\frac{\Pi_s}{\Pi_c}\ , \tag{5.23}$$

and takes the form

$$(y-1)R''+R'+\left(\frac{\ell(\ell+1)}{y^2}+\frac{\hat{\omega}^2\left((y-1)\epsilon^2+1\right)}{(y-1)y}\right)R=0\ , \tag{5.24}$$

where primes now denote derivatives with respect to y. The solution to (5.24) can be written in terms of hypergeometric functions as

$$\begin{aligned}R=&C_1y^{\ell+1}(1-y)^{-i\hat{\omega}}{}_2F_1(\ell+1-i\hat{\omega}(1+\epsilon),\ell+1-i\hat{\omega}(1-\epsilon),-2\ell,y)\\&+C_2y^{-\ell}(1-y)^{-i\hat{\omega}}{}_2F_1(-\ell-i\hat{\omega}(1+\epsilon),-\ell-i\hat{\omega}(1-\epsilon),-2\ell,y)\ .\end{aligned} \tag{5.25}$$

Note that the scaling dimensions of the scalar, i.e. the characteristic exponents of the power law as $y \to 0$, depend on the quantum numbers of the fields. This is very common occurrence in the near horizon geometries of extremal black holes, and more generally in cases where the metric is a direct product. It is as well present in geometries with non-trivial scaling properties in the UV, such as the cases studied in, for example, [98, 99, 87]. This feature is usually interpreted as some semi-local behavior of the dual theory [100]. We will encounter a similar type of dependence for the scaling dimensions of all metric and matter fluctuations, and it would be interesting to account for this holographically.

The quasi-normal modes (QNMs) of the black hole under consideration are solutions to the linearized equations of motion which satisfy regularity at the boundary $y = 0$ and ingoing boundary conditions at the horizon $y = 1$ [101, 38]. The latter condition corresponds to a near horizon behaviour of the form $R \sim (1-y)^{-i\hat{\omega}}$ times a regular power series in y. These requirements imply that the QNM frequencies are given by

$$\hat{\omega} = -\frac{i}{1 \pm \epsilon}(\ell + n) \ , \qquad n = 0, 1, 2, \dots \ . \tag{5.26}$$

From the structure of the background metric (5.16), it is very surprising that the Klein-Gordon equations for a massless field has such a simple solution. One of our goals is to investigate if the coupled metric and matter fluctuations have a similar behavior, and hence which lessons can we draw from a potential holographic dual.

5.4.2 Master equations for gravitational fluctuations

Our starting point is to decompose the fields as

$$g_{\mu\nu} = \bar{g}_{\mu\nu} + \delta g_{\mu\nu} \ , \quad \tilde{A}_\mu = \bar{\tilde{A}}_\mu + \delta \tilde{A}_\mu \ , \quad A^0_\mu = \bar{A}^0_\mu + \delta A^0_\mu \ , \quad \eta = \bar{\eta} + \delta\eta \ , \quad \chi = \bar{\chi} + \delta\chi \ , \tag{5.27}$$

where the barred variables correspond to the background values in (5.16) and the pieces proportional to δ are the fluctuations. The dynamics of these modes are, as expected from the couplings in either (5.1) or (5.5), a non-trivial coupled system of ODEs. To attack this hurdle we will build master equations by following the techniques described in section 4 and originally constructed in [88, 66]. In a nutshell, this approach gives a elegant and pragmatic approach to build master field equations for gauge invariant variables by exploiting the spherical symmetries of the systems.

Just as we saw in chapter 4, we will decompose further our fluctuations into scalar and vector modes of S^2, i.e.

$$\delta g_{\mu\nu} = h^{(V)}_{\mu\nu} + h^{(S)}_{\mu\nu} \ , \qquad \delta\tilde{A}_\mu = \tilde{A}^{(V)}_\mu + \tilde{A}^{(S)}_\mu \ , \qquad \delta A^0_\mu = A^{0(V)}_\mu + A^{0(S)}_\mu \ , \tag{5.28}$$

which can be discussed separately. The fluctuations of the dilaton η and axion χ are all in the scalar sector. Note that there are no tensor perturbations, we cannot build such structures on S^2. We will as well choose a radial gauge for which

$$\delta g_{\mu r} = 0 \ , \qquad \delta\tilde{A}_r = 0 \ , \qquad \delta A^0_r = 0 \ . \tag{5.29}$$

This condition does not fully fix the gauge. As we build the master equations, we will build combinations that are invariant under residual diffeomorphisms and $U(1)$ gauge transformations.

Vector modes

We recall the discussion of chapter 4 on vector modes: these are perturbations of the form

$$\delta g_{ab} = 0 \ , \qquad \delta g_{ai} = e^{-i\omega t} f_a^{(V)}(r) \mathbb{V}_i \ , \qquad \delta g_{ij} = e^{-i\omega t} H^{(V)}(r) \mathbb{V}_{ij} \ , \tag{5.30}$$

$$\delta \tilde{A}_a = 0 \ , \qquad \delta \tilde{A}_i = e^{-i\omega t} a(r) \mathbb{V}_i \ , \qquad \delta A^0_a = 0 \ , \qquad \delta A^0_i = e^{-i\omega t} b(r) \mathbb{V}_i \ , \tag{5.31}$$

where $(a, b) = (t, r)$ and $(i, j) = (\theta, \phi)$ and we decomposed the fluctuations in frequency eigenmodes; note that there are no fluctuations for the dilaton and axion in this sector. Here $\mathbb{V}_i$ are vector harmonics on S^2, which can be simply taken to be $\mathbb{V}_i = \epsilon^{ij} \hat{D}_j \mathbb{S}$ with $\mathbb{S}$ being the standard spherical harmonics and ϵ^{ij}, $\hat{D}_j$ are the Levi-Civita tensor and the covariant derivative on the 2-sphere. Note that they satisfy

$$(\hat{\nabla}^2 + k_V^2) \mathbb{V}_i = 0 \ , \qquad \hat{D}^i \mathbb{V}_i = 0 \ , \tag{5.32}$$

where $k_V^2 = \ell(\ell + 1) - 1$, with ℓ an integer greater or equal to 1. As explained in [88, 66], modes with $\ell = 1$ correspond to pure diffeo modes, so we consider $\ell \geq 2$ only. The $\mathbb{V}_{ij}$ are define via the symmetrized derivative

$$\mathbb{V}_{ij} = -\frac{1}{k_V} (\hat{D}_i \mathbb{V}_j + \hat{D}_j \mathbb{V}_i) \ . \tag{5.33}$$

Choosing the standard coordinates on the sphere $d\Omega^2 = d\theta^2 + \sin^2\theta d\phi^2$, these are given by

$$\begin{aligned}
\mathbb{V}_\theta &= \csc\theta \partial_\phi \mathbb{S} \ , \qquad \mathbb{V}_\phi = -\sin\theta \partial_\theta \mathbb{S} \ , \\
\mathbb{V}_{\theta\theta} &= \frac{\csc\theta}{k_V} (\cot\theta - \partial_\theta) \partial_\phi \mathbb{S} \ , \\
\mathbb{V}_{\theta\phi} &= -\frac{1}{2k_V} (\csc\theta \partial_\phi^2 + \cos\theta \partial_\theta - \sin\theta \partial_\theta^2) \mathbb{S} \ , \\
\mathbb{V}_{\phi\phi} &= -\frac{1}{k_V} (\cos\theta - \sin\theta \partial_\theta) \partial_\phi \mathbb{S} \ .
\end{aligned} \tag{5.34}$$

The diffeomorphisms that preserve the form of the ansatz in the vector sector are generated by the vector field

$$\xi_V = e^{-i\omega t} \sqrt{\Delta} \mathbb{V}^i \partial_i \ . \tag{5.35}$$

This generates the pure gauge mode

$$f_t = -i\omega\sqrt{\Delta} \ , \qquad H^{(V)} = -2k_V\sqrt{\Delta} \ , \qquad a(r) = b(r) = 0 \ . \tag{5.36}$$

Moreover, it is clear that $a(r)$ and $b(r)$ are invariant under the $U(1)$ gauge transformations associated to the gauge fields. Based on this, and just as in section 4, the gauge invariant combinations of the fluctuations we will use are $a(r)$, $b(r)$ in (5.31), in addition to $\mathcal{W}$ defined by

$$\mathcal{W}(r) \equiv \frac{X}{2ik_V \omega \Delta^{1/2}} \left((H^{(V)})' - \frac{\Delta'}{2} H^{(V)} \right) \ , \tag{5.37}$$

where prime denotes derivative with respect to r. The remaining component of the metric perturbation, f_t, can be written in terms of $\mathcal{W}$ using the equations of motion. At the linearized level, the

Einstein equations and the Maxwell equations for both gauge fields gives the following system of coupled equations

$$\begin{aligned}
&\mathcal{W}'' + \left(\frac{X'}{X} - \frac{\Delta'}{\Delta}\right)\mathcal{W}' + \left(\frac{1-k_V^2}{X} + \frac{\omega^2\Delta}{X^2}\right)\mathcal{W} + \frac{6m}{X}a + \frac{2m\Pi_c\Pi_s}{X}b = 0\,,\\
&a'' + \left(\frac{X'}{X} - \frac{\Delta'}{\Delta}\right)a' + \left(-\frac{\left(k_V^2+4\right)}{X} + \frac{\omega^2\Delta}{X^2}\right)a - \frac{\left(k_V^2-1\right)}{2mX}\mathcal{W} - \frac{\Pi_c\Pi_s}{X}b = 0\,,\\
&b'' + \left(\frac{\Delta'}{\Delta} + \frac{X'}{X}\right)b' + \left(\frac{\omega^2\Delta}{X^2} - \frac{1}{X}\left(1 + k_V^2 + \frac{(2m)^5\Pi_c^2\Pi_s^2}{\Delta^2}\right)\right)b\\
&- \frac{3(2m)^5\Pi_c\Pi_s}{X\Delta^2}a + \frac{(2m)^7\Pi_c\Pi_s\left(1-k_V^2\right)}{X\Delta^2}\mathcal{W} = 0\,.
\end{aligned} \tag{5.38}$$

These equations are valid for both the STU model in (5.1), and the effective action in (5.5). However, in the STU model we need as well to take into account the constraint (5.4), which comes from the equation of motion of the axion field. This constraint gives

$$\bar{\tilde{A}}_t'\, b + (\bar{A}_t^{0\,\prime} - 2e^{2\bar{\eta}}\bar{\tilde{A}}_t')\, a = 0\,. \tag{5.39}$$

Solving for this constraint and replacing in (5.38), it simple to see that the only possible solution is

$$a(r) = b(r) = \mathcal{W}(r) = 0\,. \tag{5.40}$$

Hence, *all* vector fluctuations in the STU model are trivial.

However, if subRN is viewed as a background solution to (5.5), we don't have additional constraints and the task ahead is to solve (5.38). Performing the redefinitions (5.22) in addition to

$$\hat{a} = \frac{1}{2m}a(r)\,, \qquad \hat{b} = \frac{1}{2m\Pi_c^2}b(r)\,, \tag{5.41}$$

the vector equations (5.38) read

$$\begin{aligned}
&\mathcal{W}'' + \left(\frac{\left(y^2\epsilon^2 - 2y\left(\epsilon^2-1\right)+\epsilon^2-1\right)}{(y-1)y\left((y-1)\epsilon^2+1\right)}\right)\mathcal{W}' + \left(\frac{k_V^2-1}{(y-1)y^2} + \frac{\hat{\omega}^2\left((y-1)\epsilon^2+1\right)}{(y-1)^2y}\right)\mathcal{W}\\
&+ \frac{\epsilon}{y^2(1-y)}\hat{b} + \frac{3}{y^2(1-y)}\hat{a} = 0\,,
\end{aligned} \tag{5.42}$$

$$\begin{aligned}
&\hat{a}'' + \left(\frac{\left(y^2\epsilon^2 - 2y\left(\epsilon^2-1\right)+\epsilon^2-1\right)}{(y-1)y\left((y-1)\epsilon^2+1\right)}\right)\hat{a}' + \left(\frac{k_V^2+4}{(y-1)y^2} + \frac{\hat{\omega}^2\left((y-1)\epsilon^2+1\right)}{(y-1)^2y}\right)\hat{a}\\
&+ \frac{\left(1-k_V^2\right)}{(y-1)y^2}\mathcal{W} + \frac{\epsilon}{(y-1)y^2}\hat{b} = 0\,,
\end{aligned} \tag{5.43}$$

$$\begin{aligned}
&\hat{b}'' + \left(\frac{\left(\left(y^2-1\right)\epsilon^2+1\right)}{(y-1)y\left((y-1)\epsilon^2+1\right)}\right)\hat{b}' + \frac{3\epsilon}{(y-1)\left((y-1)\epsilon^2+1\right)^2}\hat{a} + \left(\frac{\epsilon(1-k_V^2)}{(y-1)\left((y-1)\epsilon^2+1\right)^2}\right)\mathcal{W}\\
&+ \left(\frac{k_V^2\left((y-1)\epsilon^2+1\right)^2 + \left(y^2+2y-2\right)\epsilon^2 + (y-1)^2\epsilon^4 + 1}{(y-1)y^2\left((y-1)\epsilon^2+1\right)^2} + \frac{\hat{\omega}^2\left((y-1)\epsilon^2+1\right)}{(y-1)^2y}\right) = 0\,.
\end{aligned} \tag{5.44}$$

The near boundary analysis of (5.42)-(5.44) reveals that the characteristic behaviours near $y = 0$ are of the form y^{Δ_V} with

$$\Delta_V = \left\{ \pm \left(\frac{3}{2} + k_V^2 \pm \frac{1}{2}\sqrt{13 + 12k_V^2} \right)^{1/2}, 1 \pm \sqrt{2 + k_V^2} \right\} . \tag{5.45}$$

For $\epsilon = 0$, it is possible to decouple (5.42)-(5.44) and the resulting equations can be solved analytically in terms of hypergeometric functions. Imposing regularity at the boundary and ingoing boundary conditions at the horizon, we find that the spectrum is given by

$$\hat{\omega} = -i(\Delta_V^+ + n) , \qquad n = 0, 1, 2, \dots , \tag{5.46}$$

where Δ_V^+ are the three positive scaling dimensions in (5.45).

For $\epsilon \neq 0$, it is not clear how to further decouple (5.42)-(5.44) while keeping the system of second order. Nevertheless, it is rather straightforward to solve the system numerically, and in particular to find its QNMs. We do so by discretizing the system of equations and solving the resulting matrix eigenvalue problem numerically. We present our results in Fig. 5.1. Note that some of the frequencies acquire a non-zero real part as we increase ϵ, manifestly departing from the structure found in the Klein-Gordon equation in section 5.4.1. If the system has a hidden conformal symmetry, the quasinormal frequencies here should be compared with those in for BTZ black holes [45]: there the frequencies are always interger spaced and purely imaginary. This is not the feature we find here.

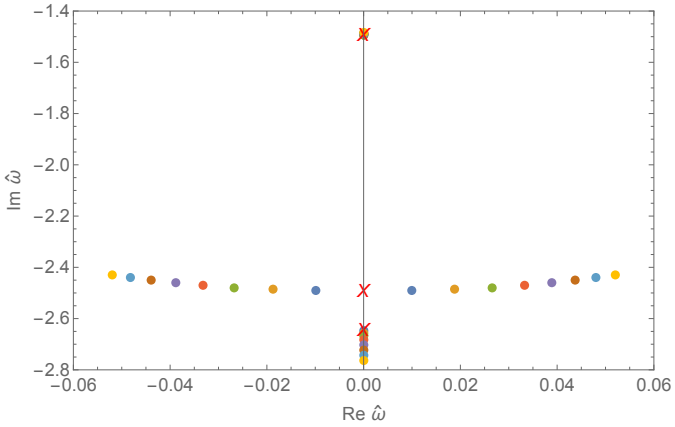

Figure 5.1: Snapshots of the lowest vector QNM in the complex plane for $\epsilon = 0.01, \dots, 0.08$. Different colors correspond to different values of ϵ. The red crosses correspond to the analytical values in (5.46), $\hat{\omega} = \{1.49265, 2.49265, 2.64575\}$. The first and third QNM remain on the imaginary axis, moving away from each other. The second QNM moves onto the complex plane.

This sharp discrepancy between the two actions in considerations is very interesting: the STU model still supports the conjecture that there is a hidden conformal symmetry in the subRN solution, whereas a different effective action, such as (5.5), shows that the quasinormal mode spectrum of subRN in the vector sector does not fit with a conformal description.

Scalar modes

We now move on to studying the scalar modes, which are much more intricate. In this case we have for the metric fluctuations

$$\delta g_{ab} = e^{-i\omega t} h_{ab} \mathbb{S} \,, \qquad \delta g_{ai} = e^{-i\omega t} f_a^{(S)}(r) \mathbb{S}_i \,, \qquad \delta g_{ij} = e^{-i\omega t} (H_T^{(S)}(r) \mathbb{S}_{ij} + H_L^{(S)}(r) \sigma_{ij} \mathbb{S}) \,, \tag{5.47}$$

for the gauge fields we take

$$\delta \tilde{A}_a = e^{-i\omega t} a_a(r) \mathbb{S} \,, \quad \delta \tilde{A}_i = e^{-i\omega t} a_\theta(r) \mathbb{S}_i \,, \quad \delta A^0_a = e^{-i\omega t} b_a(r) \mathbb{S} \,, \quad \delta A^0_i = e^{-i\omega t} b_\theta(r) \mathbb{S}_i \,, \tag{5.48}$$

and for the dilaton and axion we have

$$\delta e^\eta = e^{-i\omega t} s_1(r) \mathbb{S} \,, \qquad \delta \chi = e^{-i\omega t} s_2(r) \mathbb{S} \,. \tag{5.49}$$

As before, we have $(a, b) = (t, r)$ and $(i, j) = (\theta, \phi)$ and we will use the radial gauge (5.29). Here, $\mathbb{S}$ are vector harmonics on S^2, satisfying

$$(\hat{\nabla}^2 + k_S^2) \mathbb{S} = 0 \,, \tag{5.50}$$

with $k_S^2 = \ell(\ell + 1)$ and

$$\mathbb{S}_i = -\frac{1}{k_S} \hat{D}_i \mathbb{S} \,, \qquad \mathbb{S}_{ij} = \frac{1}{k_S^2} \hat{D}_i \hat{D}_j \mathbb{S} + \frac{1}{2} \sigma_{ij} \mathbb{S} \,. \tag{5.51}$$

Here σ_{ij} is the metric on S^2. The eigenvalue equation (5.50) implies that ℓ is a non-negative integer. However, modes with $\ell = 0, 1$, are trivial [88, 66] so we focus on $\ell \geq 2$. The diffeomorphism that preserves the form of the ansatz in the scalar sector can be written as

$$\xi = e^{-i\omega t} \Delta^{-1/2} (c_{t0} X \partial_t + c_{S0} \Delta \mathbb{S}^i \partial_i) \,, \tag{5.52}$$

where c_{t0} and c_{S0} are arbitrary constants. This generates the diffeomorphic mode

$$h_{tt} = -2 c_{t0} i\omega X \Delta^{-1/2} \,, \qquad f_t^{(S)} = -c_{t0} k X \Delta^{-1/2} - c_{S0} i\omega \Delta^{1/2} \,, \tag{5.53}$$

$$H_T^{(S)} = -2 c_{S0} k \Delta^{1/2} \,, \qquad H_L^{(S)} = c_{S0} k \Delta^{1/2} \,, \tag{5.54}$$

$$a_t = c_{t0} i\omega \bar{\tilde{A}}_t \,, \quad a_\theta = c_{t0} k \bar{\tilde{A}}_t \,, \quad b_t = c_{t0} i\omega \bar{A}^0_t \,, \quad b_\theta = c_{t0} k \bar{A}^0_t \,, \tag{5.55}$$

$$s_1 = 0 \,, \quad s_2 = 0 \,, \tag{5.56}$$

In addition, we record the linearized field strengths since they are invariant under the $U(1)$ gauge transformations

$$\delta \tilde{F}_{rt} = e^{-i\omega t} a_t' \mathbb{S}, \qquad \delta \tilde{F}_{ri} = e^{-i\omega t} a_\theta' \mathbb{S}_i \,, \qquad \delta \tilde{F}_{ti} = e^{-i\omega t} (k a_t - i\omega a_\theta) \mathbb{S}_i \,, \tag{5.57}$$

$$\delta F^0_{rt} = e^{-i\omega t} b_t' \mathbb{S} \,, \qquad \delta F^0_{ri} = e^{-i\omega t} b_\theta' \mathbb{S}_i \,, \qquad \delta F^0_{ti} = e^{-i\omega t} (k b_t - i\omega b_\theta) \mathbb{S}_i \,. \tag{5.58}$$

It should be noted, however, that expressions (5.57) and (5.58) are not invariant under diffeomorphisms. We shall take this into account when constructing our gauge invariant variables.

As we saw in the vector modes, the equation of motion for the axion field played a crucial role: it is a constraint that forced the dynamics of all fluctuations to be trivial. However, for the scalar modes its role is a bit different. This equation gives a quadratic equation for $\delta\chi$ which reads

$$s_2'' + \left(\frac{\Delta'}{\Delta} + \frac{X'}{X} \right) s_2' + \left(\frac{\omega^2 \Delta}{X^2} - \frac{k^2}{X} + \frac{2(2m)^4 \Pi_s \Pi_c}{\Delta} + 4 \right) s_2 = 0 \,. \tag{5.59}$$

Note that there is no source from other fluctuations in the scalar modes, the equation for $\delta\chi$ nicely decouples. This gives us two possible routes: we can either set $\delta\chi = 0$ and solve for the remaining modes or consider non-trivial solutions to (5.59). In the following we will consider both cases.

Scalar modes with $\delta\chi = 0$

Let us study first the scalar modes with $\delta\chi = 0$. We again closely follow [88, 66] and write the fluctuation equations in terms of gauge invariant quantities. We obtain four gauge invariant variables, each representing the degrees of freedom of the metric, the scalar and each of the gauge fields. We denote the fields as Φ for the metric, S, for the scalar, and $\mathcal{A}$, $\mathcal{A}_0$ for the gauge fields. Their expressions in terms of the basic fields are

$$\begin{aligned}\Phi &= -\frac{iX}{k_S\omega\sqrt{\Delta}}f_t'^{(S)} + \frac{4\sqrt{\Delta}}{\Delta'}H_L^{(S)} + \left(\frac{X'}{2k_S^2\sqrt{\Delta}} + 2\frac{\sqrt{\Delta}}{\Delta'} - \frac{X\Delta'}{2k_S^2\Delta^{3/2}}\right)H_T^{(S)} \\ &+ \left(\frac{iX'}{k_S\omega\sqrt{\Delta}} - \frac{iX\Delta'}{2k_S\omega\Delta^{3/2}}\right), \end{aligned} \tag{5.60}$$

$$\mathcal{A} = -\frac{s_1}{2k_Sm} - \frac{H_L^{(S)}}{2k_Sm\sqrt{\Delta}} - \frac{H_T^{(S)}}{4k_Sm\sqrt{\Delta}} - \frac{h_{tt}\sqrt{\Delta}}{4k_SmX} + \frac{a_t'}{k_S}, \tag{5.61}$$

$$\begin{aligned}\mathcal{A}_0 &= \frac{\Delta^2}{k_S}b_t' + \frac{48m^4\Pi_c\Pi_s\Delta'}{k_S(\Pi_c^2-\Pi_s^2)}s_1 - \frac{16m^4\Pi_c\Pi_s\Delta'}{k_S(\Pi_c^2-\Pi_s^2)\sqrt{\Delta}}H_L^{(S)} - \frac{8m^4\Pi_c\Pi_s\sqrt{\Delta}\,\Delta'}{k_S(\Pi_c^2-\Pi_s^2)X}h_{tt}, \\ &+ \alpha_1(r)f_t + \alpha_2(r)H_T^{(S)} + \alpha_3(r)H_T'^{(S)} + \alpha_4(r)H_T''^{(S)}, \end{aligned} \tag{5.62}$$

$$S = \frac{3}{2}k_S\sqrt{X}\Delta'\,s_1 - \frac{3X^{3/2}\Delta'^2}{8k_S\Delta^{3/2}}H_T'^{(S)} + \frac{3X^{3/2}\Delta'^3}{16k_S\Delta^{5/2}}H_T^{(S)}, \tag{5.63}$$

where the expressions for the coefficients $\alpha_i(r)$ can be found in Appendix 5.A.2.

As above we redefine the fields, the radial variable and the frequency such that the equations of motion only depend on $\epsilon = \Pi_s/\Pi_c$ and $\hat{\omega} = \omega/(4\pi T)$, and the radial coordinate $y = 2m/r$. This can be achieved by the redefinitions (5.22) alongside with

$$\hat{\mathcal{A}} := \mathcal{A}\,, \qquad \hat{\mathcal{A}}_0 := (2m)^8\Pi_c^2\mathcal{A}_0\,, \qquad \hat{S} := (2m)^5\Pi_c^2 S\,, \qquad \hat{\Phi} := \frac{(2m)^2}{k}\Phi\,. \tag{5.64}$$

The equations of motion then read

$$\hat{\mathcal{A}}'' + c_{1\hat{\mathcal{A}}'}(y)\hat{\mathcal{A}}' + c_{1\mathcal{A}}(y)\hat{\mathcal{A}} + c_{1\hat{\Phi}}(y)\hat{\Phi} + c_{1\hat{\Phi}'}(y)\hat{\Phi}' + c_{1\hat{S}}(y)\hat{S} + c_{1\hat{\mathcal{A}}_0}(y)\hat{\mathcal{A}}_0 = 0\,, \tag{5.65}$$

$$\hat{\mathcal{A}}_0'' + c_{2\hat{\mathcal{A}}_0'}(y)\hat{\mathcal{A}}_0' + c_{2\hat{\mathcal{A}}_0}(y)\hat{\mathcal{A}}_0 + c_{2\hat{\Phi}}(y)\hat{\Phi} + c_{2\hat{\Phi}'}(y)\hat{\Phi}' + c_{2\hat{S}}(y)\hat{S} + c_{2\hat{\mathcal{A}}}(y)\hat{\mathcal{A}} = 0\,, \tag{5.66}$$

$$\hat{\Phi}'' + c_{3\hat{\Phi}'}(y)\hat{\Phi}' + c_{3\hat{\Phi}}(y)\hat{\Phi} + c_{3\hat{S}}(y)\hat{S} + c_{3\hat{\mathcal{A}}}(y)\hat{\mathcal{A}} + c_{3\hat{\mathcal{A}}_0}(y)\hat{\mathcal{A}}_0 = 0\,, \tag{5.67}$$

$$\begin{aligned}\hat{S}'' + c_{4\hat{S}'}(y)\hat{S}' + c_{4\hat{S}}(y)\hat{S} + c_{4\hat{\Phi}}(y)\hat{\Phi} + c_{4\hat{\Phi}'}(y)\hat{\Phi}' + c_{4\hat{\mathcal{A}}}(y)\hat{\mathcal{A}} + c_{4\hat{\mathcal{A}}'}(y)\hat{\mathcal{A}}' \\ + c_{4\hat{\mathcal{A}}_0'}(y)\hat{\mathcal{A}}_0' + c_{4\hat{\mathcal{A}}_0}(y)\hat{\mathcal{A}}_0 = 0 \end{aligned} \tag{5.68}$$

The coefficients are complicated functions of y, ℓ, ϵ and $\hat{\omega}$, and are given in Appendix 5.A.2. It is worth mentioning that the frequency dependence occurs only through $\hat{\omega}^2$, so the equations of motion we have obtained can be thought to be of second order in time, as in [88, 66]. Note that the scalar sector is characterized by 8 degrees of freedom, corresponding to the 8 integration constants that the general solution of (5.65)-(5.68) must have.

Rather surprisingly, the system (5.65)-(5.68) can be decoupled and its physical properties can be studied analytically. In order to do so, we begin by noting that we can decouple a fourth order equation

for $\hat{\mathcal{A}}$. To obtain this equation, we take a linear combination of (5.65)-(5.68) along with up to two derivatives of (5.65) and (5.67). Choosing the coefficients of this linear combination properly, we arrive at

$$\sum_{i=0}^{4} b_i(y)\frac{d^i}{dy^i}\hat{\mathcal{A}}(y) = 0 \,, \tag{5.69}$$

where

$$b_4 = 1 \,, \qquad b_3 = 4\left(\frac{1}{y}+\frac{1}{y-1}\right) \,, \tag{5.70}$$

$$b_2 = \frac{2((y-1)\ell(\ell+1)+y(7y-6))}{(y-1)^2y^2} + \frac{\hat{\omega}^2\left(2(y-1)\epsilon^2+2\right)}{(y-1)^2y} \,, \tag{5.71}$$

$$b_1 = \frac{2\left(2y+\ell^2+\ell\right)}{(y-1)^2y^2} + \frac{\hat{\omega}^2\left((4y-2)\epsilon^2+2\right)}{(y-1)^2y^2} \,, \tag{5.72}$$

$$b_0 = \frac{\hat{\omega}^4\left((y-1)\epsilon^2+1\right)^2}{(y-1)^4y^2} + \frac{\ell(\ell+1)\left(\ell^2+\ell-2\right)}{(y-1)^2y^4} \\ \frac{\hat{\omega}^2\left((y-1)^2\epsilon^2\left(y+2\left(\ell^2+\ell+1\right)\right)+2y\ell^2+2y\ell+3y-2\ell^2-2\ell-2\right)}{(y-1)^4y^3} \,. \tag{5.73}$$

The four independent solutions of this equation are of the form

$$\hat{\mathcal{A}} = y^{\Delta_{\hat{\mathcal{A}}}}(1-y)^{-i\hat{\omega}}{}_2F_1(\Delta_{\hat{\mathcal{A}}}-i\hat{\omega}(1+\epsilon)\,,\Delta_{\hat{\mathcal{A}}}-i\hat{\omega}(1-\epsilon),2\Delta_{\hat{\mathcal{A}}},y) \,, \tag{5.74}$$

where

$$\Delta_{\hat{\mathcal{A}}} = \{2+\ell,\ell,1-\ell,-1-\ell\} \,. \tag{5.75}$$

The associated QNM are then easily found to be

$$\hat{\omega}^{(0)}_{\hat{\mathcal{A}}} = -\frac{i}{1\pm\epsilon}(\ell+n) \,, \qquad \hat{\omega}^{(2)}_{\hat{\mathcal{A}}} = -\frac{i}{1\pm\epsilon}(\ell+2+n) \,, \qquad n=0,1,2,\dots \,. \tag{5.76}$$

The labels (0) and (2) in these quantities denote the offsets of 0 and 2 with respect to ℓ that these modes have, respectively. Expressions (5.76) are as well valid at $\epsilon = 0$. Once a solution of $\hat{\mathcal{A}}$ is given, the remaining profiles can be found by plugging the solution back into (5.65)-(5.68). While for general parameters this task can be cumbersome, it is straightforward once we set the frequencies to their QNM values (5.76), since then the hypergeometrics reduce to polynomials.

The remaining four degrees of freedom can be isolated by noting that setting $\hat{\mathcal{A}} = 0$ we obtain a consistent set of equations for $\hat{\Phi}$, $\hat{S}$, and $\hat{\mathcal{A}}_0$. To see this, we set $\hat{\mathcal{A}} = 0$, and eliminate $\hat{S}$ algebraically from (5.65). By doing so, (5.66) and (5.67) become two coupled second order equations for $\hat{\Phi}$ and $\hat{\mathcal{A}}_0$, while (5.68) yields a third order equation for $\hat{\Phi}$ which does not provide independent information. The second order equations can be in fact decoupled introducing the fields $V_\pm$ via

$$\hat{\Phi} = \alpha_0(y)(V_-+V_+) \,, \qquad \hat{\mathcal{A}}_0 = \alpha_-(y)V_- + \alpha_+(y)V_+ \,, \tag{5.77}$$

$$\alpha_0(y) = \frac{4\ell^2\left((y-1)\epsilon^2+1\right)^2+4\ell\left((y-1)\epsilon^2+1\right)^2+\left(\epsilon^2-1\right)\left((y-1)^2\epsilon^2-1\right)}{y\left((y-1)\epsilon^2+1\right)} \,, \tag{5.78}$$

$$\alpha_\pm(y) = \frac{c_\pm\left((y-1)\epsilon^3+\epsilon\right)+\left(\epsilon^2-1\right)^2}{y\epsilon} \,, \tag{5.79}$$

with

$$c_\pm = \frac{(\epsilon^2-1)}{\epsilon}(1\pm\epsilon(2\ell+1))\ . \tag{5.80}$$

The decoupled equations of motion for $V_\pm$ adopt the form

$$(y-1)V_\pm'' + V_\pm' + \left[y^{-2}\frac{P_\pm(y)}{Q_\pm(y)^2} + \frac{(1+(y-1)\epsilon^2)\hat{\omega}^2}{y(y-1)}\right]V_\pm = 0\ , \tag{5.81}$$

where

$$Q_\pm = (2\ell+1)\epsilon^2(y-1) + (2\ell+1) \pm \epsilon y\ , \tag{5.82}$$

and

$$\begin{aligned} P_\pm = {}& \epsilon^4(2\ell+1)^2(y-1)(\ell(\ell+1)(y-1)-y) \\ & \pm \epsilon^3(2\ell+1)y(2\ell(\ell+1)(1-y)-y+2) \\ & + \epsilon^2\left(\left(\ell^2+\ell+1\right)y^2 + 2\ell(\ell+1)(2\ell+1)^2 y - 2\ell(\ell+1)(2\ell+1)^2\right) \\ & \mp \epsilon(2\ell+1)y(2\ell(\ell+1)-y+2) + \ell(\ell+1)\left((2\ell+1)^2-4y\right) - y\ . \end{aligned} \tag{5.83}$$

The two second order decoupled equations (5.81) capture the four degrees of freedom that we were after. We observe that the fields $V_\pm$ can be mapped into one another by the "charge conjugation" transformation $\epsilon \to -\epsilon$. For $\epsilon = 0$, we can easily find the full solution of the system in terms of hypergeometric functions, and that the spectrum is given by

$$\hat{\omega} = -i(\ell+n)\ , \qquad \hat{\omega} = -i(\ell+2+n)\ . \tag{5.84}$$

On the other hand, for any $\epsilon \neq 0$, the presence of $Q_\pm$ in (5.81) modifies the structure of the singularities in the wave equation so it is no longer of the hypergeometric type. The ODE (5.81) has four regular singular points located at $y = 0, 1, \infty$ and the zero of $Q_\pm$; this makes the solutions Heun functions.[1] Because of this, we have not been able to solve it for general parameters, but we can show that for the frequencies

$$\hat{\omega}_\pm^{(0)} = -\frac{i}{1\pm\epsilon}(\ell+n)\ , \qquad \hat{\omega}_\pm^{(2)} = -\frac{i}{1\mp\epsilon}(\ell+2+n), \qquad n = 0,1,2,\ldots, \tag{5.85}$$

the solutions satisfying ingoing boundary conditions and regularity at infinity can be written as polynomials of order n and $n+2$, for $\hat{\omega}_\pm^{(0)}$ and $\hat{\omega}_\pm^{(2)}$ respectively. More concretely, the independent solutions take the form

$$V_\pm^{(0)} = y^{\ell+1}(1-y)^{-i\hat{\omega}_\pm^{(0)}}Q_\pm(y)^{-1}\sum_{k=0}^{n} a_{k,\pm}^{(0)} y^k\ , \tag{5.86}$$

$$V_\pm^{(2)} = y^{\ell+1}(1-y)^{-i\hat{\omega}_\pm^{(2)}}Q_\pm(y)^{-1}\sum_{k=0}^{n+2} a_{k,\pm}^{(2)} y^k\ . \tag{5.87}$$

The coefficients $a_{k,\pm}^{(0)}$, $a_{k,\pm}^{(2)}$ can be computed order by order in y.[2] The profiles for the original gauge invariant fields can be easily recovered by solving the algebraic relations (5.77), and (5.65) with $\hat{\mathcal{A}} = 0$.

[1] Because ℓ is an integer, the singularity at $y = 0$ is actually a resonant singularity, but it does not affect the conclusions we draw hereafter.

[2] The polynomials in (5.86) are formally known as a particular class of Heun polynomials. The specific form is not important, rather we want to highlight that the solution truncates.

While our analysis does not *a priori* guarantee that all solutions of (5.81) are of this form, we have checked this result numerically for a wide range of parameters. Moreover, continuity with the $\epsilon = 0$ case, and analogy with the Klein-Gordon field in the subRN background, suggests that this might be the full solution of the system. This completes our analysis of the scalar modes with $\delta\chi = 0$.

Scalar modes with $\delta\chi \neq 0$

Let us now consider modes with non-vanishing axion perturbation. As mentioned above, the equation of motion for the axion decouples and adopts the form (5.59), so it can be studied on its own. In particular, this means that the QNM frequencies obtained by solving this equation, let's call them $\omega_{\rm axion}$, are QNM of the full system, despite the fact the axion does enter as a source in Maxwell's equations for $\tilde{A}$ and A^0.[3]

The near boundary fall offs that follow from (5.59) are given by $s_2 \sim r^{\pm\delta_{\rm axion}}$ with

$$\delta_{\rm axion} = \sqrt{\ell^2 + \ell + 4}\,. \tag{5.88}$$

The QNM are then solutions that decay as $r^{-\delta_{\rm axion}}$ and satisfy ingoing boundary conditions. As before, we perform the redefinitions (5.22), obtaining

$$s_2'' + \frac{\left(y^2\epsilon^2 - 2y\left(\epsilon^2-1\right) + \epsilon^2 - 1\right)}{(y-1)y\left((y-1)\epsilon^2+1\right)}s_2' + \left(\frac{\delta_{\rm axion}(y-1)\epsilon^2 + \delta_{\rm axion} + 2y\epsilon}{y^2\left((y-1)^2\epsilon^2 + y - 1\right)} + \frac{\hat{\omega}^2\left((y-1)\epsilon^2+1\right)}{(y-1)^2 y}\right)s_2 = 0\,. \tag{5.89}$$

For $\epsilon = 0$, this equation can be solved in terms of hypergeometrics, and the resulting spectrum is once again quantized according to

$$\hat{\omega} = -i(\delta_{\rm axion} + n)\,. \tag{5.90}$$

By studying the structure of the singularities of (5.89), we conclude that it is not a hypergeometric equation for $\epsilon \neq 0$; it contains four regular singular points making the equation of the Heun type. While this prevents us from finding the analytic solution for general ϵ, we can obtain the spectrum numerically as in the previous cases. All frequencies are purely imaginary, but we find that the spectrum is not evenly spaced. We plot our results in Fig. 5.2. In order to check for evenly spaced frequencies, we define the quantity

$$\nu_n = i(\hat{\omega}_{n+4} - \hat{\omega}_{n+2}) - i(\hat{\omega}_{n+2} - \hat{\omega}_n)\,. \tag{5.91}$$

where n denotes the overtone of the mode, $n = 0$ being the lowest QNM. This quantity is identically zero for all ϵ, ℓ for the frequencies (5.76). This is not the case for solutions of (5.89) with $\epsilon \neq 0$, showing that the spectrum is not evenly spaced.

5.A Appendix

5.A.1 Equations of motion in the electric frame

In this appendix we give the equations of motion for the electric frame STU action (5.1). The Einstein equation is

$$R_{\mu\nu} - \frac{1}{2}g_{\mu\nu}R + \frac{1}{2}g_{\mu\nu}\left(\frac{3}{2}\partial_\alpha\eta\partial^\alpha\eta + \frac{3}{2}e^{2\eta}\partial_\alpha\chi\partial^\alpha\chi\right) - \frac{3}{2}\partial_\mu\eta\partial_\nu\eta - \frac{3}{2}e^{2\eta}\partial_\mu\chi\partial_\nu\chi$$

[3] Similarly to the cases discussed above, in order to obtain the profiles for the remaining fields for every $\omega_{\rm axion}$, we need to find the non-homogeneous solutions with these given sources.

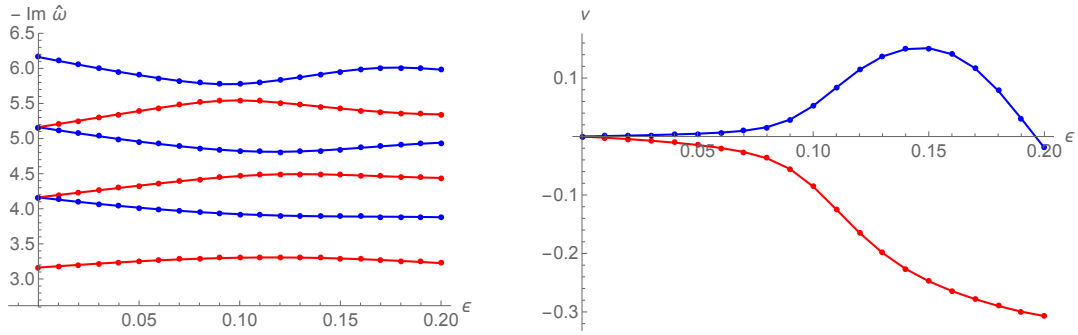

Figure 5.2: Six lowest QNM frequencies for the axion field for $\ell = 2$. All real parts are zero and the imaginary parts are negative. On the left panel we plot $-\mathrm{Im}\,\hat{\omega}$ as a function of ϵ. Modes we would expect to be evenly spaced for hypergeometric solutions are plotted in the same color. On the right panel we display our test for even spacing defined in (5.91) for $i = 0$ (red) and $i = 1$ (blue). This ceases to be zero for $\epsilon \neq 0$, so the modes are not evenly spaced.

$$
\begin{aligned}
&+\frac{1}{2}g_{\mu\nu}\left(\frac{1}{4}e^{-3\eta}(F^0)^2+\frac{3}{4}\frac{e^{-\eta}}{(4\chi^2+e^{-2\eta})}(\tilde{F}-\chi^2F^0)^2\right)\\
&-\frac{1}{2}e^{-3\eta}F^0_{\alpha\mu}F^{0,\alpha}_{\ \ \ \nu}-\frac{3}{2}\frac{e^{-\eta}}{(4\chi^2+e^{-2\eta})}(\tilde{F}-\chi^2F^0)_{\alpha\mu}(\tilde{F}-\chi^2F^0)^{\alpha}_{\ \ \nu}=0\,.
\end{aligned}
\tag{5.92}
$$

The equations for the dilaton and axion are

$$
\begin{aligned}
&\frac{1}{\sqrt{-g}}\partial_\mu(\sqrt{-g}\,\partial^\mu\eta)-e^{2\eta}\partial_\mu\chi\partial^\mu\chi+\frac{1}{4}e^{-3\eta}(F^0)^2+\frac{1}{4}e^{-\eta}\frac{4\chi^2-e^{-2\eta}}{(4\chi^2+e^{-2\eta})^2}(\tilde{F}-\chi^2F^0)^2\\
&-\frac{2\chi\,e^{-2\eta}}{(4\chi^2-e^{-2\eta})^2}(\tilde{F}-\chi^2F^0)\wedge(\tilde{F}-\chi^2F^0)=0\,,\\
&\frac{1}{\sqrt{-g}}\partial_\mu(\sqrt{-g}\,e^{2\eta}\partial^\mu\chi)+\frac{\chi\,e^{-\eta}}{(4\chi^2+e^{-2\eta})^2}(\tilde{F}-\chi^2F^0)_{\mu\nu}(2\tilde{F}+(2\chi^2+e^{-2\eta})F^0)^{\mu\nu}\\
&+\frac{4\chi^2-e^{-2\eta}}{(4\chi^2+e^{-2\eta})^2}(\tilde{F}-\chi^2F^0)\wedge(\tilde{F}-\chi^2F^0)+\frac{e^{-2\eta}}{4\chi^2+e^{-2\eta}}(\tilde{F}-\chi^2F^0)\wedge F^0=0\,,
\end{aligned}
\tag{5.93}
$$

and the Maxwell equations are

$$
\begin{aligned}
&\frac{3}{\sqrt{-g}}\partial_\mu\left(\sqrt{-g}\,\frac{e^{-\eta}}{(4\chi^2+e^{-2\eta})}(\tilde{F}-\chi^2F^0)^{\mu\nu}\right)\\
&+3\varepsilon^{\alpha\beta\mu\nu}\tilde{F}_{\alpha\beta}\partial_\mu\left(\frac{\chi}{4\chi^2+e^{-\eta}}\right)-\varepsilon^{\alpha\beta\mu\nu}F^0_{\alpha\beta}\partial_\mu\left(\frac{\chi(2\chi^2+e^{-2\eta})}{4\chi^2+e^{-\eta}}\right)=0\,,\\
&\frac{1}{\sqrt{-g}}\partial_\mu(\sqrt{-g}\,e^{-3\eta}F^{0,\mu\nu})+\frac{3}{\sqrt{-g}}\partial_\mu\left(\sqrt{-g}\,\frac{\chi^2e^{-\eta}}{(4\chi^2+e^{-2\eta})}(\tilde{F}-\chi^2F^0)^{\mu\nu}\right)\\
&+3\varepsilon^{\alpha\beta\mu\nu}\tilde{F}_{\alpha\beta}\partial_\mu\left(\frac{\chi(2\chi^2+e^{-2\eta})}{4\chi^2+e^{-\eta}}\right)-\varepsilon^{\alpha\beta\mu\nu}F^0_{\alpha\beta}\partial_\mu\left(\frac{\chi^3(\chi^2+e^{-2\eta})}{4\chi^2+e^{-\eta}}\right)=0\,,
\end{aligned}
\tag{5.94}
$$

In (5.93), the wedge notation is short hand for a contraction with an epsilon tensor

$$
\tilde{F}\wedge F^0\equiv\varepsilon^{\mu\nu\lambda\rho}\tilde{F}_{\mu\nu}F^0_{\lambda\rho}\,,
\tag{5.95}
$$

where $\varepsilon_{\mu\nu\lambda\rho}=\sqrt{-g}\epsilon_{\mu\nu\lambda\rho}$, and $\epsilon_{0123}=1$. Setting $\chi=0$ simplifies these equations to

$$
R_{\mu\nu}-\frac{1}{2}g_{\mu\nu}R-\frac{1}{2}g_{\mu\nu}\left(-\frac{3}{2}\partial_\mu\eta\partial^\mu\eta-\frac{1}{4}e^{-3\eta}(F^0)^2-\frac{3}{4}e^{\eta}(\tilde{F})^2\right)
$$

$$-\frac{3}{2}\partial_\mu\eta\partial_\nu\eta-\frac{1}{2}e^{-3\eta}F^0_{\alpha\mu}F^{0,\alpha}_{\ \ \ \nu}-\frac{3}{2}e^{\eta}\tilde{F}_{\alpha\mu}\tilde{F}^{\alpha}_{\ \ \nu}=0\ , \tag{5.96}$$

and

$$\begin{gathered}\frac{1}{\sqrt{-g}}\partial_\mu(\sqrt{-g}\partial^\mu\eta)+\frac{1}{4}(F^0)^2e^{-3\eta}-\frac{1}{4}\tilde{F}^2e^{\eta}=0\ ,\\ \partial_\mu(\sqrt{-g}\,e^{\eta}\tilde{F}^{\mu\nu})=0\ ,\qquad \partial_\mu(\sqrt{-g}\,e^{-3\eta}F^{0,\mu\nu})=0\ ,\end{gathered} \tag{5.97}$$

with the addition of the constraint

$$\tilde{F}\wedge\tilde{F}-e^{-2\eta}F^0\wedge\tilde{F}=0\ . \tag{5.98}$$

5.A.2 Details of the scalar mode calculation

The coefficients $\alpha_i(r)$ that participate in the definitions (5.60)-(5.63) are given by

$$\alpha_1 = \frac{4im^2(\Pi_c^2-\Pi_s^2)\omega\Delta^{3/2}X'}{k_S^2\Pi_c\Pi_sX}-\frac{4im(\Pi_c^2-\Pi_s^2)\omega\Delta^{5/2}}{k_S^2\Pi_c\Pi_sX\Delta'}- \tag{5.99}$$

$$-\ \frac{4im^2\omega(4m^2\Pi_c^2\Pi_s^2-(\Pi_c^2-\Pi_s^2)^2X)\sqrt{\Delta}\,\Delta'}{k_S^2\Pi_c\Pi_s(\Pi_c^2-\Pi_s^2)X},$$

$$\alpha_2 = \frac{m^2(\Pi_c^2-\Pi_s^2)\sqrt{\Delta}(X+2\omega^2\Delta)X'}{k_S^3\Pi_c\Pi_sX}-\frac{2m^2(\Pi_c^2-\Pi_s^2)\omega^2\Delta^{5/2}}{k_S^3\Pi_c\Pi_sX\Delta'}-m^2\Delta'\times \tag{5.100}$$

$$\times\ \frac{7(\Pi_c^2-\Pi_s^2)^2X^2-16m^2\Pi_c^2\Pi_s^2\omega^2\Delta+2X(8k_S^2m^2\Pi_c^2\Pi_s^2+(\Pi_c^2-\Pi_s^2)^2(2\omega^2\Delta+X'^2))}{2k_S^3\Pi_c\Pi_s(\Pi_c^2-\Pi_s^2)X\sqrt{\Delta}}+$$

$$+\ \frac{m^2(8m^2\Pi_c^2\Pi_s^2-9(\Pi_c^2-\Pi_s^2)^2X)X'\Delta'^2}{2k_S^3\Pi_c\Pi_s(\Pi_c^2-\Pi_s^2)\Delta^{3/2}}+\frac{7m^2X(4m^2\Pi_c^2\Pi_s^2-(\Pi_c^2-\Pi_s^2)X)\Delta'^3}{2k_S^3\Pi_c\Pi_s(\Pi_c^2-\Pi_s^2)\Delta^{5/2}}, \tag{5.101}$$

$$\alpha_3 = \frac{2m^2(\Pi_c^2-\Pi_s^2)\sqrt{\Delta}(3X+X'^2)}{k_S^3\Pi_c\Pi_s}-\frac{2m^2(\Pi_c^2-\Pi_s^2)\Delta^{3/2}X'}{k_S^3\Pi_c\Pi_s\Delta'}+ \tag{5.102}$$

$$+\ \frac{8m^2(m^2\Pi_c^2\Pi_s^2-(\Pi_c^2-\Pi_s^2)^2X)X'\Delta'}{k_S^3\Pi_c\Pi_s(\Pi_c^2-\Pi_s^2)\sqrt{\Delta}}-\frac{6m^2X(4m^2\Pi_c^2\Pi_s^2-(\Pi_c^2-\Pi_s^2)^2X)\Delta'^2}{k_S^3\Pi_c\Pi_s(\Pi_c^2-\Pi_s^2)\Delta^{3/2}},$$

$$\alpha_4 = \frac{2m^2(\Pi_c^2-\Pi_s^2)X\sqrt{\Delta}X'}{k_S^3\Pi_c\Pi_s}-\frac{2m^2(\Pi_c^2-\Pi_s^2)X\Delta^{3/2}}{k_S^3\Pi_c\Pi_s\Delta'}+ \tag{5.103}$$

$$+\ \frac{2m^2X(4m^2\Pi_c^2\Pi_s^2-(\Pi_c^2-\Pi_s^2)^2X)\Delta'}{k_S^3\Pi_c\Pi_s(\Pi_c^2-\Pi_s^2)\sqrt{\Delta}}.$$

The coefficients that appear in the equations of motion for the linearized perturbations in the scalar sector (5.65)-(5.68) are

$$c_{1\hat{\mathcal{A}}'} = 1/(-1+y), \tag{5.104}$$

$$c_{1\mathcal{A}} = \frac{4\hat{\omega}^2\left((y-1)\epsilon^2+1\right)}{(y-1)^2 y} + \frac{k_S^2}{(y-1)y^2} - \frac{3\left(\epsilon^2-1\right)^2}{y^2\left(8k_S^2\left((y-1)\epsilon^2+1\right)^2+\left(\epsilon^2-1\right)\left((y-1)(2y-5)\epsilon^2+3y-5\right)\right)}, \tag{5.105}$$

$$c_{1\hat{\Phi}} = -\frac{\left(\epsilon^2-1\right)k_S^3\left((y-1)\epsilon^2+1\right)}{2(y-1)y\left(8k_S^2\left((y-1)\epsilon^2+1\right)^2+\left(\epsilon^2-1\right)\left((y-1)(2y-5)\epsilon^2+3y-5\right)\right)}, \tag{5.106}$$

$$c_{1\hat{\Phi}'} = \frac{\left(\epsilon^2-1\right)^2 k_S}{4\left(8k_S^2\left((y-1)\epsilon^2+1\right)^2+\left(\epsilon^2-1\right)\left((y-1)(2y-5)\epsilon^2+3y-5\right)\right)}, \tag{5.107}$$

$$c_{1\hat{S}} = \left[4k_S^2\left((y-1)\epsilon^2+1\right)^2-\left(1-\epsilon^2\right)\left((y-1)^2\epsilon^2-1\right)\right]\times\left[24(1-y)^{3/2}y\left(\epsilon^2-1\right)\right.$$
$$\times\left.8k_S^2\left((y-1)\epsilon^2+1\right)^2+\left(\epsilon^2-1\right)\left(2y^2\epsilon^2-7y\epsilon^2+3y+5\epsilon^2-5\right)\right]^{-1},$$

$$c_{1\hat{\mathcal{A}}_0} = -\epsilon\left(\epsilon^2-1\right)^2 \times\left[256\left((y-1)\epsilon^2+1\right)^2\left(8k_S^2\left((y-1)\epsilon^2+1\right)^2+\left(\epsilon^2-1\right)\left((y-1)(2y-5)\epsilon^2+3y-5\right)\right)\right]^{-1}, \tag{5.108}$$

$$c_{2\hat{\mathcal{A}}_0'} = \frac{(y-2)(y-1)\epsilon^2+3y-2}{(y-1)y\left((y-1)\epsilon^2+1\right)}, \tag{5.109}$$

$$c_{2\hat{\mathcal{A}}_0} = \frac{k_S^2}{(y-1)y^2}+\frac{4\hat{\omega}^2\left((y-1)\epsilon^2+1\right)}{(y-1)^2 y} - \frac{\epsilon^2\left(\epsilon^2-1\right)^2}{\left((y-1)\epsilon^2+1\right)^2\left(8k_S^2\left((y-1)\epsilon^2+1\right)^2+\left(\epsilon^2-1\right)\left((y-1)(2y-5)\epsilon^2+3y-5\right)\right)}, \tag{5.110}$$

$$c_{2\hat{\Phi}} = -\frac{128\epsilon\left(\epsilon^2-1\right)k_S^3\left((y-1)\epsilon^2+1\right)}{(y-1)y\left(8k_S^2\left((y-1)\epsilon^2+1\right)^2+\left(\epsilon^2-1\right)\left((y-1)(2y-5)\epsilon^2+3y-5\right)\right)}, \tag{5.111}$$

$$c_{2\hat{\Phi}'} = \frac{64\epsilon\left(\epsilon^2-1\right)^2 k_S}{8k_S^2\left((y-1)\epsilon^2+1\right)^2+\left(\epsilon^2-1\right)\left(2y^2\epsilon^2-7y\epsilon^2+3y+5\epsilon^2-5\right)}, \tag{5.112}$$

$$c_{2\hat{S}} = \left[-32\epsilon\left(4k_S^2\left((y-1)\epsilon^2+1\right)^2+\left(\epsilon^2-1\right)\left((y-3)(y-1)\epsilon^2+2y-3\right)\right)\right] \times\left[(1-y)^{3/2}y\left(\epsilon^2-1\right)\right.$$
$$\times\left.8k_S^2\left((y-1)\epsilon^2+1\right)^2+\left(\epsilon^2-1\right)\left((y-1)(2y-5)\epsilon^2+3y-5\right)\right]^{-1}, \tag{5.113}$$

$$c_{2\hat{\mathcal{A}}_0} = -\frac{768\epsilon\left(\epsilon^2-1\right)^2}{y^2\left(8k_S^2\left((y-1)\epsilon^2+1\right)^2+\left(\epsilon^2-1\right)\left(2y^2\epsilon^2-7y\epsilon^2+3y+5\epsilon^2-5\right)\right)}, \tag{5.114}$$

$$
\begin{aligned}
c_{3\hat{\Phi}'} &= \frac{(y-2)(y-1)\epsilon^2+3y-2}{(y-1)y\left((y-1)\epsilon^2+1\right)} \qquad (5.115)\\
&- \frac{\left(\epsilon^2-1\right)\left(3(y-1)(2y-1)\epsilon^4+2(y(y+3)-3)\epsilon^2+3(y+1)\right)}{y\left((y-1)\epsilon^2+1\right)\left(8k_S^2\left((y-1)\epsilon^2+1\right)^2+\left(\epsilon^2-1\right)\left((y-1)(2y-5)\epsilon^2+3y-5\right)\right)},\\
c_{3\hat{\Phi}} &= \frac{\epsilon^2\left(7\epsilon^2+1\right)}{4(y-1)\left(y\epsilon^2-\epsilon^2+1\right)^2}-\frac{(\epsilon-1)(\epsilon+1)\left(25\epsilon^2+3\right)}{8(y-1)y\left(y\epsilon^2-\epsilon^2+1\right)^2} \qquad (5.116)\\
&- \frac{k_S^2}{(y-1)y^2}+\frac{4\hat{\omega}^2\left((y-1)\epsilon^2+1\right)}{(y-1)^2y}+\frac{\left(\epsilon^2-1\right)\left((y(2y-7)-6)\epsilon^2+3(y+2)\right)}{8(y-1)\left((y-1)y\epsilon^2+y\right)^2}\\
&- \frac{\left(\epsilon^2-1\right)\left((y-1)(2y-5)\epsilon^2+3y-5\right)\left(3(y-1)(2y-1)\epsilon^4+2(y(y+3)-3)\epsilon^2+3(y+1)\right)}{4(y-1)\left((y-1)y\epsilon^2+y\right)^2\left(8k_S^2\left((y-1)\epsilon^2+1\right)^2+\left(\epsilon^2-1\right)\left((y-1)(2y-5)\epsilon^2+3y-5\right)\right)}
\end{aligned}
$$

$$
\begin{aligned}
c_{3\hat{S}} &= \left[(y-1)(2(y-3)(y-1)y-3)\epsilon^4+(y(y(3y-5)+3)-3)\epsilon^2+y+1 \qquad (5.117)\right.\\
&- \left.4k_S^2\left((y-1)\epsilon^2+1\right)^2\left((y-1)(2y-1)\epsilon^2-y-1\right)-(y-1)^3(2y-1)\epsilon^6\right]\\
&\times \left[2(1-y)^{3/2}y^2\left(\epsilon^2-1\right)k_S\left((y-1)\epsilon^2+1\right)\right.\\
&\times \left.8k_S^2\left((y-1)\epsilon^2+1\right)^2+\left(\epsilon^2-1\right)\left((y-1)(2y-5)\epsilon^2+3y-5\right)\right]^{-1},\\
c_{3\hat{\mathcal{A}}} &= -\frac{48k_S\left((y-1)\epsilon^2+1\right)}{(y-1)y^3\left(\epsilon^2-1\right)} \qquad (5.118)\\
&+ \frac{12\left(3\left(y\left(y^2+y-4\right)+2\right)\epsilon^2+(y-1)^3(2y+3)\epsilon^4+5y-3\right)}{(y-1)y^3k_S\left((y-1)^2(2y-5)\epsilon^4+5(y-2)(y-1)\epsilon^2+3y-5\right)}\\
&+ \frac{96k_S\left((y-1)\epsilon^2+1\right)\left(3(y-1)(2y-1)\epsilon^4+2(y(y+3)-3)\epsilon^2+3(y+1)\right)}{y^3\left((y-1)(2y-5)\epsilon^2+3y-5\right)\left(8k_S^2\left((y-1)\epsilon^2+1\right)^2+\left(\epsilon^2-1\right)\left((y-1)(2y-5)\epsilon^2+3y-5\right)\right)}\\
c_{3\hat{\mathcal{A}}_0} &= -\frac{\epsilon\left(\epsilon^2-1\right)^3k_S}{16(y-1)y\left((y-1)\epsilon^2+1\right)^5} \qquad (5.119)\\
&- \frac{y^3\epsilon^9k_S}{16(y-1)\left(\epsilon^2-1\right)\left((y-1)\epsilon^2+1\right)^5}+\frac{\epsilon^3k_S\left((y(2y-3)+2)\epsilon^4+(3y-4)\epsilon^2+2\right)}{8(y-1)\left((y-1)\epsilon^2+1\right)^5}\\
&+ \frac{\epsilon\left(-6y^2+(y-1)^2(y(2y+5)-13)\epsilon^4-(y-1)((y-26)y+26)\epsilon^2+21y-13\right)}{64(y-1)yk_S\left((y-1)\epsilon^2+1\right)^3\left((y-1)(2y-5)\epsilon^2+3y-5\right)}\\
&- \left[\epsilon k_S\left(3(y-1)(2y-1)\epsilon^4+2(y(y+3)-3)\epsilon^2+3(y+1)\right)\right]\\
&\times \left[8y\left((y-1)\epsilon^2+1\right)\left((y-1)(2y-5)\epsilon^2+3y-5\right)\right.\\
&\times \left.8k_S^2\left((y-1)\epsilon^2+1\right)^2+\left(\epsilon^2-1\right)\left((y-1)(2y-5)\epsilon^2+3y-5\right)\right]^{-1},
\end{aligned}
$$

$$
\begin{aligned}
c_{4\hat{S}'} &= \frac{2}{y} \qquad (5.120)\\
&- \frac{3(y-1)\left(\epsilon^2-1\right)^3}{y\left((y-1)\epsilon^2+1\right)\left(8k_S^2\left((y-1)\epsilon^2+1\right)^2+\left(\epsilon^2-1\right)\left((y-1)(2y-5)\epsilon^2+3y-5\right)\right)},\\
c_{4\hat{S}} &= -\frac{\left(\epsilon^2-1\right)\left((y-1)(2y-5)\epsilon^2+3y-5\right)}{4(y-1)\left((y-1)y\epsilon^2+y\right)^2} \qquad (5.121)\\
&+ \frac{(y-1)^2(y(y+4)-10)\epsilon^4+2y(y+4)(3y-5)\epsilon^2+y(16-5y)+20\epsilon^2-10}{4(y-1)^2y^2\left((y-1)\epsilon^2+1\right)^2}\\
&+ \frac{k_S^2}{(y-1)y^2}+\frac{4\hat{\omega}^2\left((y-1)\epsilon^2+1\right)}{(y-1)^2y}\\
&- \frac{3(y-1)\left(\epsilon^2-1\right)^4\left(3(y-1)^2\epsilon^4+(y(y+6)-6)\epsilon^2+3\right)}{y^2\left((y-1)\epsilon^2+1\right)^2\left(8k_S^2\left((y-1)\epsilon^2+1\right)^2+\left(\epsilon^2-1\right)\left((y-1)(2y-5)\epsilon^2+3y-5\right)\right)^2}\\
&- \frac{3\left(\epsilon^2-1\right)^3\left((y-1)(2y-1)\epsilon^2-y-1\right)}{4\left((y-1)y\epsilon^2+y\right)^2\left(8k_S^2\left((y-1)\epsilon^2+1\right)^2+\left(\epsilon^2-1\right)\left((y-1)(2y-5)\epsilon^2+3y-5\right)\right)},\\
c_{4\hat{\Phi}} &= 6\left(\epsilon^2-1\right)^3k_S \qquad (5.122)\\
&\times \left[8y\hat{\omega}^2\left(\epsilon^2-1\right)\left(8k_S^2\left((y-1)\epsilon^2+1\right)^2+\left(\epsilon^2-1\right)\left((y-1)(2y-5)\epsilon^2+3y-5\right)\right)\right.\\
&- \frac{k_S^2}{(y-1)\epsilon^2+1}\\
&\times \left(\epsilon^2-1\right)\left((y-1)^2\left(8y^2-42y+37\right)\epsilon^4+3y^2+2(y-1)(y(5y-37)+37)\epsilon^2-32y+37\right)\\
&+ \left.8k_S^2\left((y-1)\epsilon^2+1\right)^2\left((y-1)(4y-5)\epsilon^2+y-5\right)\right)\Big]\\
&\times \left[\sqrt{1-y}y^2\left(8k_S^2\left((y-1)\epsilon^2+1\right)^2+\left(\epsilon^2-1\right)\left((y-1)(2y-5)\epsilon^2+3y-5\right)\right)^2\right]^{-1},\\
c_{4\hat{\Phi}'} &= -6\sqrt{1-y}\left(\epsilon^2-1\right)^4k_S \qquad (5.123)\\
&\times \left[\left(\epsilon^2-1\right)\left((y-1)^3(2y-11)\epsilon^4+(y-1)((y-22)y+22)\epsilon^2-9y+11\right)\right.\\
&+ \left.8k_S^2\left((y-1)\epsilon^2+1\right)^2\left((y-1)^2\epsilon^2-1\right)\right]\\
&\times \left[y\left((y-1)\epsilon^2+1\right)^2\left(8k_S^2\left((y-1)\epsilon^2+1\right)^2+\left(\epsilon^2-1\right)\left((y-1)(2y-5)\epsilon^2+3y-5\right)\right)^2\right]^{-1},\\
c_{4\hat{\mathcal{A}}} &= 24\left(\epsilon^2-1\right) \qquad (5.124)\\
&\times \left[-3(y-1)\left(\epsilon^2-1\right)^4\left((y-1)^3(2y-11)\epsilon^4+(y-1)((y-22)y+22)\epsilon^2-9y+11\right)\right.\\
&+ 2\left(\epsilon^2-1\right)^2\left((y-1)\epsilon^2+1\right)^2\\
&\times k_S^2\left(27y^2+(y-1)^2(4(y-11)y+67)\epsilon^4+2(y-1)(y(18y-67)+67)\epsilon^2-90y+67\right)\\
&+ \left.128k_S^6\left((y-1)\epsilon^2+1\right)^6++64\left(\epsilon^2-1\right)k_S^4\left((y-1)\epsilon^2+1\right)^4\left((y-4)(y-1)\epsilon^2+3y-4\right)\right)\Big]\\
&\times \left[\sqrt{1-y}y^3\left((y-1)\epsilon^2+1\right)^2\left(8k_S^2\left((y-1)\epsilon^2+1\right)^2+\left(\epsilon^2-1\right)\left((y-1)(2y-5)\epsilon^2+3y-5\right)\right)^2\right]^{-1},
\end{aligned}
$$

$$c_{4\hat{\mathcal{A}}'} = -\frac{72\sqrt{1-y}\left(\epsilon^2-1\right)^2\left(8k_S^2\left((y-1)\epsilon^2+1\right)^2+\left(\epsilon^2-1\right)\left((y-1)(2y-3)\epsilon^2+y-3\right)\right)}{y^2\left((y-1)\epsilon^2+1\right)\left(8k_S^2\left((y-1)\epsilon^2+1\right)^2+\left(\epsilon^2-1\right)\left((y-1)(2y-5)\epsilon^2+3y-5\right)\right)}, \tag{5.125}$$

$$c_{4\hat{\mathcal{A}}_0'} = -\frac{3\sqrt{1-y}\epsilon\left(\epsilon^2-1\right)^2\left(8k_S^2\left((y-1)\epsilon^2+1\right)^2+\left(\epsilon^2-1\right)\left(2y^2\epsilon^2-5y\epsilon^2+y+3\epsilon^2-3\right)\right)}{32\left((y-1)\epsilon^2+1\right)^3\left(8k_S^2\left((y-1)\epsilon^2+1\right)^2+\left(\epsilon^2-1\right)\left(2y^2\epsilon^2-7y\epsilon^2+3y+5\epsilon^2-5\right)\right)}, \tag{5.126}$$

$$\begin{aligned} c_{4\hat{\mathcal{A}}_0} &= -3\epsilon\left(\epsilon^2-1\right) \\ &\times \Big[(y-1)\left(\epsilon^2-1\right)^4\left((y-1)^3(2y-11)\epsilon^4+(y-1)((y-22)y+22)\epsilon^2-9y+11\right) \\ &+ 2\left(\epsilon^2-1\right)^2\left((y-1)\epsilon^2+1\right)^2 \\ &\times (3y^2+(y-1)^2(4(y-3)y+11)\epsilon^4+2(y-1)(y(2y-11)+11)\epsilon^2-10y+11)k_S^2 \\ &+ 64(y-2)\left(\epsilon^2-1\right)k_S^4\left((y-1)\epsilon^2+1\right)^5 \\ &+ 128k_S^6\left((y-1)\epsilon^2+1\right)^6\Big] \\ &\times \left[\sqrt{4-4y}y\left(2(y-1)\epsilon^2+2\right)^4\left(8k_S^2\left((y-1)\epsilon^2+1\right)^2+\left(\epsilon^2-1\right)\left((y-1)(2y-5)\epsilon^2+3y-5\right)\right)^2\right]^{-1} \end{aligned} \tag{5.127}$$

Part III

Non-supersymmetric Metastable Vacua

"How many realities do actually exist? Who cares. This is the one you are in, so you better regard it as the one and only."

— Lia Maldonado-Parada

Chapter 6

Supersymmetry Breaking with Antibranes

We have already discussed in part I how important supersymmetry breaking mechanisms are in string theory and how this fits with reality. In part II, our concern was on non-supersymmetric black holes holography. Now we focus on supersymmetry breaking in cosmological settings with antibranes. As black holes and cosmological settings share common features in this regard, we start this introduction by first recalling some key aspects of the already discussed black holes, to then move on to cosmology – the topic this part of the thesis is mostly related with.

The construction of non-supersymmetric black holes in string theory is a valuable step for extending the knowledge we have about their supersymmetric counterparts. As we already discussed in chapter 2, it is desirable to explain the entropy of these black holes through a microscopic system of bounded D-branes [10] or a dual field theory description [57]. Explicit construction of non-supersymmetric solutions gives important insight about these black holes. For example, non-supersymmetric microstate geometries[1] are crucial for testing the fuzzball proposal[2] [102, 103, 104, 105, 106, 107] beyond extremality. Various supersymmetric microstate geometries have been successfully constructed already [108, 109, 110, 111, 112, 113, 114]. The presence of supersymmetry makes the equation of motion linear, thus easier to solve [115, 116, 117, 118, 119, 120]. When there is no supersymmetry present, the non-linearity of the equations makes the solving process a highly challenging task.

The construction of non-supersymmetric microstate geometries is so technically challenging that for a long time only two classes of solutions were known: the JMaRT [121, 122, 123] and the running-Bolt [124, 125]. Eventually, generalization procedures/systematic constructions of non-supersymmetric microstate geometries were developed [126, 127, 128, 129, 130, 131]. For our purposes, we would like to focus on [127]. Therein, the authors proposed a way of constructing non-supersymmetric microstate geometries using supertubes. The supertubes break supersymmetry since they carry antibrane charge

[1] Microstate geometries are horizonless and nonsingular solutions of supergravity that asymptotically approach the black hole geometry but they differ at horizon-scale.

[2] The fuzzball proposal states that a black hole is an ensemble of horizonless and non-singular configurations called "fuzzballs." Each of these configurations carries the same conserved charges as the black hole. In the supergravity context, a microstate geometry can be seen as a fuzzball. The importance of this proposal is that it has the potential to solve many of the puzzles related to black holes, in particular, the information loss paradox and the statistical origin of the black hole entropy.

(we elaborate further on antibranes in the next subsection). Breaking supersymmetry with antibrane charge is a general feature of string theory, and it also used for the construction of de Sitter vacua within its framework.

Supersymmetry breaking antibranes were proposed by Kachru-Pearson-Verlinde (KPV) [132] and used by Kachru-Kallosh-Linde-Trivedi (KKLT) [133] to construct four-dimensional de Sitter spacetime using ten-dimensional string theory – a long-standing string cosmology problem. The latter is of great phenomenological importance, as our universe at large scales is approximately de Sitter spacetime due to the presence of a small and positive cosmological constant [134, 135]. If string theory intends to be a successful quantum theory of gravity, it should be able to describe de Sitter spacetime. De Sitter spacetime is not a supersymmetric solution; thus a supersymmetry breaking process in string theory for this purpose is also needed.

When working with supergravity in ten dimensions, building four-dimensional de Sitter is hard to achieve. As a start, we would like to work with warped compactifications, because of their role in stabilizing part of the moduli. However, following the no-go theorems [136, 137], warped compactifications to a four-dimensional Minkowski or de Sitter spacetime are not immediately possible. We need to add sources or singularities to the compact internal space, as done for example in [138]. After adding these sources/singularities and avoiding the no-go theorems, moduli might remain unfixed. Moreover, even if we manage to fix the moduli, we still need to introduce a supersymmetry breaking mechanism that does not spoil any of the previous steps.

The KKLT model has the historical importance of being the first one that managed to complete all steps above: it fixes the full moduli with warped compactifications *and* non-perturbative quantum corrections and obtains de Sitter vacua by using supersymmetry breaking anti-D3 branes. Later it was found that these vacua were not unique to anti-D3 branes; for example, turning on the gauge fields living within D7 branes gives a contribution to the four-dimensional potential that allows for de Sitter vacua [139]. However, our interest in anti-branes is founded on its ubiquitous nature in string theory. They are used in inflationary models [140, 141, 142], in dynamical supersymmetry breaking [143, 132, 144, 145, 146], and as said before, in non-extremal black holes microstate geometries [127, 126]. Thus, it is natural to dig deeper into its physics and to start asking questions about the details of how these antibranes are breaking supersymmetry.

Metastable States, Probe Level and Back-reaction

To understand better the role of anti-branes in the construction of de Sitter vacua, we review the KKLT model. We divide it into two general steps. First comes the warped compactification from ten-dimensional supergravity to an effective four-dimensional theory. After the full moduli have been fixed, we are left with supersymmetric anti-de Sitter vacua. This part of the construction is not the one that we will study further in this thesis. The details are nicely explained in the original publication [133]. Our main concern is the second step, the addition of supersymmetry breaking antibranes. Their addition can uplift the energy of the vacua to de Sitter spacetime.

Let us now discuss the details of these antibranes addition in the KPV calculation. In ten dimen-

sions, topological cycles can support non-zero fluxes. We add now *probe/non-backreacting* branes with opposite charge relative to these fluxes (hence "antibranes"), thus breaking supersymmetry. As the ground state is supersymmetric, we expect this anti-branes set-up to decay eventually. This decaying happens through brane polarization and further brane-flux annihilation. We review both effects in chapter 7, but we give here a flavor:

1. The antibranes polarize into an NS5 brane that contains in its worldvolume the antibranes charge.

2. Branes materialize out from the background flux and annihilate the antibrane charge in the NS5.

3. After all the anti-brane charge has been annihilated, the system is back to a supersymmetric state.

However, there is a bonus step between 1 and 2. If the antibrane charge is small enough in comparison to the background flux charge, there exists a metastable state where the NS5 carries anti-brane charge. This state breaks supersymmetry and gives an extra contribution to the four-dimensional potential, uplifting from anti- to de Sitter vacua.

The existence of the above mentioned metastable state has been debated for years. One known issue is the presence of a divergence in the energy density of a three-form flux. This divergence does not show up at the probe level of [132] but appears when back-reaction is approximatively taken into account [147, 148]. Divergences in the energy density are normal if they are linked to the presence of a source. In this case, one might like to attach this divergence to the source of antibrane charge. However, the behavior of the matter fields and geometry close to the divergence does not seem to indicate that. Lacking a clear interpretation, we name this divergence "unphysical." In this thesis, we focus our efforts on its study. Nevertheless, there are other related issues to the metastable state of antibranes that are open[3].

The unphysical divergence might be an artifact of the approximation scheme. A fully back-reacted solution would be welcome and might settle down the whole discussion. However, an explicit solution to the supergravity equations of motion including the back-reaction of antibranes is nowhere in sight. The absence of supersymmetry makes the solving process very challenging. Thus, we are in need of novel approaches that can extract relevant information from the equations of motion without the need to explicitly solve them. In this thesis, we make progress in this direction.

Before we go on to explain our work, a comment is in order. It might be that the divergence is evidence that supergravity is failing to capture the relevant physics. In this case, a resolution might be found in full string theory. The last was argued for a single anti-brane in [155, 154]. Even so, it is desirable to have a physical interpretation of the singularity in the supergravity picture – for example, in the lines of [156, 157, 158, 159]. A supergravity interpretation should give insights about how the divergence is resolved in string theory. If we lack this interpretation, the string theory resolution of

[3]For example: tachyonic repelling behavior of the anti-D3 branes that might jeopardize the polarized 5-brane state [149, 150], anti-D6 branes non-polarization behavior that (as a T-dual system of smeared anti-D3 branes) suggest the same behavior in the anti-D3 case [151], flux-clumping around the anti-D3 that lowers the effective potential barrier (thus eliminating the metastable state possibility) [152, 153], among others that are debated in [154].

the divergence is unclear. Moreover, there might be no resolution at all, indicating that the antibranes metastable state is unphysical. Thus, in order to clarify these uncertainties, a more in-depth supergravity study of the divergence is required.

Necessity is the Mother of Invention: the Smarr Way

Fortunately, we will not need the full solution to make progress. The antibrane sourced configuration allows for the construction of a Smarr law. A consistent Smarr law imposes constraints on the IR and UV values for the fluxes and geometry. When satisfied, these constraints are equivalent to a configuration with a divergence now attached to the antibrane source [2, 3]. Let us point out that not all the (in this thesis) studied antibrane sourced configurations satisfy these constraints. This approach is our contribution to the metastable debate, and we use it for ten- and eleven-dimensional antibranes settings in chapter 8 and 9.

Effectively, our method discloses the boundary conditions necessary for a supergravity solution that will result in a well-behaved metastable state. However, having the boundary conditions does not mean that the solution exists. The existence of the solution can only be demonstrated by constructing it explicitly or by obtaining sufficient evidence via numerical methods[4]. A proof for the existence of this solution is beyond the scope of this thesis. However, it might be a natural step to take.

Eleven-dimensional Supergravity

The mentioned KKLT mechanism and most of the previous discussion are in the frame of ten-dimensional supergravity. We also scrutinize an eleven-dimensional supergravity configuration, where we can construct analogous systems with probe anti-M-branes. At the probe level, these also break supersymmetry, polarize and reach a metastable state [161]. When backreaction is approximately included, they develop an unphysical singularity in the flux density [162]. Again, the full eleven-dimensional solution with antibrane sources is beyond our technical reach. Fortunately, we can apply the same approach again as in the ten-dimensional case and extract boundary conditions for well-behaved configurations.

Just like in the ten-dimensional case, our approach will show us under which boundary conditions the metastable state is physical. This calculation is interesting because it shows that a resolution of the unphysical divergence via a proper choice of boundary conditions is possible beyond the ten-dimensional setting[5]. It might be that these unphysical divergences due to antibrane sources in string theory are resolved just by setting proper boundary conditions. In particular, from here we can already scrutinize the construction of non-supersymmetric microstate geometries via anti-brane charged supertubes [126, 127]. Let us recall that having the boundary conditions does not prove the existence of the solution. For the last, we need to solve the full equations of motion or collect enough numerical

[4] An interesting investigation where a numerical solution for a stack of (smeared) anti-M2 branes at finite temperature has appeared not long ago [160]. Therein, the authors address the singularity in the energy density of the metastable state and a possible topological phase transition. These two behaviors agree qualitatively with [3]. We check [3] in great detail in chapter 9.

[5] Another advantage of the case of supergravity in eleven dimensions is that there is less field content (there is only one flux) making the calculation and results cleaner.

evidence.

Outline

This part of the thesis consists of three more chapters. In chapter 7 we review the brane polarization (Myers effect) [163] and brane-flux annihilation (Kachru-Pearson-Verlinde or KPV mechanism) [132]. These two effects have the leading role in the construction of the metastable non-supersymmetric state that we will scrutinize. Chapter 7 focus entirely on the ten-dimensional perspective, but the eleven-dimensional version is entirely analogous (see [161]).

In chapter 8 we introduce our work. Here we study the antibranes metastable state in ten-dimensional supergravity. We start with a more specific introduction to this ten-dimensional configuration. Then we discuss a general ansatz that solves the equations of motion for antibranes on throat geometries supported by three-form fluxes – a KPV-like setting. We then discuss how UV and IR boundary conditions are related. This relation let us obtain a consistency relation for the configuration sourced by antibranes. This last relation is used to show explicitly what are the boundary conditions where unphysical singularities arise. It also shows how to avoid them. We do this first for zero temperature, to then add finite temperature. Finally, we present our conclusions and outlook. In this section, we translate the derived consistency relation to the Smarr law of the system. After this, an appendix follows with relevant technical details.

In chapter 9 we approach antibranes metastable states in eleven-dimensional supergravity. We start again with a more particular introduction to this case. We then move to the technical set-up and probe results for anti-M2 branes. Then, we build the Smarr law of the backreacted system and discuss its relation to on-shell brane actions. Note that in this chapter we start our analysis by building the Smarr law, unlike chapter 8 where our analysis led us to a Smarr law. We continue with the study cases of smeared antibranes, the non-smeared and extremal branes. We then study finite temperature black branes. In all the previously mentioned cases, we use the Smarr law to find the boundary conditions that avoid the unphysical divergence. We conclude with the discussion. Some useful technical details can be found in the appendix.

Chapter 7

Brane Polarization and Brane-flux Annihilation

As we reviewed in the previous chapter, antibranes put in backgrounds with fluxes have important applications in black hole physics and the KKLT (Kachru-Kallosh-Linde-Trivedi) construction of non-supersymmetric de Sitter spaces in string theory. In this chapter, we quickly review the basics of two important aspects of supersymmetry breaking antibranes in flux backgrounds. First, we discuss brane polarization [163]. Second, we explain the decay mechanism of this system called brane-flux annihilation [132] and its application to the KKLT setting [133]. For both, we focus on the probe limit, where the back-reaction of the anti-D3 branes on the flux background is neglected. In the following two chapters, we will discuss the potential issues after back-reaction and our work on how to address some of these issues.

Brane polarization [163], also known as the Myers effect, happens when a number N of Dp-branes are put in a background with fluxes, forming a stack. In contrast to when the branes are apart, the stacked systems can develop a new ground state that is understood as a bound state of the Dp-branes and a higher dimensional D$(p+2)$-brane. Geometrically, the background flux has puffed-up the Dp-branes to a higher dimensional worldvolume, whose dynamics can be approximatively captured via a D$(p+2)$-brane description. This approximation improves when the number N of Dp-branes becomes large.

As an example, we can look at D0-branes polarizing into a D2-brane. This example comes from Myers himself, where he put a stack of D0-branes on a flat background electrically charged with respect to an F_4 four-form. In this setting, the stack polarizes into a D0-D2 bound state [163]. The polarized system has two equivalent descriptions:

1. A non-abelian theory of a stack of N D0-branes, effectively giving rise to a local D2-brane charge coupling.

2. An abelian theory of a single D2-brane that carries N D0-brane in its worldvolume.

How a D2-brane can carry lower dimensional D0-brane charge can be seen from the Chern-Simons term of the D2-brane action. Let us write it for a flat background that only has C_3 and C_1 Ramond-Ramond

three- and two-forms turned on,

$$\begin{aligned} S_{CS} &= \mu_2 \int \left(P[C_3] + 2\pi\alpha' P[C_1] \wedge F \right) \\ &= \mu_2 \int P[C_3] + \left(2\pi\alpha' \mu_2 \int F \right) \int P[C_1]. \end{aligned} \tag{7.1}$$

In this expression, μ_2 is the D2-brane charge, $\sqrt{\alpha'}$ is the string length scale, F is the two-form field strength living in the worldvolume of the D2, and $P[...]$ represents the pullback of the background fields to the D2 worldvolume. The term involving C_3 is the natural coupling for a D2-brane. The second term is an effective D0 coupling arising due to the F two-form presence. It is then said then that the D2-brane carries D0-brane charge in its worldvolume.

Geometrically, the D0-branes form a "fuzzy sphere"[1] [164], or equivalently, a spherical D2-brane with N D0-brane charge in its worldvolume, as in (7.1). The spherical D2-brane does not carry a net D2-brane charge. However, these configurations carry a local dipole D2-brane charge. We can make here an analogy between brane polarization and the dielectric effect: just as an uncharged material in an exterior electric field can have an electric dipole, a D0-brane configuration with no D2-charge can have a dipole D2-charge induced by an external field. See figure 7.1 for a visual representation of the D0-D2 polarize state.

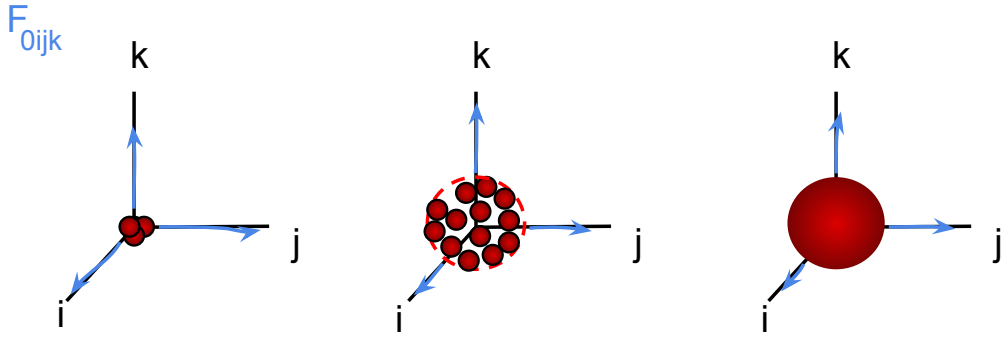

Figure 7.1: Left: D0-branes previous to polarization. Middle: Polarized D0-branes into an S^2 at a given radius R (fuzzy sphere). Right: D2-brane with $\mathbb{R} \times S^2$ topology, where the S^2 has approximately the same radius R as the fuzzy sphere picture. The D2-brane carries dissolved N D0-brane charge in its worldvolume. In the three cases, there is an influence of an electrically sourced background four-form F_4.

Branes immersed in flux background can also annihilate against the flux, in a process closely related to the polarization we just discussed. This process is called brane-flux annihilation. We review now the brane-flux annihilation example introduced by Kachru, Pearson, and Verlinde (KPV) [132]. For this, we need to introduce first the antibranes, which are our supersymmetry breaking ingredient. Antibranes are branes that are oppositely charged relative to the flux background. For example, in the

[1]The explanation of the "fuzzy sphere" name goes as follows. Transversal coordinates describe the brane position in its transversal space. For a stack of branes, these coordinates no longer commute. In the D0-D2 polarization case, they form an $SU(2)$ algebra. Thus, the stack is a rotational invariant configuration in transversal space.

KPV setting, the background three-form fluxes carry D3-brane charge. Hence, the anti-D3-branes are carrying minus D3-brane charge. As reviewed in the previous chapter, antibranes break supersymmetry. We can roughly explain this by comparing them with branes. For branes, the gravitational and flux interactions between brane and background cancel out. For antibranes, they add up, thus violating the no-force condition. This violation is equivalent to say that supersymmetry is broken in this configuration.

We return now to the review of the KPV brane-flux annihilation example. In this example, a stack of anti-D3-branes polarizes into an anti-D3-NS5 bound state that further annihilates its antibrane charge against D3-branes that materializes out from the background three-form fluxes. The polarization here occurs in a more complex configuration than the D0-D2 polarized state of Myers. The background is an explicit example of the Giddings-Kachru-Polchinski (GKP) solution [138], a type IIB supersymmetric warped geometry product of a four-dimensional Minkowski external spacetime and a topologically non-trivial six-dimensional manifold. In this GKP example, the compact manifold is a Calabi-Yau threefold that locally allows the reproduction (or embedding) of the non-compact Klebanov-Strassler (KS) warped geometry [165]. Thus, when focusing in this region, the system can be well described by the KS geometry: the Calabi-Yau threefold can be seen as a non-compact six-dimensional deformed conifold of topology $S^3 \times S^2$, with background five-form F_5 and three-form fluxes F_3 and H_3 present. There are M F_3-flux units threading the A-cycle of the deformed conifold, and K H_3-flux units threading its dual B-cycle – see figure 7.2, left. F_5 vanishes in the "near the tip" region of the KS geometry, which is the region that we want to focus in for reasons that we explain below.

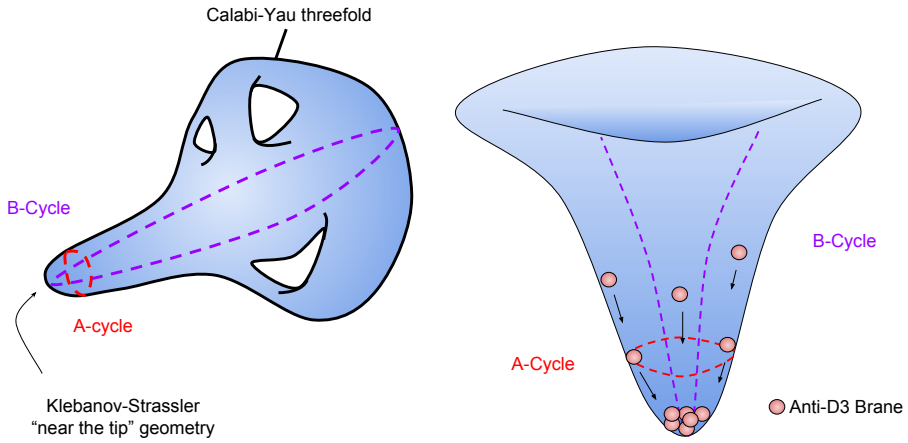

Figure 7.2: Left: Representation of the compact Calabi-Yau threefold in the KPV setting. It has a local region described by the Klebanov-Strassler geometry. In this region, the internal manifold can be described by a deformed conifold with an A-cycle and a dual B-cycle. Right: The "near the tip" region where the anti-branes gather.

We put now an amount of $p \ll M$ antibranes on this background. This limit allows us to neglect the backreaction of the antibranes – this probe level assumption is used for the whole KPV calculation. The influence of the background F_5 flux and gravitational attraction will gather the antibranes to the tip of the deformed conifold – see figure 7.2, right. We assume then that the relevant dynamics are concentrated to this region; thus we work in the "near the tip" limit from now on. This antibrane

gathering in the tip makes evident that the configuration is no longer supersymmetric: if D3-branes were the ones to be placed on the KS geometry, the F_5 and gravitational contributions would cancel out, and the no-force condition will be satisfied, as expected from a supersymmetric configuration.

The p antibranes form a stack at the tip of the cone that further polarizes into an NS5-brane wrapping an S^2 within the S^3 of the deformed conifold. This NS5 moves from one pole of the S^3 to the other while annihilating its worldvolume anti-D3-brane charge against M D3-branes that materializes out from the background three-form fluxes. The annihilation process finishes in the opposite pole, leaving $(M-p)$ D3-branes as a residuum, which can also be seen as the decay of a non-supersymmetric state to a supersymmetric one. See figure 7.3 for a visual representation of the NS5 brane-flux annihilation.

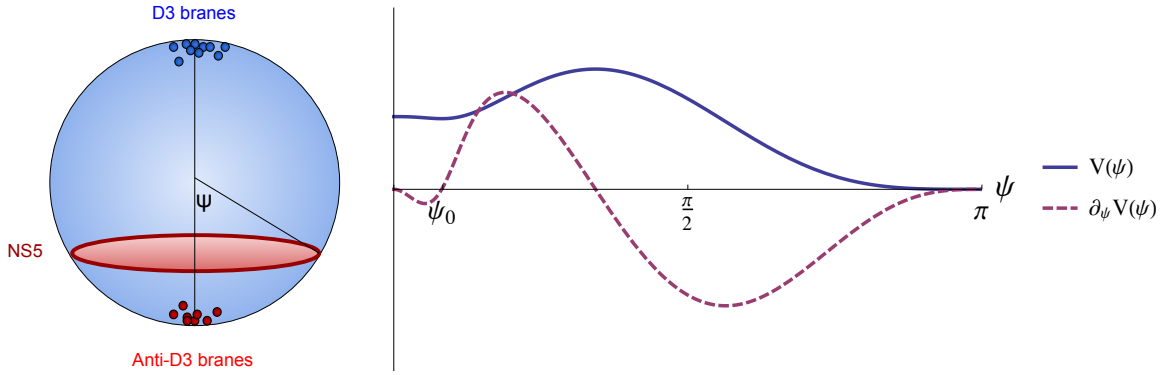

Figure 7.3: Left: A schematic picture of the brane-flux annihilation. Right: A qualitative representation of the potential $V(\psi)$ and $\partial_\psi V(\psi)$ felt by the NS5-brane for $p/M = 0.03$. The initial configuration consists of p anti-D3-branes, which polarize into an NS5 wrapping the S^2 within the deformed conifold's S^3. The NS5 rolls through the S^3 until it reaches the final $(M-p)$ D3-branes supersymmetric configuration. When $p \ll M$, the NS5 can sit at a small polar angle ψ_0 in a metastable state.

In the limit $p \ll M$, the NS5-brane can sit still in the S^3 at a small polar angle (see figure 7.3, right)

$$\psi_0 = \frac{2\pi p}{b_0^4 M}, \quad b_0^2 \approx 0.93266, \tag{7.2}$$

where the NS5 has a radius

$$R_{NS5} = \sin\psi_0 R_{S^3} \sim \frac{p}{M} R_{S^3}. \tag{7.3}$$

This is a metastable state containing anti-D3-brane charge with remarkable phenomenological consequences. Following the KKLT construction [133], the GKP solution can be compactified to four dimensions with all its moduli fixed due to the presence of fluxes and the introduction of non-perturbative quantum effects. Initially, the four-dimensional vacuum is supersymmetric anti-de Sitter spacetime. The existence of the antibrane-charged metastable state allows us to add an extra contribution to the four-dimensional potential that uplifts in a controlled way – thanks to the GKP solution space warping – the vacuum energy from anti-de Sitter to de Sitter spacetime.

The KPV mechanism is a calculation done at the probe level. When including backreaction corrections to the calculation, the H_3 flux energy density has a singularity near the anti-D3-charge source

[147, 148]. This singularity does not match the radial dependence expected from standard anti-D3-branes, so its origins are not immediately obvious. With no physical interpretation, this singularity might be a reason to doubt on the existence of this metastable state, and therefore, de Sitter vacua constructions that use anti-D3-branes as an uplifting method. The next two chapters are devoted to scrutinizing the existence of antibrane-charged metastable states in ten and eleven dimensions supergravity. We study the UV and IR boundary conditions of a (putative) full solution. This study allows us to discover some boundary conditions for the matter fields of the full solution that permits to avoid the unphysical singularities.

Chapter 8

Antibranes Metastable States in Type II Supergravity

This chapter is based on [2].

In this chapter, we revisit under which gluing conditions a stack of anti-D3 branes can be added into flux throats with opposite charge, i.e., how the UV and IR of the would-be solution should be consistently related. These consistency conditions typically reveal singularities in the 3-form fluxes whose meaning is being debated. Yet, we prove (under well-motivated assumptions) that unphysical singularities can potentially be avoided when the anti-branes polarize into spherical NS5 branes, with a specific radius. If a consistent solution can then indeed be found, our analysis seems to suggests a rather large correction to the radius of the polarization sphere compared to the KPV probe result [132]. We furthermore comment on the gluing conditions at finite temperature and point out that one specific assumption of a no-go theorem [166] can be broken if anti-branes are indeed to polarize into spherical NS5 branes at zero temperature.

8.1 Introduction

Supersymmetric throat geometries supported by fluxes are stable string theory solutions with important applications for holography, flux compactifications and black holes. As we briefly introduced in chapter 6, one explicit method to break the supersymmetry in the throat while preserving classical stability is adding anti-branes to the flux background, which carry charges opposite to the charge dissolved in flux [143, 132, 133, 145, 127]. We focus on anti-D3 branes in the Klebanov–Strassler (KS) throat as first studied in the KPV paper [132]. If the anti-brane charge p is small compared to the background RR-flux M, then their addition can be seen as a small perturbation of the KS throat; the limit of small anti-brane charge is what guarantees metastability, at least at probe level. The decay channel is the annihilation of the p anti-D3 branes with some of the background NSNS flux. If the corrections to the probe result come with positive powers of p/M it guarantees the self-consistency of the approach as long as $p/M \ll 1$.

If the above reasoning is to hold, then the results of [132] suggest that the supergravity solution

describing the metastable state should be spherical NS5 branes wrapping a contractible two-cycle of finite size. These spherical NS5 branes carry no monopole NS5 brane charge but the original p anti-D3 charges instead. This supergravity picture should hold in the following limit:

$$g_s \ll 1\,, \qquad g_s p \gg 1\,, \qquad g_s M \gg 1\,, \tag{8.1}$$

and at the same time $p/M \ll 1$ as required for stability. The above limit ensures that string loop corrections can be ignored and that the length scales of the tip of the KS throat and of the contractible 2-cycle are large in string units such that higher derivate corrections are also suppressed. Interesting arguments have been presented that for $p = 1$ the metastability is not threatened by backreaction [155, 167]. A single anti-brane is however beyond the scope of this thesis since it cannot be understood within the supergravity limit. The complementary regime of p/M of order unity or larger cannot be regarded as a perturbation to the KS throat and the would-be supergravity solution in this case can better be thought of as being $AdS_5 \times S^5$ perturbed by M units of three-form flux [156]. We do not go into that limit in this work since it does not correspond to meta-stable supersymmetry breaking by perturbatively small amounts as originally intended in [132].

The first attempts for constructing the supergravity solutions (in certain approximate schemes) revealed "non-physical" singularities: singularities which were claimed to be different from the usual ones associated to brane sources [147, 148]. The singularity is such that the scalar $e^{-\phi}|H_3|^2$, which gives the contribution of the H_3 flux to the energy-momentum tensor in Einstein frame, diverges near the sources. Although it is tempting to interpret this divergence as the self-energy of the NS5 brane, it was claimed this is not the correct interpretation, because the orientation of the fluxes and the magnitude of the divergence was not right for NS5 branes. One might worry that this mismatch is inherent to the approximations of the original papers [147, 148], but in fact the singularity was shown to persist beyond those approximations [168, 166]. Nonetheless, that interpretation of the singularity as unphysical is incomplete since the computations of [168, 166] assume genuine anti-D3 branes instead of spherical NS5 branes carrying anti-D3 charges, thus, one could therefore speculate that when one looks instead for supergravity solutions describing spherical NS5 branes at the tip of the throat, one finds acceptable singularities. This is the first point we investigate in this chapter and we find that, under well motivated assumptions, certain fields can be tuned near the horizon such that the singularity corresponds to the usual divergent self-energy of the NS5 brane. There is no guarantee that this tuning is possible in the sense that the UV can be glued consistently to the IR, but at least we find that all earlier no-go theorems against that gluing can be circumvented.

Second we investigate the configuration at finite temperature [169]. The temperature acts as an IR cut-off in field theory. If there is a mechanism in string theory that can resolve the singularity or turn it into a physical divergence (such as with brane polarisation), one expects the singularity to be shielded at finite temperature. Numerical evidence has shown that this hope was in vain [170, 171] at least for anti-D3 branes that are smeared over the finite tip at the bottom of the throat or for localised anti-D6 branes [172]. In addition, a no-go theorem was found for localised anti-Dp branes with $p \leq 6$ [166]: the would-be supergravity solution will develop a divergent flux density $e^{-\phi}|H_3|^2$ at the horizon. However, as all no-go results, the theorem is only as strong as its assumptions. In this chapter we argue that NS5 polarization is a priori consistent with relaxing one assumption in [166] on the

boundary conditions. If finite T solutions exist, our results should then be a useful lead on how to pick boundary conditions near the brane sources. In fact, some progress on the existence of smooth finite T solutions was reported in [173] and we verify that indeed this boundary condition was used. Still the construction of [173] misses a compact 'A'-cycle, which is crucial for the physics of anti-brane metastable states. Without such a compact A-cycle the construction of smooth finite temperature solutions was also argued earlier in [174].

We start the remainder of this chapter with a review of the main results of [166]. Then we analyse the H_3 flux density. At zero temperature, we review the singular flux for anti-D3 brane boundary conditions in the IR region of the flux throat and extend the analysis to spherical NS5-branes carrying anti-D3 charge. We show the flux energy density is again singular, but it is possible to obtain the appropriate power of divergence expected for a local NS5-source. This turns out to be only possible at a NS5 radius which scales as $R \sim \sqrt{p/M}$ for small p/M, which differs from the probe prediction $R \sim p/M$. We then heat up the background, and elaborate on a caveat in the arguments of [166] and discuss under which conditions the singularity can be cloaked by a smooth horizon. The discussion and interpretation of our results is found in section 8.5.

8.2 Gluing IR to UV at $T = 0$

We recall the formalism of [166]. This formalism extends the results in [168] and using the equations of motion with a general ansatz relates the boundary conditions near the anti-brane in the IR to the generalized ADM mass, which is measured in the UV. This allows to elaborate analytic arguments about the existence of the supergravity solution without knowing its explicit version – which is quite involved to obtain. Thus, these relations between the UV and IR tell us which consistency relations are necessary – but not sufficient – for the existence of well-behaved interpolating solutions. They have proven useful to demonstrate the absence of solutions in many non-trivial circumstances, which are otherwise only amenable to heavy numerical techniques.

We focus the discussion on throat geometries supported by 3-form fluxes in which anti-D3 branes are added at the tip, i.e. we will pay special attention for the $p = 3$ case. The example to have in mind is the Klebanov–Strassler throat [165]. The would-be solution takes the following form in 10D Einstein frame,

$$\begin{aligned} \mathrm{d}s_{10}^2 &= \mathsf{e}^{2A}\Big(-e^{2f}\mathrm{d}t^2 + \delta_{ij}\mathrm{d}x^i\mathrm{d}x^j\Big) + \mathrm{d}s_6^2\,, \\ C_4 &= \tilde{\star}_4\alpha, \\ H_3 &= -\mathsf{e}^{\phi-4A-f}\star_6\left((\alpha+\alpha_0)F_3 + X_3\right)\,. \end{aligned} \tag{8.2}$$

The functions ϕ, A, f, α only depend on the internal coordinates and α_0 is a constant. The horizon is located at $e^{2f} = 0$. At this point the throat metric $\mathrm{d}s_6^2$ is completely general. As said, we use notation with tildes for metrics and Hodge duals without any warp factor e^{2A} nor e^{2f}. For instance $\tilde{g}_{\mu\nu} = \eta_{\mu\nu}$ is the Minkowski metric.

We require the throat geometries to have a 3-dimensional subspace non-trivial in homology, which we call the A-cycle, and F_3 to have a fixed quantised flux $\int_A F_3 = 4\pi^2 M$. This piece of information is

crucial to describe the backreaction of anti-branes in the Klebanov-Strassler background. The A-cycle is present in the UV limit of the supergravity solution [147] and was essential in proving the presence of the original non-perturbative brane-flux instabilities [132] and the singularity [166]. For a relatively low number of anti-branes p such that $p/M \ll 1$ we expect the topology to remain the same and the A-cycle to be present.

Remember that the 3-form fluxes H_3 and F_3 are closed and we choose them to take values inside the 6-dimensional throat geometry. Then H_3 is the most general form that solves the B_2 equation of motion

$$\mathrm{d}(\mathrm{e}^{-\phi} \star_{10} H_3) = -F_5 \wedge F_3 \,, \tag{8.3}$$

provided that X_3 is closed as well. The ansatz for the H_3 flux (8.2) seems to have a redundancy, as any shift in X_3 along F_3 shifts the constant α_0. This redundancy can be fixed by demanding that

$$\int_A X_3 = 0. \tag{8.4}$$

We will furthermore fix the gauge for C_4 (and hence α) such that $\alpha_0 = 0$. This is the gauge used in [147, 175], whose results we use below.

The key observation of [166], which we repeat in the appendix, is that the following 9-form

$$\mathcal{B} = -C_4 \wedge F_5 - \tilde{\star}_4 1 \wedge B_2 \wedge X_3 + \star_{10} \mathrm{d}\Big(\phi - 4A - f\Big) \tag{8.5}$$

integrates over a spacetime volume $\mathcal{M}$ to

$$\frac{1}{\tilde{v}_4} \oint_{\partial \mathcal{M}} \mathcal{B} = M_{ADM} \,, \tag{8.6}$$

if the closed surface $\partial\mathcal{M}$ encapsulates the anti-brane sources; otherwise the integral vanishes. In this expression, $\tilde{v}_4$ is the four-dimensional volume. This is very much like Gauss' law in electrodynamics with the role of the electric charge played by the generalized ADM mass. When supersymmetry is broken by p anti-branes, M_{ADM} is proportional to p and positive [166]. This condition can then be used to constrain the behavior of the supergravity fields near the source by letting the closed surface approach the anti-brane horizon. We want to stress that this integral has only been shown to reproduce the ADM mass for the perturbative solution of [147]. We come back to more general asymptotics allowing $p/M \gg 1$ in Section 8.5.3.

The above formalism needs to be altered in order to apply it to spherical NS5 branes. The reason is that we intend to integrate the 9-form (8.5) on a surface $\partial\mathcal{M}_{IR}$ infinitesimally close to the spherical NS5 horizon. But along this surface B_2 is not everywhere defined since an NS5 acts as a magnetic source for B_2. This would imply that we need to compute the contribution from a surface of Dirac "strings" stretching from one side of the spherical NS5 to the opposite side, as depicted in Figure 8.1[1].

[1] In a first version of this work we missed that contribution and we are grateful to J. Polchinski for pointing that out. See also comments in [154].

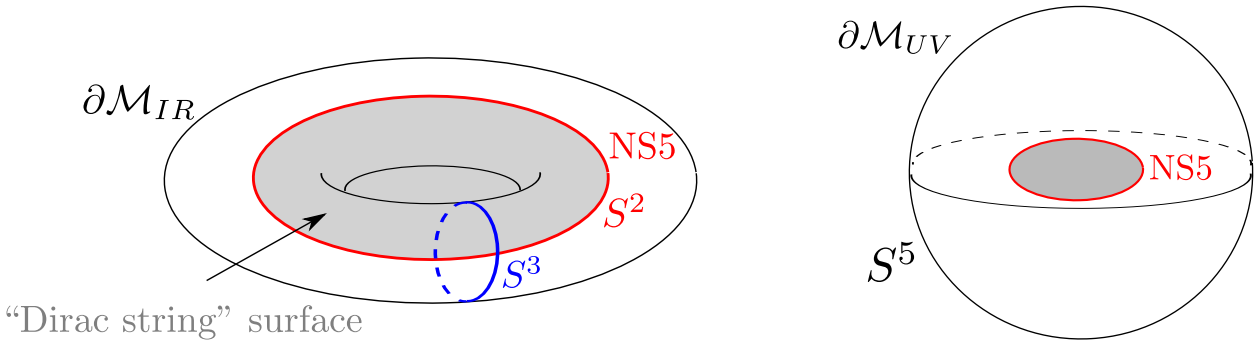

Figure 8.1: Boundaries $\partial\mathcal{M}$, with 4d Minkowski directions suppressed. Left: the IR surface that encapsulates the NS5 corresponds to an $S^3 \times S^2$ close to the brane. The spherical NS5 is drawn symbolically as a red circle. We can choose a patch such that the B_2 gauge field is well-defined everywhere except in they gray surface stretching from one side of the NS5-brane to another. Right: the UV boundary can be taken to be S^5.

Luckily this complication can be avoided by using B_6 as the fundamental potential instead of B_2. Going through an analogous computation as in [166], but using B_6, one finds:

$$\mathcal{B} = -C_4 \wedge F_5 - B_6 \wedge H_3 + \star_{10}\mathrm{d}\Big(\phi - 4A - f\Big)\,, \tag{8.7}$$

where we made use of

$$\mathrm{e}^{-\phi} \star H_3 \equiv \mathrm{d}B_6 - C_4 \wedge F_3\,, \tag{8.8}$$

such that

$$\mathrm{d}B_6 = -\tilde{\star}_4 1 \wedge X_3\,. \tag{8.9}$$

Again, notice that we ignore a possible closed but not exact piece in X_3. Such a harmonic piece would give a non-zero bulk contribution

$$\int_{\mathcal{M}} H_3 \wedge \tilde{\star}_4 1 \wedge X_3 \tag{8.10}$$

to the ADM mass. This harmonic contribution to the ADM mass would be similar to the mechanism to smooth support black hole microstate geometries [176]. This connection will be explored in more detail in future work.

8.3 Flux divergences

We focus on the density of the NS-NS 3-form flux as it appears in the energy-momentum tensor. From the ansatz (8.2) we find

$$\mathrm{e}^{-\phi}|H_3|^2 = e^{\phi-8A-2f}|\alpha F_3 + X_3|^2\,. \tag{8.11}$$

It is the aim of this chapter to infer whether this quantity stays finite near the source or not, by using consistency relations for gluing the IR solution to the UV solution.

8.3.1 Anti-D3 boundary condition

Consider eq. (8.11) and take zero temperature ($e^{2f} = 1$). Close to the anti-D3 brane, we can use the near-D3 solution of the appendix, eq. (8.42). The factor e^{-8A} is expected to blow up whereas ϕ remains finite. The metric transverse to the brane scales as $\mathrm{d}s_6^2 = e^{-2A}\widetilde{\mathrm{d}s}_6^2$, such that

$$\mathrm{e}^{-\phi}|H_3|^2 \sim e^{-2A}|\alpha F_3 + X_3|^2_{\widetilde{\mathrm{d}s}_6^2}\,, \tag{8.12}$$

where the subscript indicates we take the contraction without warp factors using $\widetilde{\mathrm{d}s}_6^2$. Hence unless the combination $\alpha F_3 + X_3$ vanishes at the position of the brane, we find a singular H_3 density scaling. This is the infamous 3-form singularity encountered in many places in the literature.

One can argue that the combination $\alpha F_3 + X_3$ indeed does not vanish at the anti-D3-brane position using eq. (8.6). As we are dealing with anti-D3 branes, we are free to use the (8.5) boundary term, since we do not expect a contribution from Dirac strings. For the standard anti-D3 boundary condition, the last term (whole bracket) in (8.5) does not contribute. Hence X_3 and α cannot both vanish since $M_{ADM} > 0$. As F_3 has a non-vanishing component along the A-cycle, the combination $\alpha F_3 + X_3$ is nonzero by construction and hence introduces a three-form singularity. Note that for a D3-brane boundary condition with $M_{ADM} = 0$, this issue is not present.

A possible way out would be that F_3 and X_3 vanish at the position of the anti-D3 brane, while α is non-zero (see the discussion in [168]). This is a priori not impossible since only the integral along the A-cycle of F_3 equals $4\pi^2 M$ and the flux could be distributed inhomogeneously along that cycle. If one tracks down what is needed for a regular H-flux density, one finds that the charge density in the fluxes has to scale to zero near the source as

$$H_3 \wedge F_3 \sim e^{4A} \star_6 1\,. \tag{8.13}$$

We consider this to be an unphysical boundary condition, since the anti-brane attracts both gravitationally and electromagnetically the charges dissolved in flux; therefore one expects that the maximal value for $H_3 \wedge F_3$ is reached near the source, instead of going to zero. We leave it for further research to find a full mathematical proof of this.

8.3.2 NS5 boundary condition

In the probe limit, the anti-D3 brane is unstable towards puffing up into an NS5-brane that wraps a contractible 2-cycle inside the A-cycle [132]. This NS5 brane carries no NS5 monopole charge, but rather anti-D3 charge through flux on its worldvolume. Since the probe NS5-branes can sit at a classically stable position, one expects a consistent supergravity solution with an NS5 brane boundary condition in the IR. We argue now that this possibility can indeed not be excluded from the gluing conditions.

With NS5 boundary conditions at the brane position, the four-dimensional transverse metric scales as e^{-6A}, while e^{ϕ} scales as e^{-4A}. Three non-trivial conditions have to be met in order for the H_3 density (8.11) to be consistent with an NS5 brane (the interested reader can corroborate them using the expressions in Appendix 8.A.2):

1. Near the NS5 source, the H_3 density should be singular of a specific degree: $e^{-\phi}|H_3|^2 \sim \mathrm{e}^{-2A}$.
2. Near the source, the dominating legs of H_3 are perpendicular to the NS5 worldvolume.
3. $\oint_{\partial\mathcal{M}} \mathcal{B}$ has to be finite and positive by (8.6), with $\mathcal{M}$ a spacetime volume encapsulating the source.

The ansatz (8.2) and the second requirement imply that $\alpha F_3 + X_3$ must have two legs on the NS5 worldvolume and one transverse leg. Together with the local metric scaling of an NS5 brane this implies

$$\mathrm{e}^{-\phi}|H_3|^2 = \mathrm{e}^{-10A}|\alpha F_3 + X_3|^2_{\widetilde{\mathrm{d}s_6}^2}\,. \tag{8.14}$$

Then condition 1 requires that $\alpha F_3 + X_3$ scales as e^{4A}. F_3 indeed has two legs on the NS5 when it threads the A-cycle, but we assume it cannot scale to zero near the NS5 brane for exactly the same reasons mentioned around equation (8.13).

Hence either α and X_3 scale as e^{4A}, or one does and the other one vanishes still more rapidly. We now argue that neither of these two possibilities can be excluded since sending α and X_3 to zero can still be consistent with a positive $1/\tilde{v}_4 \oint_{\partial\mathcal{M}} \mathcal{B}$ integral.

Consider (8.7) and its integral over the 9-surface in the IR along the NS5 horizon. Again one finds that the last term does not contribute by comparing with the known flat space solution. Interestingly the first two terms can be integrated explicitly, such that we find the equality

$$M_{ADM} = \mathrm{Vol}_4\Big(\alpha_H Q_3 + b_H Q_5 \mathrm{Vol}_2\Big)\,, \tag{8.15}$$

where Q_3 is the *monopole* anti-D3 charge and Q_5 the *dipole* NS5 charge carried by the spherical NS5 brane defined as

$$Q_3 = \int_{S^5} F_5\,, \qquad Q_5 = \int_{S^3} H_3\,, \tag{8.16}$$

for an S^5 surrounding the D3-branes and an S^3 linking the NS5-brane, as in Figure 8.1.

The values of the gauge potentials near the horizon are denoted

$$C_4 = \alpha_H \tilde{\star}_4 1\,, \qquad B_6 = b_H \tilde{\star}_4 1 \wedge \epsilon_2\,, \tag{8.17}$$

with ϵ_2 the volume-form of the 2-cycle wrapped by the NS5 brane, whose integrated value is denoted Vol_2. The above value formula for the ADM mass computed near the horizon coincides exactly with what would have been found using the formalism of [168] – and [166] – that relates the ADM mass to the on-shell brane action $S_{DBI} + S_{WZ}$. Indeed, the above expression is the on-shell Wess-Zumino term for a spherical NS5 brane carrying anti-D3 charge. The DBI probe action always vanishes on-shell since the warp-factor vanishes near the horizon. This is a nice consistency check of our results. It is now clear that we can take α_H to vanish as long as b_H remains finite to account for the ADM mass. At the same time this is consistent with X_3 scaling down as e^{4A} such that the expression for the flux divergence (8.14) is consistent with a spherical NS5 brane. The way X_3 scales down is not affected by the finite value of b_H - needed to account for the ADM mass - since X_3 relates to the derivatives of b_H but not b_H itself, see (8.9).

We can glean interesting quantitative information from our analysis concerning the NS5 position as well. Consider the 2-cycle wrapped by the NS5. Its volume scales as $g_s M$

$$\text{Vol}_2 = \int \epsilon_2 = g_s M R^2 \,, \tag{8.18}$$

where R is the radius of the S^2 on the A-cycle wrapped by the NS5 brane, with the overall $g_s M$ scaling taken out and we ignored numerical prefactors[2]. Since the ADM mass is proportional to the number of anti-branes p [175, 177]

$$M_{ADM} = 2\text{Vol}_4 e^{4A_{\text{tip}}} p \,, \tag{8.19}$$

we find from combining the last two equations with (8.15) that

$$R^2 \sim \frac{p}{M} \,. \tag{8.20}$$

This differs from the probe level (7.3), where it was found that for small p/M,

$$R \sim \frac{p}{M} \,. \tag{8.21}$$

In the discussion we comment on the interpretation of this mismatch.

Finally a word on the assumption of having a spherical NS5 brane as an IR configuration. This is clearly motivated by the probe analysis of [132]. Nevertheless, it could be that the NS5 polarisation channel comes with partner five-brane polarisation channels when backreaction is taken into account, similar to the Polchinski-Strassler (PS) background [156]. Therefore, if the supergravity solution locally is a non-supersymmetric version of PS, there could be a rather involved web of (p, q) 5-branes spanning different directions. The natural direction for D5 polarisation in the KS throat is the contractible B-cycle as drawn schematically in fig. 8.2. If the D5 channel is also present, our computations

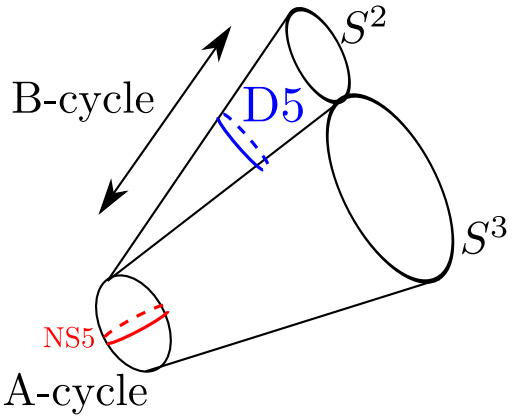

Figure 8.2: Pictorial representation of the Klebanov-Strassler geometry. There are a priori two polarization channels for anti-D3 branes: NS5 polarization on an S^2 inside the A-cycle, or D5 polarization on the S^2 of the B-cycle.

are not valid for at least two reasons. First, having two intersecting branes around complicates the

[2]This is a consequence of the fact that the S^3 tip of the KS cone has a radius set by $\sqrt{g_s M}$.

metric scaling such that our above arguments are invalidated. Second, we have relied on a trivial Bianchi identity for F_3, which is altered in the presence of D5 charges. It has been argued in the regime when $p/M \gg 1$ that D5 polarisation does not occur [178, 149]. This seems to be a peculiar property of anti-branes. For the purpose of this paper, the absence of a D5-polarization channel also for small values of p/M would imply a big simplification: we would then simply discard the analysis of boundary conditions where a spherical D5 polarization accompanies the NS5 brane.

However the full story seems more intricate. As suggested in [149] in the regime $p/M \gg 1$, the preferred channel might well be an oblique phase, a combination of D5 and NS5 polarisation along resp. B- and A-cycles. We leave a full treatment of possible oblique phases and more general asymptotics that allow to go beyond the limit $p/M \ll 1$ to future work.

8.4 Revisiting $T > 0$ no-go claims

Let's go further in our investigation of the near brane behavior of anti-branes by heating up the background. If the metastable state persists in the supergravity regime, one expects to cover all the involved 5-brane polarisation processes behind a smooth horizon [174]. For that reason we ignore the issue of not having a well defined B_2 field along the IR surface.

Once we introduce temperature in the form of a non-zero blackening factor, we find

$$e^{-\phi}|H_3|^2 \sim e^{-2f}|\alpha F_3 + X_3|^2\,, \tag{8.22}$$

where we assume that e^{2A} and ϕ are finite at the horizon. It was shown in [166] that also at finite T one can argue that α and X_3 cannot simultaneously vanish at the horizon: this is necessary in order to have a non-zero finite boundary integral $\oint \mathcal{B}$ at the horizon. Hence we seem to have a singular H_3 density since e^{-2f} becomes infinite at the horizon.

There is however one assumption that went into the no-go result of [166] that should perhaps be relaxed. Five assumptions were made explicitly. Let us take r to be the coordinate perpendicular to the horizon:

1. The temperature shows up under the form of $g_{tt} \sim e^{2f}, g_{rr} \sim e^{-2f}$, with $e^{2f} \sim r - r_h$.
2. e^{2A}, e^{2f}, ϕ depend only on r near the horizon r_h.
3. The ansatz (8.2) for metric and form fields .
4. The component of F_3 with all legs along the horizon is non-zero.
5. The relevant part of the boundary term,

$$\oint_{\partial \mathcal{M}_{horizon}} \tilde{\star}_4 1 \wedge [\alpha F_5 + B_2 \wedge X_3]\,, \tag{8.23}$$

is finite and non-zero.

These assumptions are rather solid, following either from black brane solutions – points 1 and 2 – the expectation of the backreaction in the KS background – points 3,4 – or the study of the boundary term – point 5. Condition 4 however was used in a stronger form: not only F_3, but $\alpha F_3 + X_3$ was assumed to always have a component *along* the horizon. This was partially inspired by former smeared branes setups in which this was necessary for preserving the symmetries [170]. We think that this requirement might be too strong, and indeed some comments about this were already present in [166]. Our aim here is to further clarify this issue.

First, one of the distinguishing features is that F_3 has flux along the topological A-cycle. This leads to $\star_6 H_3 = e^{\phi-4A-f}(\alpha F_3 + X_3)$ also having flux through this cycle. This H_3 flux is the cause of the Myers effect that polarizes the probe branes into NS5-branes and we expect it to be present in the backreaction as well. In general, the radial coordinate along the A-cycle will not be identified with the radial component r orthogonal to the horizon. Nevertheless, these coordinates will have a non-trivial relation, leading to the near-horizon behaviour:

$$\alpha F_3 + X_3 = \mathrm{d}r \wedge \omega_2 + \dots \,, \tag{8.24}$$

for some two-form ω_2. In case the terms $\dots$ vanish we find that the H_3 density remains finite since $g_{rr} \sim e^{-2f}$:

$$e^{-\phi}|H_3|^2 \sim |\alpha F_3 + X_3|^2_{\widetilde{\mathrm{d}s_6}} \,, \tag{8.25}$$

where now the contraction does not include e^{2A} factors nor blackening factors e^{2f}. Intriguingly, this is exactly the mechanism in [173] that provides a finite solution. However, it is unclear whether this extends to a viable finite T version of anti-D3 branes in KS backgrounds. In [173], there was no topological compact A-cycle. Rather the simplification was made that the six-dimensional transverse space was $\mathbb{R}^6$, the role of the A-cycle being played by an $\mathbb{R}^3$ factor. Also, the work of [173] included the first order backreaction of the fluxes on the black D3-brane geometry, but did not include the backreaction of the metric nor second order effects that can turn up in the flux density. Thus the believe that this issue still has to be settled.

8.5 Conclusions and outlook

In this chapter we emphasized the importance of exploring the boundary term that evaluates to the generalized ADM mass to shed new light on the back-reaction of anti-branes in flux throats. This method is very powerful, as it gives strong constraints on the back-reacted supergravity solutions without having to construct them explicitly. Our main result is the application of this method to the polarized NS5 state of supersymmetry-breaking anti-D3 branes in warped throats. Our method allows for the first time to study the polarized NS5 state in the regime where supergravity and probe limits are both expected to be applicable – $g_s p \gg 1$ and $p/M \ll 1$, with p the anti-brane charge and M the 3-form flux through the A-cycle of the KS throat.

8.5.1 Summary of results

The main result is the observation that the 3-form flux divergence, typical to anti-brane solutions, can potentially be made physical by polarising the anti-D3 branes into spherical NS5 branes. This polarisa-

tion process is expected from probe computations [132] and the presence of local NS5 sources offers a natural explanation for the presence of singular three-form fluxes. We found that the conditions for gluing the IR geometry to the UV geometry do not forbid such a three-form singularity. Furthermore the computation suggests that there is a unique radius R for the spherical NS5 brane and that the radius scales as $R \sim \sqrt{p/M}$. The probe analysis however suggests that $R \sim p/M$. So for small values of p/M, which is the regime in which one can expect meta-stable SUSY-breaking, the radius of the NS5 brane is much bigger than the radius predicted by the probe computation. This is a clear indication that, if the full back-reacted supergravity solution exists, the flux clumping process described in [152, 153] indeed significantly pushes the NS5 brane towards the equator. However, in contrast with [152, 153] we cannot conclude that it actually goes over the equator nor that the system becomes locally unstable.

The result rests on the absence of D5 polarisation in the B-cycle of the KS throat, which was argued based on the computations carried out in [178, 149]. This turns out to be the simplification needed to apply the techniques of [168, 166] to compute the 3-form flux density near the source without the need for the full supergravity solution. Our proof does not depend on any details of the background – aside the absence of D5 polarisation: the only requirement is that supersymmetry is broken such that the – generalised – ADM mass is positive. But as mentioned in [149] there can be oblique D5/NS5 polarisation channels. It is an interesting challenge to extend the result to that case.

As an aside, we reinvestigated the assumptions that went into the no-go theorem for the existence of smooth finite temperature anti-brane solutions [166]. In view of the possible NS5 polarisation channel we argued that a specific assumption about the directions of the 3-form flux near the horizon could be relaxed. If the 3-form $\star_6 H_3$ near the horizon is of the form $\mathrm{d}r \wedge \omega_2$, with ω_2 a two-form and r the local coordinate transverse to the horizon, the flux density at the horizon will be smooth. This condition cannot be satisfied for smeared anti-D3 solutions [170] or localised anti-D6 branes [172]. Hence if smooth finite T solutions exist, then their construction will necessarily involve the boundary condition $\star_6 H = \mathrm{d}r \wedge \omega_2$ at the horizon, which can be natural for NS5 branes.

We used that at large enough T we expect that the details of the NS5 polarization are hidden behind the horizon. One can still try to heat up the NS5-polarization itself to see the effect of small temperature. This is an interesting question to adress in the future.

8.5.2 Numerical analysis

We hope that this analysis can be the starting point for a numerical investigation of fully backreacted NS5 solutions. These results could be useful for choosing boundary conditions near the horizon in order to find a solution. We showed that boundary conditions exist, consistent with the ADM mass, that evade unphysical singularities. Having certainty that anti-brane supersymmetry breaking is meta-stable as indicated by probe computations [132] requires that a well-behaved supergravity solution can be found. At least this statement is true for large flux numbers and charges such that all typical length scales are within the classical gravity level. For small charges, arguments beyond the probe approximation have been suggested in [155, 154].

If a numerical study suggests that our IR boundary conditions cannot be chosen, then an unphysical

3-form singularity remains that can only be interpreted as a fatal attraction of the D3 charges dissolved in flux towards the anti-D3 brane. In that case we speculate that this could be an explanation for the tachyon found in the analysis of Bena et. al. [149]. The tachyon corresponds to a force on anti-D3 branes that has a non-zero projection towards the top of the A-cycle. The same should hence apply to spherical NS5 branes carrying anti-D3 charge [150]. If the picture of [152, 153, 179] is correct, then one expects exactly a tachyonic mode that pushes spherical NS5 branes towards the North Pole of the S^3 A-cycle, consistent with [150].

8.5.3 Connection to Smarr relations and black hole physics

In [166], the boundary term (8.5) has only been related to the ADM mass for KS-like throats with added anti-brane charge of [175] based on the perturbation of [147]. However, we believe that it can be applied much more widely. The expression for the mass in terms of a boundary term that we used in this paper is a special case of a Smarr relation. For instance in five-dimensional supergravity, the generalized ADM mass for asymptotically flat or AdS solutions with horizons – black holes, black rings – can be derived from a boundary term that evaluates to – see [180, 181] and references therein:

$$M_{ADM} = TS + \Phi Q + \phi q + V\Lambda\,. \tag{8.26}$$

The parameters in this expression are charges and dual potentials: entropy S and temperature T, electric monopole charge Q and electrostatic potential Φ, magnetic dipole charge q and its magnetic potential ϕ, and (minus) the effective inside the horizon and the cosmological constant Λ . The appearance of the dipole charge might be surprising: it is not a global conserved charge, but can only be measured locally for instance for dipole black rings. Still, it contributes to the Smarr relation because it is impossible to define the dipole potential ϕ using only a single patch, as explained in great detail in [182]. Recently the Smarr relation was shown to allow also for a bulk contribution (not a boundary term), that is non-zero only for non-trivial topology, which was previously overlooked. This topological contribution makes the construction of stationary spacetimes possible even in absence of horizons and underpins the black hole microstate geometry programme [176].

The form of the Smarr relation (8.26) is not restricted to asymptotically flat or AdS spaces, but to more general asymptotics. The prescription for the conserved energy (mass) in generic spacetimes with a timelike Killing vector has been discussed by Hawking and Horowitz in a Hamiltonian formalism [183]. Its application to flat space or AdS reduces to the known form of the Smarr formula in terms of Komar integrals, while for the anti-branes in KS it should become our boundary term (8.5). We sketched the analogy between Smarr relations for black holes and warped throats in [4].

8.A Appendix

This appendix has three sections with more technical details. We rederive the boundary term that integrates to the ADM mass in 8.A.1, give a quick review of p-brane solutions in flat space in secction 8.A.2 and in section 8.A.3 we conclude with the details for extending our finite temperature results from anti-D3 to anti-Dp branes for any $p \leq 6$.

8.A.1 Boundary term

Here we rederive the boundary term from the Einstein equations and other equations of motion. First we choose a shorthand notation X_7 in the ansatz that solves the B_2 equation of motion (8.3):

$$e^{-\phi} \star_{10} H_3 = -C_4 \wedge F_3 + X_7 \,, \qquad \mathrm{d}X_7 = 0 \,. \tag{8.27}$$

In the main body of the text we used Poincaré invariance in four dimensions to write $X_7 = \tilde{\star}_4 1 \wedge X_3$ with X_3 closed.

With the ansatz we describe in section 8.2, the Einstein equations can be massaged to [166]

$$R_4 = -\nabla^2 \phi - e^{-\phi}|H_3|^2 - |F_5|^2 - \mu_3 \delta(\Sigma). \tag{8.28}$$

Here, R_4 is the trace of the Ricci tensor along the four macroscopic dimensions and Σ denotes the brane world-volume. The ansatz (8.2) together with the equations of motion for the form fields also imply that

$$\star_{10} e^{-\phi}|H_3|^2 = -C_4 \wedge F_3 \wedge H_3 + X_7 \wedge H_3 \,, \tag{8.29}$$

$$\star_{10}|F_5|^2 = \mathrm{d}(C_4 \wedge F_5) + C_4 \wedge F_3 \wedge H_3 - \mu_3 \delta(\Sigma) C_4 \wedge \star_6 1 \,, \tag{8.30}$$

$$C_4 = \star_4 (e^{-4A}\alpha) \tag{8.31}$$

From these equations, it follows that

$$\star_{10} R_4 = \mathrm{d} \star_{10} \mathrm{d}\phi - \mathrm{d}(C_4 \wedge F_5) - X_7 \wedge H_3 + \star_{10}(\alpha e^{-4A} - 1)\mu_3 \delta(\Sigma). \tag{8.32}$$

In order to get a still more suggestive form, we use the following relation between the Ricci scalars of the metrics with and without warp factors:

$$R_4 = e^{-2A}\tilde{R}_4 + \star_{10} \mathrm{d} \star_{10} \mathrm{d}\,(4A) \,. \tag{8.33}$$

Then with (8.8) and $\tilde{R}_4 = 0$ (Minkowski space), we are left with

$$\star_{10}(1 - \alpha e^{-4A})\mu_3 \delta(\Sigma) = \mathrm{d} \star_{10} \mathrm{d}(\phi - 4A) - \mathrm{d}(C_4 \wedge F_5) - X_7 \wedge H_3. \tag{8.34}$$

The first two terms on the right-hand side are total derivatives, but not the last one. However, we can remark that since X_7 is closed we can write it as

$$X_7 = dB_6 + X_7^{\mathrm{harm}} \,, \tag{8.35}$$

where B_6 is globally well-defined and X_7^{harm} is harmonic. From now on we assume that $X_7^{\mathrm{harm}} = 0$. We will come back to the contribution of such harmonic terms to the ADM mass and the comparison to black hole microstate geometries and fuzzballs in future work. Then we can write

$$X_7 \wedge H_3 = \mathrm{d}(B_6 \wedge H_3) - B_6 \wedge \mathrm{d}H_3. \tag{8.36}$$

Now, we integrate both sides of (8.34) along a region of spacetime $\mathcal{M}$ not containing the source. The region $\mathcal{M}$ we have in mind has two boundaries: one IR boundary surrounding the branes at a

small distance, which we will let go to zero; and another one far in the UV of the KS throat. In the region $\mathcal{M}$, there is no NS5 charge such that $\mathrm{d}H_3 = 0$ and we get

$$\int_{\partial\mathcal{M}_{UV}} \mathcal{B} = \int_{\partial\mathcal{M}_{IR}} \mathcal{B}\,. \tag{8.37}$$

where

$$\mathcal{B} = -C_4 \wedge F_5 - B_6 \wedge H_3 + \star_{10}\mathrm{d}(\phi - 4A)\,. \tag{8.38}$$

In [166] it was shown that in the UV the integral

$$\frac{1}{\tilde{v}_4}\int_{\partial\mathcal{M}_{UV}} (-C_4 \wedge F_5 + \mathrm{d}B_6 \wedge B_2 + \star_{10}\mathrm{d}(\phi - 4A)) = M_{ADM} \tag{8.39}$$

is equal to the ADM mass M_{ADM}, where $\tilde{v}_4$ is a volume factor accounting for the integration along the Minkowski directions. This ADM mass is non-vanishing whenever supersymmetry is broken by (anti-)D3 branes, as it is in the KPV set-up for metastable states. In the UV, B_2 can be integrated over $\partial\mathcal{M}_{\mathrm{UV}}$. By partial integration and taking into account the fact that we integrate along a boundary, we see that

$$\frac{1}{\tilde{v}_4}\int_{\partial\mathcal{M}_{UV}} \mathcal{B} = M_{ADM} \neq 0. \tag{8.40}$$

When we combine this with (8.37) and realize that the dilaton and the warp factor do not contribute at the IR, we obtain the remarkable result

$$\frac{1}{\tilde{v}_4}\int_{\partial\mathcal{M}_{IR}} (C_4 \wedge F_5 + B_6 \wedge H_3) = M_{ADM} \neq 0. \tag{8.41}$$

This is what we need to argue for the singularities in section 8.3.

8.A.2 Supergravity brane solutions

Near the branes sources (D3 or NS5), we approximate the geometry by a p brane metric:

$$\mathrm{d}s^2 = e^{2A}(-e^{-2f}\mathrm{d}t^2 + \mathrm{d}\vec{x}_p^2) + e^{2\frac{p+1}{p-7}A}(\mathrm{d}r^2 + r^2\mathrm{d}\Omega_{8-p}^2)\,, \tag{8.42}$$

where the dilaton and sourced field strength for a Dp brane are

$$e^{\phi} = e^{4\frac{3-p}{p-7}A}\,, \qquad F_{8-p} = e^{2f}\coth\beta Q_p \mathrm{d}\Omega_{8-p} \tag{8.43}$$

and for an NS5/F1 are

$$e^{\phi} = e^{-4\frac{3-p}{p-7}A}\,, \qquad H_{8-p} = e^{2f}\coth\beta Q_p \mathrm{d}\Omega_{8-p}\,. \tag{8.44}$$

Also,

$$e^{\frac{16}{p-7}A} = 1 + \sinh^2\beta r_0^{7-p}/r^{7-p}\,, \quad e^{2f} = 1 - \frac{r_0^{7-p}}{r^{7-p}}\,. \tag{8.45}$$

The $T \to 0$ limit is $\beta \to \infty, r_0 \to 0$ while keeping $Q_p \equiv \sinh^2\beta r_0^{7-p}$ fixed.

Finally we note that at $T = 0$, the flux density near p-branes scales with the warp factor A as:

$$NS5/F1: \quad e^{(3-p)\phi/2}|H_{8-p}|^2 \sim e^{-2\frac{(p-3)^2}{(7-p)^2}A}\,, \tag{8.46}$$

$$Dp: \quad e^{-(3-p)\phi/2}|F_{8-p}|^2 \sim e^{-2\frac{(p-3)^2}{(7-p)^2}A}\,. \tag{8.47}$$

8.A.3 Anti-Dp branes at finite T

The extension of the finite temperature results to anti-Dp branes inserted in throat geometries that carry Dp brane charges dissolved in fluxes is immediate [166]. The ansatz generalizes to

$$\begin{aligned} &\mathrm{d}s_{10}^2 = \mathrm{e}^{2A} g_{\mu\nu}\mathrm{d}x^\mu \mathrm{d}x^\nu + \mathrm{d}s_{9-p}^2\,, \\ &C_{p+1} = \tilde{\star}_{p+1}\alpha, \\ &H_3 = \mathrm{e}^{\phi-(p+1)A} \star_{9-p} \Big(\alpha F_{6-p} + X_{6-p}\Big)\,. \end{aligned} \tag{8.48}$$

Such backgrounds exist up to $p = 6$, which describes an anti-D6 brane in a background with Romans mass and H_3 flux carrying D6 charges. As with anti-D3 branes, there is a conserved current that entails a non-trivial gluing condition between the IR and the UV. Near the horizon in the IR the conserved charge is given by

$$\oint_{IR} \frac{2}{1-p} \tilde{\star_{p+1}} 1 \wedge [F_{8-p} + B_2 \wedge X_3] + \frac{4}{p+1} \star_{10} \mathrm{d}f\,, \tag{8.49}$$

and as before this integral has to be positive and finite.

In complete analogy with anti-D3 branes we can investigate necessary gluing conditions to obtain the same conclusions, except for anti-D6 branes where we find a different result. When $p = 6$, the three-form H_3 is always proportional to the volume form in the three-dimensional transverse space (there is no A-cycle) and there is no X_0 term: $H_3 = e^{\phi-7A} \star_3 F_0$. For finite T solutions we furthermore cannot evade the no-go result as sketched earlier, since $\star_3 H_3 \sim F_0$ is a zero-form and hence cannot have a direction along $\mathrm{d}r$. Therefore we still find a singular horizon for anti-D6 branes in flux background and their T-dual equivalents such as anti-D3 branes smeared on the tip of the Klebanov-Strassler throat.

Chapter 9

Antibranes Metastable States in M-theory

This chapter is based on [3].

In this chapter, we study the backreaction of smeared and localised anti M2-branes placed at the tip of the Cvetic-Gibbons-Lu-Pope (CGLP) background [184]. To this end we derive a Smarr relation for backreacted antibranes at zero and finite temperature. For extremal antibranes we show that if smeared they cannot have regular horizons, whereas localised M2-branes can potentially be regular when polarised into M5-branes, in agreement with the probe result of Klebanov and Pufu [161]. We further discuss antibranes at finite temperature and argue that localised antibrane solutions with regular horizons are not excluded.

9.1 Introduction

Just as in ten-dimensional supergravity (chapter 8), breaking supersymmetry in eleven dimensions in a controlled manner remains one of the hard challenges in constructing string theory vacua. In eleven dimensions, this game can be played by the addition of anti M2-branes to a nontrivial background flux, in the same manner of anti-D3 branes in ten-dimensional supergravity. As we already briefly mentioned in chapters 6 and 8.1, brane/flux set-ups have already proved useful in string cosmology [133, 185], the black hole microstate program [127, 126] and dynamical supersymmetry breaking in holographic field theories [143, 132, 144, 145, 146]. In eleven dimensions, the stability of such a background is again complicated to analyse since the decay generically occurs through the Myers effect [163], with the M2-branes polarising into M5-branes that then subsequently decay. The M2-branes are then effectively annihilated against flux quanta via brane/flux annihilation [132].

A concrete set-up involves placing anti M2-branes in the resolved cone background of Cvetič, Gibbons, Lü and Pope (CGLP) [184] analogous to the Klebanov-Strassler background in type IIB supergravity [165]. The CGLP background plus anti M2-branes set-up was analysed using a probe brane in [161] where it was found that the M2 would polarise to a spherical M5-brane which finds a metastable state close to the original M2-brane location. Later, various approaches used to study the backreaction of M2-branes on the geometry revealed a divergent energy density for G_4 which could not be attributed to the presence of M2-branes [162, 186, 187, 188, 189]. One reasonable interpretation of the singu-

larity is that because the M2s want to polarise to an M5-brane they induce the observed singularity in G_4. The singular flux pile-up could signal that the brane/flux annihilation process occurs classically rather than through quantum tunnelling [152, 153, 179]. If not, we would expect to be able to hide the singularity or any polarised metastable state behind a horizon by heating up the branes [169]. Reference [189] found that *smeared* antibranes exhibit a singular horizon at any temperature. A toy model analysis of localised branes showed that the result of [189] might be an artifact of the smearing [173]. In this chapter we aim to determine what is required so that a extremal polarised state exists, but we also revisit the non-extremal scenario.

In this chapter, we study the backreaction of anti M2-branes and polarised M5-branes in the background of [184], using the same technique as previous chapter – employed in [168] and further developed in [166, 2]. After reviewing the essential ingredients of the CGLP background in section 9.2, we derive in section 9.3 the Smarr relation for a system of M2 and M5-branes placed at the tip of that geometry. It relates the energy measured far away from the branes to the charge and surface gravity of the M2/M5 system,

$$\boxed{\mathcal{E} = \frac{7}{6}\frac{\kappa\mathcal{A}}{8\pi G_N} + \Phi_{\text{M2}}Q_{\text{M2}} + \Phi_{\text{M5}}Q_{\text{M5}}\ ,} \tag{9.1}$$

where κ and $\mathcal{A}$ denote the surface gravity and area respectively, Φ_{M2} and Q_{M2} denote the potential and M2-charge of the system, while Φ_{M5} and Q_{M5} denote the *dipole* potential and charge of the brane system. Note that since the M5-branes are contractible, as we explain later, their monopole charge vanishes. However, we find similar to [190, 2] that the dipole charge of the M5s contribute with a non-vanishing term to the Smarr relation. A non-vanishing dipole contribution is only possible for horizons with a non-trivial topology.[1] In Section 9.4 we warm up by discussing smeared antibranes, which we will show cannot be regular. Then, in Section 9.5, we extend the results of [162, 186, 189] to localised branes, showing that extremal anti M2-branes with trivial horizon topology cannot have a regular horizon. If the horizon topology is non-trivial on the other hand, then the Smarr relation does not constrain the horizon to be singular. This is most likely the metastable state found by Klebanov and Pufu [161], although a full solution remains to be found. Finally in Section 9.6 we consider non-extremal branes. There we argue that localised branes posses at least two possible phases, differing in their horizon topology, which we briefly discuss. We conclude with Section 9.7.

9.2 Anti M2-branes in CGLP

In this section the smooth background of [184] is reviewed, which is a warped product of $\mathbb{R}^{1,2}$ and a Stenzel manifold. We start with the construction of Stenzel spaces before turning to the full supergravity field configuration.

Let us consider Calabi-Yau hypersurfaces in $\mathbb{C}^{n+1}$ with a conical singularity at the origin:

$$\mathcal{C}^n = \left\{ z \in \mathbb{C}^{n+1} \ :\ z_i z_i = 0 \right\} . \tag{9.2}$$

[1] One could wonder whether the backreacted solution has no horizon but is rather supported by a topological contribution as in [176]. In this paper we will not explore this possibility as we assume a presence of a horizon.

For $n \geq 3$, the base spaces of the cones are Sasaki-Einstein manifolds of dimension $2n-1$ and can be identified by intersecting $\mathcal{C}^n$ with the unit sphere in $\mathbb{C}^{n+1}$:

$$\mathcal{B}^{2n-1} = \left\{ z \in \mathcal{C}^n \ : \ z_i \bar{z}_i = 1 \right\} . \tag{9.3}$$

For $n = 3$ the base space is $\mathcal{B}^5 = T^{1,1}$ whereas for $n = 4$ the base is $\mathcal{B}^7 = V_{5,2}$. A resolution of the conical singularity of (9.2) can be achieved by modifying the defining equation by adding an inhomogeneous term to the right hand side

$$\mathcal{C}^n_\epsilon = \left\{ z \in \mathbb{C}^{n+1} \ : \ z_i z_i = \epsilon^2 \right\} , \tag{9.4}$$

where $\epsilon \in \mathbb{R}$. For $n = 2$ the hypersurface is the Eguchi-Hanson resolution of the A_1 singularity [191] while $n = 3$ gives the well-known deformed conifold [192]. The explicit metrics can be derived using a Kähler potential K which only depends on the variable

$$\rho = z_i \bar{z}_i , \tag{9.5}$$

and satisfies the differential equation [193]

$$\rho (K')^n + (\rho^2 - \epsilon^4) K'' (K')^{n-1} = c^2 , \tag{9.6}$$

for some normalization constant c. After solving this equation the metric can be written down

$$\mathrm{d}s^2_{2n} = K'(\rho) \sum_{i=1}^{n+1} \mathrm{d}z_i \mathrm{d}\bar{z}_i + K''(\rho) \sum_{i=1}^{n+1} |z_i \mathrm{d}\bar{z}_i|^2 . \tag{9.7}$$

We will focus exclusively on $n = 4$ with $c = 9/4\epsilon^3$ for which an explicit form of the metric can be found in [161]. Since we do not require its explicit form we omit writing it. From now on we will rescale our coordinates to absorb ϵ, then the coordinate ρ ranges between 1 and ∞ and for large ρ the metric reduces to that of the cone (9.2). Finally, for $\rho = 1$ the metric reduces to that of a 4-sphere with radius $\sqrt{3/2}$.

The CGLP background

The supergravity background of [184] is a warped product of the metric (9.7) with $n = 4$ and flat 3-dimensional spacetime:

$$\mathrm{d}s^2 = H^{-2/3} \big(-\mathrm{d}t^2 + (\mathrm{d}x^1)^2 + (\mathrm{d}x^2)^2 \big) + H^{1/3} \mathrm{d}s^2_8 . \tag{9.8}$$

This metric solves the Einstein equation derived from the action of 11-dimensional supergravity

$$S = \frac{1}{16\pi G_N} \int \left\{ \star_{11} R - \frac{1}{2} \star_{11} G_4 \wedge G_4 - \frac{1}{6} G_4 \wedge G_4 \wedge A_3 \right\} , \tag{9.9}$$

where the form fields are

$$G_4 = -\mathrm{vol}_3 \wedge \mathrm{d}H^{-1} + m\omega_4 \tag{9.10}$$

$$G_7 \equiv \star_{11} G_4 = H^2 \star_8 \mathrm{d}H^{-1} - mH^{-1} \mathrm{vol}_3 \wedge \omega_4 . \tag{9.11}$$

Here $\text{vol}_3 = \mathrm{d}t \wedge \mathrm{d}x^1 \wedge \mathrm{d}x^2$ and ω_4 is an anti self-dual closed 4-form on $\mathcal{C}^4_\epsilon$, m is a constant and $\star_8$ is the Hodge operator on $\mathrm{d}s^2_8$. The Bianchi identity $\mathrm{d}G_4 = 0$ is trivially solved for (9.10) whereas the Bianchi identity for G_7:

$$\mathrm{d}G_7 + \frac{1}{2} G_4 \wedge G_4 = 0 \,, \tag{9.12}$$

implies

$$\mathrm{d} \star_8 \mathrm{d}H = \frac{1}{2} m^2 \star_8 \omega_4 \wedge \omega_4 \,, \tag{9.13}$$

which can be written as

$$\nabla^2_8 H = -\frac{1}{2} m^2 |\omega_4|^2 \,. \tag{9.14}$$

This equation can be integrated assuming $H \equiv H(\rho)$ and regularity at $\rho = 1$ [184, 161]

$$H = c_0 + \left(12^3\ 3^8\right)^{1/4} m^2 \int_{(2+\rho)^{1/4}}^{\infty} \frac{\mathrm{d}t}{(t^4-1)^{5/2}} \,. \tag{9.15}$$

The constant c_0 controls the asymptotic behaviour of the solution. We will consider both $c_0 = 0$ for which the metric is asymptotically $\text{AdS}_4 \times V_{5,2}$, and $c_0 \neq 0$ for which the solution is asymptotically Ricci flat, $\mathbb{R}^{1,2} \times \mathcal{C}^4$. For $c_0 \neq 0$ we can rescale the coordinates as well as m to absorb c_0. Therefore we will only consider $c_0 = 1$ in addition to $c_0 = 0$.

Probe anti M2-branes

Anti M2-branes placed in the M-theory background just described experience a radial force which pulls them towards the resolved tip of the cone. In [161] Klebanov and Pufu performed a probe analysis to determine the behaviour of p anti M2-branes sitting at the tip. In this section we review their results.

Locally, close to the tip, the metric (9.7) reduces to the metric on the 4-sphere

$$\mathrm{d}s^2_8 \underset{\rho \to 1}{\longrightarrow} \frac{3}{2} \left[\mathrm{d}\psi^2 + \sin^2\psi \mathrm{d}\Omega^2_3\right] \,, \tag{9.16}$$

where $\mathrm{d}\Omega^2_3$ is the metric on the round three-sphere and $\psi \in [0, \pi]$ is the azimuthal angle on the four-sphere. Without loss of generality, one may assume that the antibranes are initially located at the North pole, with $\psi = 0$. The interaction between the branes and the background flux gives rise to a polarisation process through the Myers effect. Concretely, the anti M2-branes polarise into an M5-brane carrying finite M2 charge wrapping a finite size S^3 at a certain value of ψ.

The probe calculation follows closely the initial work of [132]. By evaluating the Lagrangian of a probe M5-brane with p units of M2 charge, one obtains an effective potential as a function of the azimuthal angle and the ratio p/M, where M is the total G_4 flux threading the four-sphere:[2]

$$M = \frac{1}{(2\pi\ell_p)^3} \int_{S^4} G_4 = \frac{18\pi^2 m}{(2\pi\ell_p)^3} \,. \tag{9.17}$$

Depending on the value of p/M, this potential has either only one absolute minimum at $\psi = \pi$, corresponding to the supersymmetric state where the M5-brane has $p - M$ units of M2-brane charge which

[2] We use conventions where $16\pi G_N = (2\pi)^8 \ell_p^9$.

preserves the same supersymmetry as the flux background, or one absolute minimum at $\psi = \pi$ plus a local minimum at some value $\psi = \psi_{\text{min}}$, corresponding to a metastable polarised state.

The analysis of [161] was carried out after a dimensional reduction along one of the coordinates of the anti M2-branes. We then have anti fundamental strings in type IIA supergravity, which polarise into D4-branes. The polarisation angle ψ_{min} is found at the minimum of the polarisation potential

$$V(\psi) = \sqrt{h \sin^6 \psi + U^2(\psi)} - U(\psi) \,, \tag{9.18}$$

where

$$U(\psi) = \frac{1}{8}\cos^3\psi - \frac{3}{8}\cos\psi + \frac{1}{4} - \frac{p}{2M} \,, \tag{9.19}$$

and

$$h = \frac{H(1)}{96m^2} = \frac{c_0}{96m^2} + \left(\frac{3}{4}\right)^{7/4} \int_{3^{1/4}}^{\infty} \frac{\mathrm{d}t}{(t^4-1)^{5/2}} \approx 0.0114 \,, \tag{9.20}$$

where we used that $m \gg 1$. In Figure 9.1 we plot the polarisation potential for different values of p/M. A metastable minimum of the potential only exists for small range of parameters $0 < p/M \lesssim 0.0538$. Furthermore, for small p/M the minimum satisfies

$$\psi_{\text{min}}^2 \approx \frac{1}{8h}\frac{p}{M} \,. \tag{9.21}$$

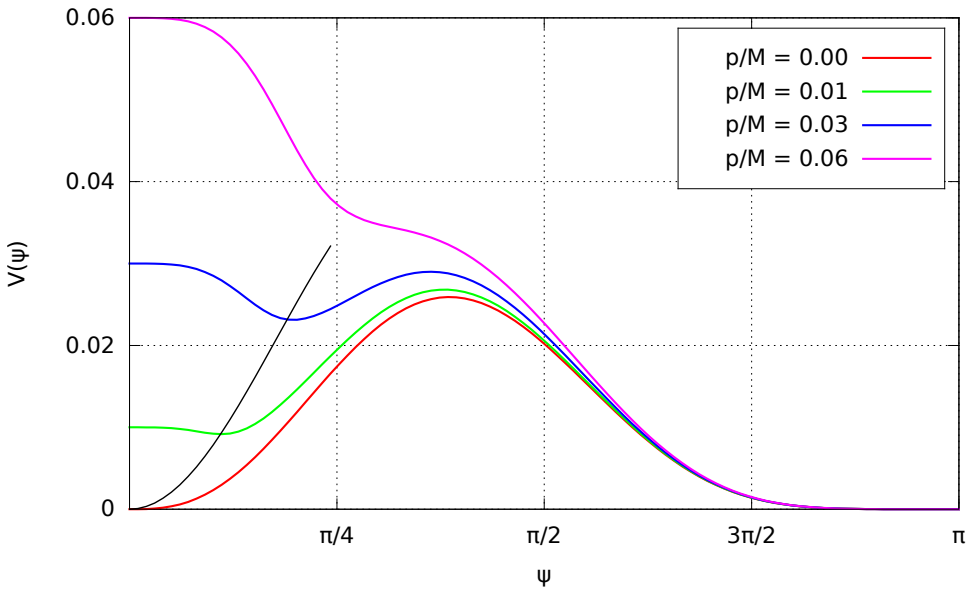

Figure 9.1: The polarisation potential $V(\psi)$ for different values of p/M. The black line shows the estimate for the position of the metastable minimum given in eq. (9.21).

9.3 A Smarr relation for M2-branes

In this section the Smarr relation (9.1) for p anti M2-branes in the CGLP background with flux number M is derived. It will be assumed that $p/M \ll 1$, in line with [161]. In Sections 9.4, 9.5 and 9.6 we then use this formula to constrain both extremal and non-extremal antibrane solutions. It is found that smeared and extremal pointlike anti M2-branes are not consistent with the Smarr relation, whereas polarised and non-extremal states are. Our approach is reminiscent of the one employed in [168] and later [166] for type II antibrane systems. In Appendix 9.A.4 we derive the Smarr relation for such set-ups.

In order to perform the calculation, an important assumption is made that asymptotically, far away from the tip of the cone, the solution should look like the CGLP solution described above. In particular the M2 charge measured at infinity is fixed to the one for a CGLP background for a given m. When the antibranes are introduced m is adjusted so that the charge remains the same. This will lead to a nonvanishing ADM mass measured at infinity as it will be explained in Section 9.5. It is the aim of this section to obtain the Smarr relation between the ADM energy density, area, charge and chemical potentials of the antibrane system.

The full antibrane metric is assumed to take the form

$$\mathrm{d}s_{11}^2 = e^{2A}\left(-\mathrm{e}^{2f}\mathrm{d}t^2 + (\mathrm{d}x^1)^2 + (\mathrm{d}x^2)^2\right) + \mathrm{d}\bar{s}_8^2 \,, \tag{9.22}$$

where $\mathrm{d}\bar{s}_8^2$ is a modification of the metric on $\mathcal{C}_\epsilon^4$ which takes into account the backreaction of the M2 branes on the flux background. We omit writing an explicit warp factor in front of the 8-dimensional metric but assume that asymptotically, for large ρ,

$$\mathrm{d}\bar{s}_8 \to H^{1/3}\mathrm{d}s_8^2 \,, \tag{9.23}$$

where $\mathrm{d}s_8^2$ is given in eq. (9.7). Note that we have introduced a metric function e^{2f} that breaks the Lorentz symmetry of $\mathbb{R}^{1,2}$ to incorporate a possible non-extremal state. The metric is general enough to describe either a stack of anti M2-branes or polarised M5-branes carrying M2 charge.

In the following it will be useful to introduce notation for the gauge fields that is adapted to the metric (9.22). We write

$$G_4 = -\mathrm{e}^{3A+f}\mathrm{vol}_3 \wedge F_1 + \tilde{F}_4 \,, \tag{9.24}$$

$$G_7 = \mathrm{e}^{3A+f}\mathrm{vol}_3 \wedge F_4 + F_7 \,, \tag{9.25}$$

which implies $F_4 = \star_8 \tilde{F}_4$ and $F_7 = -\star_8 F_1$. In this section $\star_8$ refers to the Hodge operator on $\mathrm{d}\bar{s}_8^2$. With these definitions the equations of motion in absence of source terms take the form

$$\mathrm{d}F_7 + \frac{1}{2}\tilde{F}_4 \wedge \tilde{F}_4 = 0 \,, \tag{9.26}$$

$$\mathrm{d}(e^{3A+f}F_4) + e^{3A+f}F_1 \wedge \tilde{F}_4 = 0 \,, \tag{9.27}$$

$$\mathrm{d}(e^{3A+f}F_1) = 0 \,, \tag{9.28}$$

$$\mathrm{d}\tilde{F}_4 = 0 \,. \tag{9.29}$$

For pointlike M2-branes in the internal space, only eq. (9.26) receives a delta function contribution on the right hand side. For M5-branes that wrap three internal dimensions only eq. (9.29) receives a contribution, unless the M5 carries M2 charge which then disguises itself as a contribution to eq. (9.26). For large ρ, the asymptotic expansion of all field strengths and warp factor should equal the one for the CGLP background to leading order. Beyond leading order, fields will generically differ from their background values. We therefore let

$$\mathrm{e}^{2f} \to 1 \,, \quad \mathrm{e}^{2A} \to H^{-2/3} \,, \tag{9.30}$$

as $\rho \to \infty$.

We will from now on assume that there are globally well-defined gauge potentials for F_4 and F_1, defined by

$$e^{3A+f} F_1 = \mathrm{d}C_0 \qquad \text{and} \qquad e^{3A+f} F_4 = \mathrm{d}C_3 - C_0 \tilde{F}_4 \,. \tag{9.31}$$

Despite the suggestive notation, C_0 appears in the Wess-Zumino (WZ) terms for M2-branes while C_3 appears in the WZ terms for M5-branes. In the limit $\rho \to \infty$ the potentials reduce to

$$C_0 \to H^{-1} \quad \text{and} \quad C_3 \to 0 \,, \tag{9.32}$$

and so these are globally defined for the CGLP background. The presence of M2-branes or their polarised state does not affect the existence of C_0 and C_3 in line with the discussion below eqs. (9.26-9.29). The gauge transformations that leave the field strengths invariant are

$$\delta C_0 = 0 \,, \quad \delta C_3 = \mathrm{d}\lambda_2 \,. \tag{9.33}$$

ADM energy

We now turn our attention to the ADM energy density of the anti M2-branes. We will relate it to the potentials C_0 and C_3 evaluated at the horizon of the brane configuration. The general expression for the ADM energy density of a p-brane configuration in D dimensions is derived in Appendix 9.A.1, which extends the results of [194] to spacetimes which are not transverse asymptotically Ricci flat. The result is

$$\mathcal{E} = -\frac{1}{16\pi G_N} \oint_\infty \star_D \left[\mathrm{d}\eta \wedge \Lambda_p + \xi \wedge \eta \wedge \Lambda_p + \frac{1}{D-p-3} \mathrm{d}(\eta \wedge \Lambda_p) \right] \,, \tag{9.34}$$

where $\Lambda_p = \lambda_{(1)} \wedge \cdots \wedge \lambda_{(p)}$, η is a one-form dual to the timelike Killing vector ∂_t and $\lambda_{(i)}$ are one-forms dual to p spacelike killing vectors ∂_{x^i}, $i = 1, \ldots, p$. Finally, ξ is a one-form that takes care of subtracting the background contribution to the energy density and corresponds to adding a counter-term to the action

$$\int \mathrm{d} \star_D \xi \,. \tag{9.35}$$

We normalize the energy with respect to the CGLP background for which (see Appendix 9.A.1)

$$\xi = \mathrm{d} \log H \,. \tag{9.36}$$

Using this (9.34) reduces to

$$\mathcal{E} = \frac{1}{16\pi G_N} \frac{1}{3} \oint_\infty \mathrm{e}^{3A+f} \star_8 \mathrm{d}(9A + 7f + 3 \log H) \,. \tag{9.37}$$

We now use the Einstein equation to bring the integration surface from $\rho \to \infty$ close to the horizon of the branes. To this end we write the components of the Einstein equation along the brane worldvolume,

$$R_{\mu\nu} + \frac{1}{6} g_{\mu\nu} \left(2|F_7|^2 + |\tilde{F}_4|^2 \right) = 0 \,, \tag{9.38}$$

for $\mu, \nu = 0, 1, 2$. Using the form of the metric (9.22) the Ricci tensor on $\mathbb{R}^{1,2}$ can be explicitly written down,

$$R_{00} = -g_{00} \left[\Box_8 (A + f) + \nabla(3A + f) \cdot \nabla(A + f) \right] \,, \tag{9.39}$$

$$R_{ij} = -g_{ij} \left[\Box_8 A + \nabla(3A + f) \cdot \nabla A \right] \,, \tag{9.40}$$

where $i, j = 1, 2$ and the dot-product is performed using the transverse metric $\mathrm{d}\bar{s}_8^2$. The Einstein equation (9.38) reduces to two differential equations that will enable us to rewrite the ADM energy,

$$\mathrm{d}\left(\mathrm{e}^{3A+f} \star_8 \mathrm{d}f \right) = 0 \,, \tag{9.41}$$

$$\mathrm{d}\left(\mathrm{e}^{3A+f} \star_8 \mathrm{d}A \right) = -\frac{\mathrm{e}^{3A+f}}{3} \star_8 \left(|F_7|^2 + \frac{1}{2}|\tilde{F}_4|^2 \right) \,. \tag{9.42}$$

We define an 8-dimensional submanifold $\mathcal{M}_8$ that has boundaries at $\rho \to \infty$ and at the horizon of the brane configuration. Using the above differential equations together with (9.37) yields

$$\begin{aligned} \mathcal{E} = & \frac{1}{16\pi G_N} \frac{1}{3} \oint_H \mathrm{e}^{3A+f} \star_8 \mathrm{d}(9A + 7f) \\ & - \frac{1}{16\pi G_N} \int_{\mathcal{M}_8} \mathrm{e}^{3A+f} \star_8 \left(|F_7|^2 + \frac{1}{2}|\tilde{F}_4|^2 \right) \\ & + \frac{1}{16\pi G_N} \oint_\infty \mathrm{e}^{3A+f} \star_8 \mathrm{d}\log H \,, \end{aligned} \tag{9.43}$$

where the subscript H in the first term denotes the horizon.

We will analyse the three terms of (9.43) individually. First, by construction the warp factor A is completely regular at the horizon and[3]

$$\mathrm{e}^{3A+f} \to 0 \quad \text{as} \quad \rho \to \rho_H \,. \tag{9.44}$$

This implies that we can rewrite the first term of (9.43) as

$$\frac{1}{3} \oint_H \mathrm{e}^{3A+f} \star_8 \mathrm{d}(9A + 7f) = -\frac{7}{6} \oint_H \star_{11} \mathrm{d}\eta \wedge \lambda_{(1)} \wedge \lambda_{(2)} \,. \tag{9.45}$$

The integral on the right-hand side above yields exactly minus two times the horizon surface gravity κ times the *effective area* of the horizon $\mathcal{A}$ [195, 194] (see also Appendix 9.A.2), and so

$$\frac{1}{16\pi G_N} \frac{1}{3} \oint_H \mathrm{e}^{3A+f} \star_8 \mathrm{d}(9A + 7f) = \frac{7}{6} \frac{\kappa \mathcal{A}}{8\pi G_N} \,. \tag{9.46}$$

[3]Note that for extremal horizons A diverges, wheras f vanishes. It is simple to verify that all results obtained in this section are valid also for extremal horizons taking the limit $f \to 0$.

The second term of eq. (9.43) can be rewritten using (9.26-9.28) together with the definitions (9.31)

$$\mathrm{e}^{3A+f} \star_8 \left(2|F_7|^2 + |\tilde{F}_4|^2\right) = \mathrm{d}(C_3 \wedge \tilde{F}_4 + 2C_0 F_7) \ . \tag{9.47}$$

The bulk integral can therefore be transformed into a surface integral evaluated at the horizon and at infinity. At infinity we can use the behaviour of the fields (9.30-9.32) so that

$$-\frac{1}{16\pi G_N}\oint_\infty \left(\frac{1}{2}C_3 \wedge \tilde{F}_4 + C_0 F_7\right) = -\frac{1}{16\pi G_N}\oint_\infty C_0 F_7 = -Q_{\text{M2}} \lim_{\rho\to\infty} H^{-1}(\rho) \ , \tag{9.48}$$

where[4]

$$Q_{\text{M2}} = Q_{\text{CGLP}} = \frac{\mu_{\text{M2}}}{(2\pi\ell_p)^6}\int F_7 = \mu_{\text{M2}}\frac{M^2}{4} \ , \tag{9.49}$$

is the M2 charge of our solution which we assume to be the same as the one of the CGLP background (see Appendix 9.A.3). When $c_0 = 0$ the term (9.48) diverges as $\rho^{9/4}$ but is exactly cancelled by the last term in (9.43)

$$\frac{1}{16\pi G_N}\oint_\infty \mathrm{e}^{3A+f} \star_8 \mathrm{d}\log H = Q_{\text{CGLP}} \lim_{\rho\to\infty} H^{-1}(\rho) \ . \tag{9.50}$$

Combining the above results we can write the ADM energy as

$$\mathcal{E} = \frac{7}{6}\frac{\kappa\mathcal{A}}{8\pi G_N} + \frac{1}{16\pi G_N}\oint_H \left(\frac{1}{2}C_3 \wedge \tilde{F}_4 + C_0 F_7\right) \ . \tag{9.51}$$

For the CGLP background the horizon area vanishes and the regularity of the background ensures that the second integral also vanishes so that we end up with the expected result

$$\mathcal{E}_{\text{CGLP}} = 0 \ . \tag{9.52}$$

The equation (9.51) has non-trivial implications for the consistency of the supergravity solutions describing anti M2-branes and polarised M5-branes at the tip of the cone. It allows us to relate the UV behaviour of the solution, characterized by the ADM energy measured at infinity, to the IR structure of the horizon. In [166] and in the previous chapter such a relation was used to argue for a singular flux at the horizon of localised anti D3-branes sitting at the tip of the Klebanov-Strassler background as a result of demanding a non-vanishing ADM energy. However, we will use (9.51) in a somewhat different way: we will assume that the solutions have regular horizons, and from there on investigate what it implies for the ADM energy measured in the UV.

Charges and potentials

We now close the ADM discussion by interpreting the last term in (9.51). First of all, from the equations of motion (9.26)-(9.29) we can write a local gauge potential for $\tilde{F}_4$:

$$\tilde{F}_4 = \mathrm{d}\mathcal{H}_3 \ , \qquad F_7 = \tilde{F}_7 - \frac{1}{2}\mathcal{H}_3 \wedge \tilde{F}_4 \ , \tag{9.53}$$

where $\tilde{F}_7$ is a closed 7-form. With this we can rewrite the horizon integral as

$$\oint_H \left(\frac{1}{2}(C_3 - C_0\mathcal{H}_3) \wedge \tilde{F}_4 + C_0\tilde{F}_7\right) \ . \tag{9.54}$$

[4] In our units the charge of a single M2-brane is $\mu_{\text{M2}} = 2\pi/(2\pi\ell_p)^3$ and the unit charge of an M5-brane is $\mu_{\text{M5}} = 2\pi/(2\pi\ell_p)^6$.

The integral involving C_0 and $\tilde{F}_7$ has the structure of the potential-charge ($\Phi_{\text{M2}} Q_{\text{M2}}$) term that is standard in Smarr relations for black holes. Indeed, we will see that C_0 is constant at the horizon. Moreover, the integral of $\tilde{F}_7$ corresponds to the Page charge sourced by the branes, and hence measures the localised M2 charge present in the geometry through

$$Q_{\text{M2}} = \frac{\mu_{\text{M2}}}{(2\pi\ell_p)^6} \oint \tilde{F}_7. \tag{9.55}$$

We are left with

$$\frac{1}{16\pi G_N} \oint_H C_0 \tilde{F}_7 = \Phi_{\text{M2}} Q_{\text{M2}}, \tag{9.56}$$

where Φ_{M2} equals to the gauge potential C_0 evaluated at the horizon:

$$\Phi_{\text{M2}} = C_0|_H \ . \tag{9.57}$$

As for the other term in the integral (9.54), we will now argue that the three form $(C_3 - C_0 \mathcal{H}_3)$ restricted to the horizon is closed. The Einstein equation for 11-dimensional supergravity takes the form

$$R_{\mu\nu} - \frac{1}{2 \cdot 3!} G_{\mu\rho_1\rho_2\rho_3} G_\nu{}^{\rho_1\rho_2\rho_3} + \frac{1}{6} g_{\mu\nu} |G_4|^2 = 0 \ , \tag{9.58}$$

from which we derived eq. (9.38). At the Killing horizon of the timelike Killing vector ξ we have[5]

$$|\xi|^2 = 0 \quad \text{and} \quad \xi^\mu \xi^\nu R_{\mu\nu} = 0 \ . \tag{9.59}$$

Contracting the Einstein equation with ξ at the horizon yields

$$|\iota_\xi G_4|^2 = 0 \ . \tag{9.60}$$

Analogously we can write the Einstein equation in terms of the dual field strength G_7 and run the same argument to show that at the horizon

$$|\iota_\xi G_7|^2 = 0 \ . \tag{9.61}$$

Using the definitions (9.24) and (9.25), we can rewrite the previous equations as:

$$\mathrm{e}^{-4A} |\mathrm{e}^{3A+f} F_1|^2 = \mathrm{e}^{-4A} |\mathrm{d}C_0|^2 = 0 \ , \tag{9.62}$$

$$\mathrm{e}^{-4A} |\mathrm{e}^{3A+f} F_4|^2 = \mathrm{e}^{-4A} |\mathrm{d}C_3 - C_0 \tilde{F}_4|^2 = 0 \ . \tag{9.63}$$

It follows that C_0 is constant along the horizon as stated before and furthermore that $C_3 - C_0 \mathcal{H}_3$ restricted to the horizon is closed. The latter allows us to write

$$C_3 - C_0 \mathcal{H}_3 = \omega_3 + \text{exact} \ , \tag{9.64}$$

where ω_3 is harmonic at the horizon. Furthermore since $\mathrm{d}\tilde{F}_4 = 0$, the integral of $(C_3 - C_0 \mathcal{H}_3) \wedge \tilde{F}_4$ reduces to

$$\oint_H (C_3 - C_0 \mathcal{H}_3) \wedge \tilde{F}_4 = \oint_H \omega_3 \wedge \tilde{F}_4 = \frac{(2\pi\ell_p)^9}{\pi} \ \Phi_{\text{M5}} Q_{\text{M5}} \ . \tag{9.65}$$

[5]The second equality follows from the Raychaudhuri equation.

Here the M5-charge Q_{M5} is defined by

$$Q_{\text{M5}} = \frac{\mu_{\text{M5}}}{(2\pi\ell_p)^3}\int_{\mathcal{M}_4}\tilde{F}_4 \ , \tag{9.66}$$

where $\mathcal{M}_4$ is a submanifold of the horizon which is related to the Poincaré dual of ω_3 by a constant of proportionality $2\Phi_{\text{M5}}$. We are now in position to write Smarr's relation for a system of anti M2-branes normalised for the background energy of the CGLP background:

$$\mathcal{E} = \frac{7}{6}\frac{\kappa\mathcal{A}}{8\pi G_N} + \Phi_{\text{M2}}Q_{\text{M2}} + \Phi_{\text{M5}}Q_{\text{M5}} \ . \tag{9.67}$$

The numerical factor $7/6$ seems rather ad-hoc in this equation but is correct. We can see this by deriving the first law of black hole thermodynamics. It is easy to verify that κ scales with the area in a non-trivial way

$$[\kappa] = L^{-1} = [\mathcal{A}]^{-1/7} \ , \tag{9.68}$$

whereas the chemical potentials do not scale with the charge. Using this, the first law takes the expected form

$$\mathrm{d}\mathcal{E} = \frac{\kappa}{8\pi G_N}\mathrm{d}\mathcal{A} + \Phi_{\text{M2}}\ \mathrm{d}Q_{\text{M2}} + \Phi_{\text{M5}}\ \mathrm{d}Q_{\text{M5}} \ . \tag{9.69}$$

Relation to on-shell brane actions

In [168] a similar relation between brane charges and the cosmological constant of a compactification of type II supergravity was obtained. There the derivation relied on using delta functions in the equations of motion, which result from varying the brane worldvolume action. This is only relevant for extremal branes for which the worldvolume actions are known. We can also do this in 11-dimensional supergravity where the modified form equations of motion (9.26) take the form

$$\begin{aligned}\mathrm{d}F_7 + \frac{1}{2}\tilde{F}_4\wedge\tilde{F}_4 &= Q_{\text{M2}}\delta_8 - Q_{\text{M5}}\mathcal{F}_3\wedge\delta_5 \ , &(9.70)\\ \mathrm{d}\tilde{F}_4 &= -Q_{\text{M5}}\delta_5 \ . &(9.71)\end{aligned}$$

In these equations $\mathcal{F}_3$ is the self-dual tensor field living on the M5 brane. It is fixed by gauge invariance of the M5 action to be $\mathcal{F}_3 = \mathrm{d}b_2 + A_3$ with b_2 a 2-form and A_3 the gauge potential for G_4. The Einstein equation will also receive delta function contributions from the DBI actions of the branes but since we only use its external components in the derivation of the ADM energy, we only need to consider the couplings to form fields.

We can now repeat the evaluation of the ADM energy using delta functions in the equations of motion, following closely the calculation performed in the last two subsections. All equations remain unchanged up to (9.47), which now takes the form:

$$\begin{aligned}\mathrm{e}^{3A+f}\star_8\left(2|F_7|^2 + |\tilde{F}_4|^2\right) &= \mathrm{d}(C_3\wedge\tilde{F}_4 + 2C_0F_7)\\ &\quad -(C_3 - 2\mathcal{F}_3C_0)\wedge Q_{\text{M5}}\delta_5 - 2C_0Q_{\text{M2}}\delta_8 \ ,\end{aligned} \tag{9.72}$$

where b_2 is assumed to only have legs transverse to the M2 worldvolume. The first term of equation (9.43) is zero since we only discuss extremal branes, the second one reduces to an integral over the delta functions after cancelling the infinite contribution using the third term:

$$\mathcal{E} = Q_{\text{M2}}\int C_0\delta_8 + \frac{Q_{\text{M5}}}{2}\int(C_3 - 2\mathcal{F}_3C_0)\wedge\delta_5 \ . \tag{9.73}$$

Note that we have assumed that the delta functions take care of the singularities and that the total derivative in (9.72) is free of any singularities. Identifying the chemical potential Φ_{M2} with C_0 and Φ_{M5} with the integral

$$\Phi_{\text{M5}} = \frac{1}{2}\int (C_3 - 2\mathcal{F}_3 C_0) \wedge \delta_5 \ , \tag{9.74}$$

we reproduce the Smarr relation (9.67). It is interesting to note that the Smarr relation has the form of a sum of on-shell brane actions in analogy with the results of [168]. A recent paper has suggested that this is not an accident and in general the on-shell actions of branes will arise in the calculation of the on-shell gravitational action (or free energy) of a given system [196].

9.4 Smeared anti M2-branes

As a warm-up we will start by considering smeared antibranes. Smeared branes preserve the full SO(5) symmetry of the 4-sphere at the tip of the background. This implies that the gauge potential C_3 vanishes. Regularity of the horizon then implies that

$$\Phi_{\text{M2}} = C_0|_H = 0 \ , \tag{9.75}$$

as follows from eq. (9.63). Finally, it easy to verify that a Smarr relation for smeared branes cannot have a dipole contribution. This follows from eq. (9.65) together with the previous result that $C_3 = C_0 = 0$. The final Smarr relation for smeared branes then takes the form

$$\mathcal{E} = \frac{7}{6}\frac{\kappa\mathcal{A}}{8\pi G_N} \ . \tag{9.76}$$

Such a Smarr relation cannot be attributed to branes with antibrane charge. In particular an extremal limit would give zero energy to the Smarr relation which cannot represent a stack of supersymmetry breaking antibranes sitting at the tip of the geometry.

This result has previously been observed as singular backreaction of the antibranes on the flux background [162, 186, 189]. Our calculation does not allow for such a singularity since we assumed a regular horizon. If we would not have done so, then we could not conclude that Φ_{M2} vanishes, but we would then also see that the solution exhibits the previously found singularity, so the final outcome it is the same in both approaches.

9.5 Extremal anti M2-branes

In this section we use eq. (9.67) to constrain localised extremal antibrane solutions. Extremality implies that (9.67) reduces to

$$\mathcal{E} = \Phi_{\text{M2}} Q_{\text{M2}} + \Phi_{\text{M5}} Q_{\text{M5}} \ . \tag{9.77}$$

All quantities on the right hand side of (9.77) are evaluated in the limit of zero horizon area. For the set-up in question, the ADM energy measured at the UV is proportional to two times the red-shifted tension of the p anti M2-branes sitting at the tip of the throat [161],

$$\mathcal{E} = 2pT_{\text{M2}} e^{3A/2} \ . \tag{9.78}$$

Here e^{3A} is the red-shift factor generated by the warping of the background *evaluated* at the tip. This equation can be understood as follows. We fix the M2-charge at infinity to be the same as for a CGLP background with a given m, which is proportional to the total G_4 flux threading the 4-sphere M, see (9.17). This charge is calculated in Appendix 9.A.3 and it is given by

$$Q_{\text{CGLP}} = \frac{\mu_{\text{M2}}}{(2\pi\ell_p)^6}\int_{V_{5,2}} F_7 = \mu_{\text{M2}}\frac{81\pi^4 m^2}{(2\pi\ell_p)^6} = \mu_{\text{M2}}\frac{M^2}{4}\ . \tag{9.79}$$

For every anti M2-brane introduced into the background, m must be adjusted so that the charge remains constant. This is equivalent to adding an M2-brane together with every anti M2-brane at the tip of the geometry which explains the factor of 2 in eq. (9.78).

There is the further constraint from eq. (9.63) that restricted to the horizon,

$$\mathrm{d}C_3 = C_0\tilde{F}_4\ . \tag{9.80}$$

We now focus on the component of this equation along the 4-sphere at the tip. $\tilde{F}_4$ must be proportional to the volume form on the 4-sphere at the tip, since its integral there is proportional to M. The symmetries of the solution require that the only component of C_3 along the 4-sphere takes the form

$$f(\rho,\psi)\text{vol}_{S^3} \tag{9.81}$$

for a function f of the cone coordinate ρ and the azimuthal angle ψ on the 4-sphere with the antibranes sitting at $\psi = 0$. Since C_3 is globally defined by construction, we conclude that $f(\rho,\psi)$ should reach either a minimum or a maximum at the poles, and therefore $\mathrm{d}C_3$ restricted to $\psi = 0$ at the tip vanishes. Then eq. (9.80) yields:

$$C_0|_H = \Phi_{\text{M2}} = 0 \tag{9.82}$$

for pointlike antibranes. The conclusion is that the first term in the right-hand side of (9.77) cannot contribute and the Smarr relation reduces to

$$\mathcal{E} = \Phi_{\text{M5}}Q_{\text{M5}}\ . \tag{9.83}$$

Moreover, it is simple to see that for a pointlike horizon, just like for a smeared one, the M5-charge Q_{M5} as defined in (9.66) is zero. This can be seen by freely transforming the integration domain in the definition of Q_{M5} in (9.66) to infinity using the fact that $\tilde{F}_4$ is closed. Since we demand CGLP asymptotics, and therefore no M5 charge as measured at infinity, we obtain

$$Q_{\text{M5}} = 0\ . \tag{9.84}$$

This means that the Smarr relation will imply $\mathcal{E} = 0$, which cannot be because there is a stack of antibranes sitting at the tip which do contribute to $\mathcal{E}$. We conclude then that there is no way to satisfy the Smarr relation (9.77) for extremal anti M2-branes present at the tip.

Crucial steps in our argument above was that $\tilde{F}_4$ was regular at the horizon and that we could freely transform the integral of $\tilde{F}_4$ to infinity where it is zero, thereby leading to a contradiction. Once the antibranes polarise to spherical M5 branes with induced anti M2-charge both of these arguments break

down. First of all we *do* expect a singular $\tilde{F}_4$ close to an M5-brane to account for the charge. Secondly, since the topology of the polarised state is non-trivial one cannot freely transform the integral of $\tilde{F}_4$ to infinity. In fact, there will be obstructions whenever the integration surface $\mathcal{M}_4$ is non-trivial in homology on the horizon (see figure 9.2). Note that for M5-branes the horizon is not 7-dimensional as for M2-branes, so three of the directions in the integral

$$\oint_H (C_3 - C_0 \mathcal{H}_3) \wedge \tilde{F}_4 \ , \tag{9.85}$$

are *parallel* to the brane worldvolume. It is for this reason that we clarify that the integration surface in eq. (9.66) must be non-trivial as for example in figure 9.2 in order to give a non-vanishing contribution. As already noticed in section 8.5.3 for the polarized NS5 brane, the polarized antibranes have much in common with black ring solutions in five dimensions [190], whose thermodynamics was studied in [182]. The black rings had the surprising feature that the dipole charge entered into the first law. This was understood as a consequence of the horizon not being spherical as was previously assumed in the black hole thermodynamics literature. If Q_{M5}, which we will denote as the *dipole* charge, is non-vanishing we can obviously satisfy eq. (9.77).

In the set-up we are considering, we expect the M5-branes to source a component of C_3 extending along the three-sphere they are wrapping. In fact there is a very natural way of satisfying the Smarr relation by letting again $C_0|_H = \mathrm{d}C_3|_H = 0$ and $C_3 = f(\psi)\text{vol}_{S^3}$, so that the gauge potential C_3 equals the volume from on the brane times a function $f(\psi)$. Then the potential Φ_{M5} is proportional to $f(\psi_H)$, the function $f(\psi)$ evaluated at the polarisation radius. The Smarr relation (9.77) reduces to

$$2pT_{\text{M2}}\mathrm{e}^{3A} = \mathcal{E} = \Phi_{\text{M5}} Q_{\text{M5}} = \mu_{\text{M5}} f(\psi_H) \ . \tag{9.86}$$

Where we used that Q_{M5} is the charge of a single M5-brane, μ_{M5}. Comparing to the probe result (9.21) we can rewrite this as

$$f(\psi_H) = \frac{3\pi^2}{8hm}\frac{p}{M} \ . \tag{9.87}$$

We learn that in order to recover the probe result in the $p/M \to 0$ limit of the backreacted solution, the function $f(\psi_H)$ should scale as ψ_H^2.

9.6 Black branes

After having discussed extremal antibranes, let us take a look at what would be the effect of heating up the system away from extremality. The Smarr relation (9.67) now also includes non-zero contributions from the area,

$$\mathcal{E} = \frac{7}{6}\frac{\kappa\mathcal{A}}{8\pi G_N} + \Phi_{\text{M2}} Q_{\text{M2}} + \Phi_{\text{M5}} Q_{\text{M5}} \ . \tag{9.88}$$

Remember that

$$\frac{\kappa\mathcal{A}}{8\pi G_N} = TS \ , \tag{9.89}$$

where T is the temperature and S is the entropy of the black brane. Starting from the extremal state discussed in last section we expect a near-extremal antibrane to have a non-trivial horizon topology.

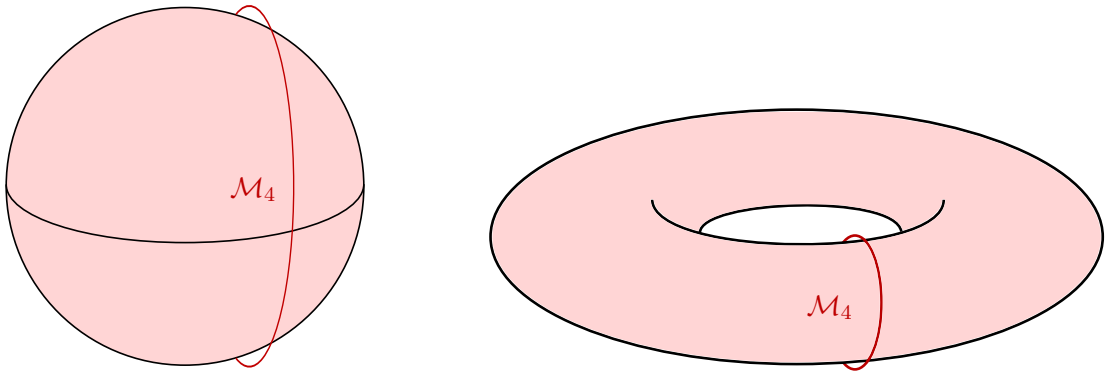

Figure 9.2: The left figure depicts a black M2 horizon for which the dipole charge vanishes. Since $\tilde{F}_4$ is regular and closed, the integration surface $\mathcal{M}_4$ can be shrunk down to zero size which implies that $Q_{\text{M5}} = 0$. In contrast the fact that polarised antibranes have a nontrivial horizon implies that the dipole charge can be non-zero.

This corresponds to a black M5-brane wrapping a contractible three-cycle on the four-sphere at the tip of the cone. The dipole M5-charge does not vanish (see figure 9.2) if the topology is non-trivial and Φ_{M2} can be small, or zero as in last section. As the horizon area increases we expect an instability towards a collapse to a spherical black brane which cannot support a dipole charge (see figure 9.2). A regular horizon then demands a cancellation between the form fields

$$\mathrm{d}C_3 - C_0\tilde{F}_4 = 0 \,, \tag{9.90}$$

when restricted to the horizon. This spherical phase, however, does not have a regular extremal limit and so we expect that below some critical area $\mathcal{A}_{\text{crit}}$ the dominant phase has non-trivial topology. In figure 9.3 we sketch these two phases as horizons in the $\rho - \psi$ plane close to the tip.

Let us remark that the spherical phase of anti M2-branes (as well as anti D3-branes) was studied in a linear approximation in [173], where the branes were inserted in a toy model background which captures some of the features of the set-up studied here. There it was observed that the spherical antibranes become singular as the area shrinks to zero size which is consistent with our results.

9.7 Conclusion

In this chapter we derived the Smarr relation for anti M2-branes (and their polarised state) immersed in the CGLP background [184]. We followed a similar procedure as in [168, 166] where the supergravity equations of motion were combined to find a constraint on the boundary conditions of the solutions at the antibrane location. We showed that these constraints arise when trying to satisfy the Smarr relation (9.1). We argued that smeared antibranes do not satisfy the Smarr relation without a singular horizon in agreement with [162, 186, 189]. We extended these results to localised extremal anti M2-branes in the CGLP background, and showed that these also cannot be regular while satisfying the Smarr relation. The relation can however be satisfied for an extremal polarised antibrane, *i.e.* an M5-brane with induced antibrane charge. A crucial feature of the polarised brane is that the dipole

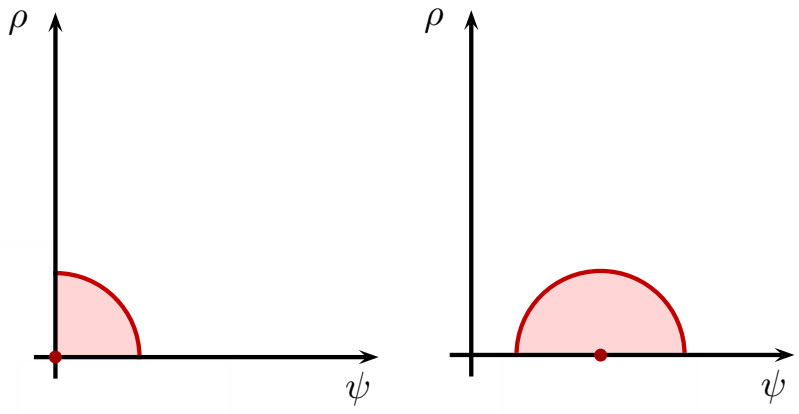

Figure 9.3: The left figure represents a spherical black M2 horizon for which Q_{M5} vanishes. The right figure depicts a non-extremal M5-brane with induced antibrane charge. For small horizon area we expect the latter to be the dominant phase.

M5-charge is nonzero. We do therefore not find a contradiction with the probe results of Klebanov and Pufu [161]. Let us stress that moving away from smeared branes and discussing fully localised branes was crucial to reach this conclusion. Finally, by combining the probe results with ours, we give boundary values for the form fields that could serve as starting points for numerical study of the full supergravity solution.

We briefly discussed non-extremal antibranes where we expect at least two phases differing in their horizon topology. We argued that an antibrane with trivial horizon area is unstable towards a black ring-like state for a small horizon area. We leave a closer study of the different phases of antibranes in flux backgrounds and their instabilities to future research. The technology used in this chapter could also be employed to study black hole microstate backgrounds that make use of antibranes as their method of breaking supersymmetry. The antibrane charge is carried by a non-supersymmetric supertube that polarises and carries dipole charge. It would certainly be interesting to analyse whether conditions posed by the Smarr relation can be used to evaluate the accuracy of probe calculations for supersymmetric and non-supersymmetric supertubes.

9.A Appendix

9.A.1 ADM energy for *p*-branes in general backgrounds

In this appendix we extend the Komar integrals for asymptotically flat black branes of [194] to black branes with arbitrary asymptotics. This is the Noether procedure presented for instance in [197], namely the its Section 4.1.2, where it is explained that the Einstein-Hilbert action, as it is invariant under general coordinate transformation, it let us define a Noether current which will help us to define the Komar mass (in its Section 6.2). What is more important is that, in the same Section 4.1.2, we are learned how to by adding boundary terms in the action this will we can correct or renormalize conserved quantities that otherwise will be infinite. This method leads to Komar-like integrals and is closely related to the approach of [198], which one can use to calculate the energy of a p-brane in

D dimensions with an asymptotically flat transverse space [194]. So the moral of the history is that the main ideas of [194] generalize to non-asymptotically flat p-branes in a natural way, by adding a counter-term to the action that takes care of the infinite contribution of the background.

First of all, we consider the solution obtained by dimensionally reducing along the p spatial dimensions of the brane. The reason for doing this is that if we are willing to work with Komar surface integrals, we have to acknowledge the fact that they are are *uniquely* defined for $p = 0$ (up to a normalisation factor) as opposed to $p > 0$, where the formula for the energy density it is not an obvious generalization of the $p = 0$ case, because there will be contributions of the brane tension as well [194]. Luckily it is easy to avoid this subtlety performing first the dimensional reduction and reach the $p = 0$ picture. To this end, we write the metric as a warped product

$$\mathrm{d}s_D^2 = g_{IJ}(x)\mathrm{d}x^I\mathrm{d}x^J + v(x)g_{mn}(y)\mathrm{d}y^m\mathrm{d}y^n \ , \tag{9.91}$$

with $I, J = 0, p+1, p+2, \ldots, D-1$ and $m, n = 1, 2, \ldots, p$. We will assume that the solution is maximally symmetric along the p spatial directions of the brane. In the D-dimensional theory, the Einstein-Hilbert term in the action is

$$\frac{1}{16\pi G_N^{(D)}}\int \mathrm{d}^D x\sqrt{g}R = \frac{1}{16\pi G_N^{(D)}}\int \mathrm{d}^{D-p}x\mathrm{d}^p y\sqrt{-g_{D-p}}\sqrt{g_p}\ v^{p/2}R \ , \tag{9.92}$$

where g_{D-p} and g_p are the determinants of the $(D-p)$ and p-dimensional metrics, respectively. Let us now define

$$\tilde{g}_{IJ} = v^{\frac{p}{D-p-2}}g_{IJ} \ . \tag{9.93}$$

For this tilde metric $\tilde{g}_{IJ}$, one has

$$\sqrt{-\tilde{g}_{D-p}}\tilde{R}_{D-p} = \sqrt{-g_{D-p}}v^{p/2}R_{D-p} + (\cdots) \ , \tag{9.94}$$

where $(\cdots)$ are terms containing the vector and scalar fields that we get from the metric when dimensionally reducing. With the transformation to $\tilde{g}_{IJ}$ we get the usual Einstein-Hilbert term in the reduced action, with Newton's constants related as usual through

$$G_N^{(D)} = G_N^{(D-p)}\cdot \mathrm{Vol}_p \ , \qquad \mathrm{Vol}_p = \int \mathrm{d}^p y\sqrt{g_p} \ . \tag{9.95}$$

Our solution is here just a point-like black hole, for which we can use the Noether approach in order to compute its mass as explained in [197]. To do this, we need to find a one-form ζ such that the combination $(\mathrm{d}\tilde{\eta} + \zeta\wedge\tilde{\eta})$ vanishes asymptotically, and is identically zero for the background metric. Here, $\tilde{\eta}$ is the timelike Killing vector of the tilde metric. To find this ζ, we can can evaluate $\tilde{\eta}$ for the background:

$$\tilde{\eta} = \tilde{g}_{00}\mathrm{d}t = e^{\frac{2(D-2)}{D-p-2}A^B}\mathrm{d}t \tag{9.96}$$

$$\mathrm{d}\tilde{\eta} = \frac{2(D-2)}{D-p-2}\mathrm{d}A^B\wedge\tilde{\eta} \ , \tag{9.97}$$

where e^{2A^B} is the warp factor of the background solution. This implies that

$$\zeta = -\frac{2(D-2)}{D-p-2}\mathrm{d}A^B. \tag{9.98}$$

We are now in state of calculating the ADM energy. It is given by [197, 194]

$$M = N \oint \tilde{\star}_{D-p} \left(\mathrm{d}\tilde{\eta} + \zeta \wedge \tilde{\eta} \right) , \qquad N \equiv -\frac{1}{16\pi G_N^{(D-p)}} \frac{D-p-2}{D-p-3} . \tag{9.99}$$

This formula follows from adding a total derivative $\mathrm{d}\tilde{\star}_{D-p}\zeta$ to the original Lagrangian [197], which will serve as a counter-term for the infinite contribution of the background to the energy. We remark that

$$\tilde{\star}_{D-p}(\mathrm{d}t \wedge \mathrm{d}r) = e^{\frac{p(D-p-4)}{D-p-2}A} \star_{D-p} (\mathrm{d}t \wedge \mathrm{d}r) . \tag{9.100}$$

Further, we know that $\tilde{\eta} = e^{\frac{2p}{D-p-2}A}\eta$, so our expression for the mass becomes

$$M = N \oint e^{pA} \star_{D-p} \left[\mathrm{d}\eta + \frac{p}{D-p-2} \mathrm{d}(2A) \wedge \eta + \zeta \wedge \eta \right] . \tag{9.101}$$

For the next step, we need the following relation:[6]

$$\star_D \mathrm{d}y^1 \wedge \cdots \wedge \mathrm{d}y^p \wedge \mathrm{d}t \wedge \mathrm{d}r = e^{-pA} \star_{D-p} \mathrm{d}t \wedge \mathrm{d}r , \tag{9.105}$$

so that

$$M = N \oint e^{2pA} \star_D \mathrm{d}y^1 \wedge \cdots \wedge \mathrm{d}y^p \wedge \left[\mathrm{d}\eta + \frac{p}{D-p-2} \mathrm{d}(2A) \wedge \eta + \zeta \wedge \eta \right] . \tag{9.106}$$

Finally, recalling our definitions of the one forms associated with the spatial Killing vectors

$$\lambda_i = g_{ii} \mathrm{d}y^i = e^{2A} \mathrm{d}y^i , \tag{9.107}$$

we get

$$M = -\frac{1}{16\pi G_N^{(D)}} \oint \star_D \Big[\mathrm{d}\eta \wedge \lambda_1 \wedge \cdots \wedge \lambda_p + \frac{1}{D-p-3} \mathrm{d}(\eta \wedge \lambda_1 \wedge \cdots \wedge \lambda_p) + \xi \wedge \eta \wedge \lambda_1 \wedge \cdots \wedge \lambda_p \Big] , \tag{9.108}$$

where we defined

$$\xi \equiv \frac{D-p-2}{D-p-3} \zeta . \tag{9.109}$$

For our set-up, we have

$$\xi = \mathrm{d} \log H . \tag{9.110}$$

[6] We normalise the Hodge operators in different dimensions by demanding $\mathrm{vol}_D = \mathrm{vol}_p \wedge \mathrm{vol}_{D-p}$, where

$$\mathrm{vol}_D = \sqrt{g_D} \mathrm{d}t \wedge \mathrm{d}r \wedge \mathrm{d}y^1 \wedge \cdots \wedge \mathrm{d}y^p \wedge \mathrm{d}x^{p+2} \wedge \cdots \wedge \mathrm{d}x^{D-1} , \tag{9.102}$$

$$\mathrm{vol}_p = \sqrt{g_p} \mathrm{d}y^1 \wedge \cdots \wedge \mathrm{d}y^p , \tag{9.103}$$

$$\mathrm{vol}_{D-p} = \sqrt{g_{D-p}} \mathrm{d}t \wedge \mathrm{d}r \wedge \mathrm{d}x^{p+2} \wedge \cdots \wedge \mathrm{d}x^{D-1} . \tag{9.104}$$

9.A.2 Surface gravity and horizon area

In this appendix we derive the form of the $\kappa\mathcal{A}$ term appearing in (9.46) in a general set-up, with that equation being a special case. Let us consider a static metric of the form

$$\mathrm{d}s^2 = -e^{2f(r)}\tilde{g}_{00}\mathrm{d}t^2 + g_{\mu\nu}\mathrm{d}x^\mu\mathrm{d}x^\nu + e^{-2f(r)}\mathrm{d}r^2 + g_{ij}\mathrm{d}x^i\mathrm{d}x^j \ , \tag{9.111}$$

where $\mu,\nu = 1,\ldots,p$ and $i,j = p+2,\ldots,D-1$. The factor e^{2f} vanishes at the horizon, while the component $\tilde{g}_{00}$ is regular.

For the timelike Killing vector with components $\xi^\mu = \delta^\mu_0$, the surface gravity κ is defined as

$$\kappa = \sqrt{\partial_\mu V \partial^\mu V} \ , \qquad V = \sqrt{-\xi_\mu \xi^\mu} \ , \tag{9.112}$$

with both terms evaluated at the horizon. Clearly for the metric at hands

$$V = \sqrt{e^{2f}\tilde{g}_{00}} \ , \tag{9.113}$$

so that at the horizon

$$\partial_\mu V \partial^\mu V = g^{rr}(\partial_r V)^2 = \frac{(\partial_r e^{2f})^2 g^{rr}\tilde{g}_{00}}{4f} = \frac{(\partial_r e^{2f})^2\tilde{g}_{00}}{4} \ , \tag{9.114}$$

where we have taken into account the fact that there $e^{2f} \to 0$. Hence

$$\kappa = \frac{1}{2}\sqrt{\tilde{g}_{00}}\partial_r e^{2f} \ . \tag{9.115}$$

Next, we have

$$\mathrm{d}\eta = \mathrm{d}(-e^{2f}\tilde{g}_{00}\mathrm{d}t) = -\tilde{g}_{00}(\partial_r e^{2f})\mathrm{d}r\wedge\mathrm{d}t \ . \tag{9.116}$$

Therefore

$$\star_D\, \mathrm{d}\eta\wedge\lambda_1\wedge\cdots\wedge\lambda_p = -\sqrt{\tilde{g}_{00}}(\partial_r e^{2f})\sqrt{g_p}\,\mathrm{vol}_{D-2-p} \tag{9.117}$$

$$= -2\kappa\sqrt{g_p}\,\mathrm{vol}_{D-2-p} \tag{9.118}$$

at the horizon, so that

$$\oint_H \star_D\, \mathrm{d}\eta\wedge\lambda_1\wedge\cdots\wedge\lambda_p = -2\kappa\mathcal{A}_{\text{eff}} \ , \tag{9.119}$$

with

$$\mathcal{A}_{\text{eff}} = \oint_H \sqrt{g_p}\mathrm{vol}_{D-2-p} \ . \tag{9.120}$$

In the main text we avoid writing explicitly the subscript of $\mathcal{A}_{\text{eff}}$.

9.A.3 M2 charge of the CGLP background

The total M2 charge of the background as measured at the UV can be computed by integrating G_7 along the base of the cone for large values of the radial coordinate ρ. Asymptotically, from (9.15) we see that

$$H(\rho) \approx c_0 + 2^{\frac{3}{2}} 3^{\frac{3}{4}} m^2 \rho^{-\frac{9}{4}} \ . \tag{9.121}$$

At the UV, the component F_7 of G_7 with all its legs on the base of the cone is

$$F_7 \approx 2^{\frac{1}{2}} 3^{\frac{11}{4}} m^2 \rho^{-\frac{13}{4}} \star_8 \mathrm{d}\rho \ . \tag{9.122}$$

As explained in [161], it is useful to perform the coordinate transformation

$$\rho = \frac{3^{\frac{1}{3}}}{4} r^{\frac{8}{3}}, \tag{9.123}$$

in which the metric of the cone becomes $\mathrm{d}s_8^2 = \mathrm{d}r^2 + r^2 \mathrm{d}V_{5,2}^2$. Then we find

$$F_7 \approx 2^7 3 m^2 r^{-7} \star_8 \mathrm{d}r \ . \tag{9.124}$$

From the form of the metric, it is clear that $\star_8 \mathrm{d}r = r^7 \mathrm{vol}_{V_{5,2}}$. The volume of the base is calculated in [199], and it turns out to be equal to $3^3\pi^4/2^7$. Therefore the total M2 Maxwell charge of the CGLP background is

$$Q_{\text{CGLP}} = \frac{\mu_{\text{M2}}}{(2\pi\ell_p)^6} \int_{V_{5,2}} F_7 = \mu_{\text{M2}} \frac{81\pi^4 m^2}{(2\pi\ell_p)^6} = \mu_{\text{M2}} \frac{M^2}{4} \ . \tag{9.125}$$

9.A.4 ADM energy for D-branes

In this appendix we present a general derivation of the ADM energy for Dp-branes immersed in flux backgrounds of type II supergravity with $p+1$-dimensional maximally symmetric spacetime. We assume a background three-form flux H_3 and $(6-p)$-form flux F_{6-p} which are internal and support a smooth asymptotically Ricci flat metric. We also allow for a fluctuating internal $(8-p)$-form F_{8-p}. Asymptotically AdS metrics can be treated in a similar way as was done in the chapter.

Once the Dp-brane is introduced into the game, we expect a backreaction onto the metric and the form fields. The metric splits into the worldvolume metric and a transverse part

$$\mathrm{d}s^2 = \mathrm{e}^{2A} \left(-\mathrm{e}^{2f} \mathrm{d}t^2 + \mathrm{d}x_p^2 \right) + \mathrm{d}s_{9-p}^2 \ , \tag{9.126}$$

where t and x_p span the worldvolume coordinates of the antibrane.

The trace reversed Einstein equation (in Einstein frame) along the brane worldvolume is

$$R_{\mu\nu} = -\frac{1}{16} \left(2\mathrm{e}^{-\phi} |H_3|^2 + (7-p) \mathrm{e}^{\frac{p-3}{2}\phi} |F_{8-p}|^2 + (5-p) \mathrm{e}^{\frac{p-1}{2}\phi} |F_{6-p}|^2 \right) g_{\mu\nu}. \tag{9.127}$$

The form field equations can be written in terms of the magnetic dual forms

$$\begin{aligned} \mathrm{d}F_{p+2} &= 0 \ , & (9.128) \\ \mathrm{d}F_{p+4} - H_3 \wedge F_{p+2} &= 0 \ , & (9.129) \\ \mathrm{d}H_7 + \eta F_{6-p} \wedge \sigma(F_{p+2}) &= 0 \ , & (9.130) \end{aligned}$$

where $\eta = (-1)^p$ and the operator σ reverses all form indices. The forms in these equations are related to the ones in the Einstein equation by the usual duality rules

$$H_7 = \mathrm{e}^{-\phi} \star_{10} H \ , \quad F_{p+2} = \mathrm{e}^{\frac{p-3}{2}\phi} \star_{10} \sigma(F_{8-p}) \ , \quad F_{p+4} = \mathrm{e}^{\frac{p-1}{2}\phi} \star_{10} \sigma(F_{6-p}) \ . \tag{9.131}$$

Using the form equations above we write a set of globally defined gauge potentials:

$$\begin{aligned} F_{p+2} &= -\eta\, \sigma(\mathrm{vol}_{p+1}) \wedge \mathrm{d}A_0 \ , & (9.132)\\ F_{p+4} &= -\eta\, \sigma(\mathrm{vol}_{p+1}) \wedge [\mathrm{d}A_2 + HA_0] \ , & (9.133)\\ H_7 &= \eta\, \mathrm{vol}_{p+1} \wedge [\mathrm{d}A_{5-p} - \eta F_{6+p} A_0] \ . & (9.134) \end{aligned}$$

The existence of these potentials is not affected by the presence of the anti-Dp brane or its polarised states. We can now rewrite the right hand side of the Einstein equation as

$$\begin{aligned} &\star_{10} 1 \left(2\mathrm{e}^{-\phi} |H|^2 + (7-p)\mathrm{e}^{(p-3)\phi/2} |F_{8-p}|^2 + (5-p)\mathrm{e}^{(p-1)\phi/2} |F_{6-p}|^2 \right) \\ &= -\mathrm{vol}_{p+1} \wedge \mathrm{d}\left(-2A_{5-p} \wedge H - (7-p) A_0\, F_{8-p} - (5-p) A_2 \wedge F_{6-p} \right) \ . \end{aligned} \tag{9.135}$$

Since we want to end up with a ADM energy *density* we redefine the potentials we work with. Finally using the form of the metric the worldvolume Einstein equations can now be written as two PDEs

$$\begin{aligned} \mathrm{d}\left(\mathrm{e}^{(p+1)A+f} \star_{9-p} \mathrm{d}f \right) &= 0 \ , & (9.136)\\ \mathrm{d}\left(\mathrm{e}^{(p+1)A+f} \star_{9-p} \mathrm{d}A - \mathcal{B} \right) &= 0 \ . & (9.137) \end{aligned}$$

where

$$\mathcal{B} = -\frac{1}{16} \left[2A_{5-p} \wedge H + (7-p) A_0\, F_{8-p} + (5-p) A_2 \wedge F_{6-p} \right] \ . \tag{9.138}$$

Evaluating the general ADM energy density formula (9.34) we obtain

$$\mathcal{E} = \frac{1}{16\pi G_N} \frac{1}{7-p} \oint_\infty \mathrm{e}^{(p+1)A+f} \star_{9-p} \left[16\mathrm{d}A + 2(8-p)\mathrm{d}f \right] \ . \tag{9.139}$$

The equations (9.136-9.137) allow us to move the integration surface down to the horizon

$$16\pi G_N \mathcal{E} = \frac{1}{7-p} \oint_H \left\{ \mathrm{e}^{(p+1)A+f} \star_{9-p} \left[16\mathrm{d}A + 2(8-p)\mathrm{d}f \right] + 16\mathcal{B} \right\} - \frac{1}{7-p} \oint_\infty 16\mathcal{B} \tag{9.140}$$

At infinity we expect that $A_{5-p}, A_2 \to 0$ while the $A_0 \to 1$. The last term will therefore give the Dp charge of the background, and we can normalise this away in the same way as in the main text by including a counter-term in the action. Here we will simply drop this finite term from the expression. The first term in the integrand gives the surface gravity times the area as explained in appendix 9.A.2. This leaves us with

$$\mathcal{E} = \frac{8-p}{7-p} \frac{\kappa \mathcal{A}}{8\pi G_N} + \frac{1}{16\pi G_N} \oint_H \frac{16\mathcal{B}}{7-p} \ . \tag{9.141}$$

At this stage we define local gauge potentials at the horizon

$$\mathrm{d}B_2 = H_3 \ , \quad \mathrm{d}B_{5-p} = \eta F_{6-p} \ . \tag{9.142}$$

These can be used to rewrite $\mathcal{B}$ at the horizon

$$16\mathcal{B} = -2(A_{5-p} + A_0 B_{5-p}) \wedge H_3 - (7-p) A_0 \, \tilde{F}_{8-p} - (5-p)(A_2 + A_0 B_2) \wedge F_{6-p} \,, \tag{9.143}$$

where

$$\tilde{F}_{8-p} = F_{8-p} - \frac{5-p}{7-p} B_2 \wedge F_{6-p} - \frac{2}{7-p} B_{5-p} \wedge H_3 \,, \tag{9.144}$$

and is closed. The Einstein equations imply that on a regular horizon[7]

$$H_7 \,, \quad F_{p+4} \,, \quad F_{p+2} \tag{9.145}$$

go to zero, which implies that the forms

$$A_0 \,, \quad A_{5-p} + A_0 B_{5-p} \,, \quad A_2 + A_0 B_2 \tag{9.146}$$

are closed when restricted to the horizon. This implies that on the horizon we can write

$$A_{5-p} + A_0 B_{5-p} = \omega_{5-p} + \text{exact} \,, \quad A_2 + A_0 B_2 = \omega_2 + \text{exact} \,, \tag{9.147}$$

where ω_{5-p} and ω_2 are harmonic. Repeating the same arguments as in the main text, *i.e.* identifying the Poincaré duals of the harmonic forms and defining the chemical potentials as their proportionality factors, we are left with

$$\mathcal{E} = \frac{8-p}{7-p} \frac{\kappa \mathcal{A}}{8\pi G_N} + \Phi_{\mathrm{D}p} Q_{\mathrm{D}p} + \Phi_{\mathrm{D}(p+2)} Q_{\mathrm{D}(p+2)} + \Phi_{\mathrm{NS5}} Q_{\mathrm{NS5}} \,. \tag{9.148}$$

All the terms in this expression are analogous to the ones we discussed in the main text. $Q_{\mathrm{D}p}$ is the Page charge, defined as the integral of $\tilde{F}_{8-p}$ over the horizon.

[7] Here we make use of the fact that the D-branes in question are at finite temperature, which regularises their horizon. All extremal D-branes have singular horizon except for the D3-brane.

Part IV

Prospect

“Some people see things that are and ask, Why? Some people dream of things that never were and ask, Why not? Some people have to go to work and don’t have time for all that.”

— George Carlin

Chapter 10

Epilogue

In this section, we discuss our most relevant results in the context of how do they complement ongoing research, the puzzles that they leave open, and possible future studies where they can be used as a starting point.

10.1 Non-supersymmetric Black Holes Holography

The understanding of the microscopics of general asymptotically flat black holes in four- and five-dimensions (which includes the Kerr black hole) remains incomplete. Our focus in this thesis was the subtracted geometry program, where we concluded that further study is needed on its holographic properties. It is desirable to know what is the underlying structure giving rise to behavior that, in principle, one would attach to a dual CFT_2.

As we have shown in Part II, the quasinormal frequencies of static subtracted geometries qualitatively depart from the BTZ black hole spectrum, casting doubts then on the subtracted geometry/CFT_2 conjecture. However, it is important to remember that this result holds only for static (non-rotating) subtracted black holes. Adding rotation is a natural generalization of our work, and it would help to increase the knowledge over the underlying structure of the subtracted geometry/CFT_2. It would also be interesting to study the conformal properties of subtracted geometries in the magnetic frame, which after an uplift are locally a product of AdS_3 and a sphere. If this non-uplifted subtracted geometry also shows non-conformal features, just as in the electric frame, it would be interesting to see how the uplift restores the conformal symmetry.

Another interesting research direction is the holographic study of subtracted geometries. Subtracted geometries have non-standard time scaling, reminiscent of Schrodinger [200, 86] and hyperscaling violating Lifshitz spacetimes [87]. These non-relativistic spacetimes are known for their applications to condensed matter systems via the gauge/gravity duality [201, 202, 203]. They also extend our knowledge of this duality beyond the traditional AdS/CFT, allowing a better understanding of the holographic relation between field theories and gravity. It is interesting then to see if subtracted geometries can make contributions in the same fashion of the above-mentioned non-relativistic space-

times.

10.2 Metastable Nonsupersymmetric Vacua

In Part III of this thesis, we discussed metastable states in string theory. Related to this, we consider that there are two studies interesting to pursue. One is to apply the same method used in chapter 8 and 9 to scrutinize supergravity configurations consisting of antibrane charged supertubes on supersymmetric black holes microstate geometries. At the probe level, this configuration gives rise to non-supersymmetric stable and metastable states [126], in an analogous way to the NS5 or M5 branes systems studied in part III. These supertube configurations are interpreted as non-extremal black holes microstates geometries [126], which are needed to test the fuzzball proposal beyond extremality. However, these probe results are just a proxy for supergravity solutions; the existence of a full solution awaits to be proven. The method used in this thesis can give valuable insights into the existence of a full solution by pointing out which boundary conditions allow for a physical solution. This investigation is a natural continuation of our findings related to the NS5 and M5 brane cases.

Regarding the proof of the existence of the NS5, M5 or supertube non-supersymmetric (meta)stable state solutions, though technically challenging, we are positive about numerical techniques that might be able to prove/disprove the existence of these solutions. In this thesis, we gave valuable input by showing a method useful for finding the boundary conditions that physical antibrane metastable states should satisfy. These boundary conditions are an important ingredient in their further numerical construction. Interesting findings on finite temperature smeared M2 branes in asymptotically CGLP backgrounds have been revealed in [160], where it has been shown that negatively charged smeared M2 black branes do not exist. This can be interpreted as that the unphysical singularity of the anti-M2 branes cannot be cloaked behind a horizon, agreeing with our findings in chapter 9. We hope that similar numerical techniques will be applied to the localized antibrane settings studied in chapters 8 and 9. This would give valuable insight about the existence of antibranes metastable states, which in its ten-dimensional version, is relevant for de Sitter construction with supersymmetry breaking antibranes in string theory.

Bibliography

[1] T. Andrade, A. Castro, and D. Cohen-Maldonado, "The spectrum of static subtracted geometries," *Class.Quant.Grav. 34 (2017) no.9, 095009*, 2017.

[2] D. Cohen-Maldonado, J. Diaz, T. van Riet, and B. Vercnocke, "Observations on fluxes near anti-branes," *JHEP*, vol. 01, p. 126, 2016.

[3] D. Cohen-Maldonado, J. Diaz, and F. F. Gautason, "Polarised antibranes from smarr relations," *JHEP 1605 (2016) 175*, 2016.

[4] D. Cohen-Maldonado, J. Diaz, T. Van Riet, and B. Vercnocke, "From black holes to flux throats: polarization can resolve the singularity," in *21st European String Workshop: The String Theory Universe Leuven, Belgium, September 7-11, 2015*, 2015.

[5] M. Bañados and D. Cohen, "Short note on gravity with tensor auxiliary fields," *Phys.Rev. D89 (2014) no.4, 047505*, 2013.

[6] J. D. Bekenstein, "Black holes and entropy," *Phys. Rev. D 7, 2333*, 1973.

[7] S. W. Hawking, "Black holes and thermodynamics," *Phys. Rev. D 13, 191*, 1976.

[8] J. Brown and M. Henneaux, "Central charges in the canonical realization of asymptotic symmetries: An example from three-dimensional gravity," *Commun.Math.Phys. 104 (1986) 207-226*, 1986.

[9] M. Banados, C. Teitelboim, and J. Zanelli, "The black hole in three-dimensional space-time," *Phys.Rev.Lett. 69 (1992) 1849-1851*, 1992.

[10] A. Strominger and C. Vafa, "Microscopic origin of the bekenstein-hawking entropy," *Phys.Lett. B379 (1996) 99-104*, 1996.

[11] J. M. Maldacena and A. Strominger, "Statistical entropy of four-dimensional extremal black holes," *Phys. Rev. Lett. 77*, 1996.

[12] C. Callan and J. Maldacena, "D-brane approach to black hole quantum mechanics," *Nuclear Physics B*, 1996.

[13] G. Horowitz and A. Strominger, "Counting states of near-extremal black holes," *Physical Review Letters*, 1996.

[14] M. Middleton, "Black hole spin: theory and observation," *arXiv:1507.06153*, 2015.

[15] J. E. McClintock, R. Shafee, R. Narayan, R. A. Remillard, S. W. Davis, and L.-X. Li, "The spin of the near-extreme kerr black hole grs 1915+105," *Astrophys.J. 652 (2006) 518-539*, 2006.

[16] L. Gou, J. E. McClintock, M. J. Reid, J. A. Orosz, J. F. Steiner, R. Narayan, J. Xiang, R. A. Remillard, K. A. Arnaud, and S. W. Davis, "The extreme spin of the black hole in cygnus x-1," *Astrophys.J. 742 (2011) 85*, 2011.

[17] L. Gou and et al., "Confirmation via the continuum-fitting method that the spin of the black hole in cygnus x-1 is extreme," *Astrophys.J. 790 (2014) no.1, 29*, 2013.

[18] M. Guica, T. Hartman, W. Song, and A. Strominger, "The Kerr/CFT Correspondence," *Phys. Rev.*, vol. D80, p. 124008, 2009.

[19] A. Castro and F. Larsen, "Near extremal kerr entropy from ads(2) quantum gravity," *JHEP 0912 (2009) 037*, 2009.

[20] A. P. Porfyriadis and A. Strominger, "Gravity waves from the kerr/cft correspondence," *Phys.Rev. D90 (2014) no.4, 044038*, 2014.

[21] S. Hadar, A. P. Porfyriadis, and A. Strominger, "Gravity waves from extreme-mass-ratio plunges into kerr black holes," *Phys.Rev. D90 (2014) no.6, 064045*, 2014.

[22] S. E. Gralla, A. P. Porfyriadis, and N. Warburton, "Particle on the innermost stable circular orbit of a rapidly spinning black hole," *Phys.Rev. D92 (2015) no.6, 064029*, 2015.

[23] S. Hadar and A. P. Porfyriadis, "Whirling orbits around twirling black holes from conformal symmetry," *JHEP 1703 (2017) 014*, 2016.

[24] S. E. Gralla, S. A. Hughes, and N. Warburton, "Inspiral into gargantua," *Class.Quant.Grav. 33 (2016) no.15, 155002*, 2016.

[25] G. Compère, K. Fransen, T. Hertog, and J. Long, "Gravitational waves from plunges into gargantua," *arXiv:1712.07130*, 2017.

[26] M. Cvetic and D. Youm, "Entropy of nonextreme charged rotating black holes in string theory," *Phys.Rev. D54 (1996) 2612-2620*, 1996.

[27] A. Castro, A. Maloney, and A. Strominger, "Hidden Conformal Symmetry of the Kerr Black Hole," *Phys. Rev.*, vol. D82, p. 024008, 2010.

[28] M. Cvetic and F. Larsen, "Conformal Symmetry for General Black Holes," *JHEP*, vol. 02, p. 122, 2012.

[29] M. Cvetic and F. Larsen, "Conformal Symmetry for Black Holes in Four Dimensions," *JHEP*, vol. 09, p. 076, 2012.

[30] M. Cvetic, M. Guica, and Z. H. Saleem, "General black holes, untwisted," *JHEP*, vol. 09, p. 017, 2013.

[31] A. Virmani, "Subtracted Geometry From Harrison Transformations," *JHEP*, vol. 07, p. 086, 2012.

[32] A. Sahay and A. Virmani, "Subtracted Geometry from Harrison Transformations: II," *JHEP*, vol. 07, p. 089, 2013.

[33] D. Fursaev and D. Vassilevich, *Operators, Geometry and Quanta: Methods of Spectral Geometry in Quantum Field Theory*. Springer, 2011.

[34] M. Kac, "Can one hear the shape of a drum?," *Am. Math. Mon. 73,1–23*, (1966).

[35] W. Press, "Long wave trains of gravitational waves from a vibrating black hole," *Astrophys. J., 170, L105–L108*, 1971.

[36] K. D. Kokkotas and B. G. Schmidt, "Quasi-normal modes of stars and black holes," *Living Rev.Rel. 2 (1999) 2*, 1999.

[37] P. K. Kovtun and A. O. Starinets, "Quasinormal modes and holography," *Phys.Rev. D72 (2005) 086009*, 2005.

[38] E. Berti, V. Cardoso, and A. O. Starinets, "Quasinormal modes of black holes and black branes," *Class. Quant. Grav.*, vol. 26, p. 163001, 2009.

[39] R. Konoplya and A. Zhidenko, "Quasinormal modes of black holes: From astrophysics to string theory," *Rev.Mod.Phys. 83 (2011) 793-836*, 2011.

[40] L. Scientific, V. Collaborations, and B. A. C. et al.), "Observation of gravitational waves from a binary black hole merger," *Phys.Rev.Lett. 116 (2016) no.6, 061102*, 2016.

[41] O. Dreyer, B. J. Kelly, B. Krishnan, L. S. Finn, D. Garrison, and R. Lopez-Aleman, "Black hole spectroscopy: Testing general relativity through gravitational wave observations," *Class.Quant.Grav. 21 (2004) 787-804*, 2003.

[42] N. Yunes and X. Siemens, "Gravitational-wave tests of general relativity with ground-based detectors and pulsar timing-arrays," *Living Rev.Rel. 16 (2013) 9*, 2013.

[43] L. Scientific, rgo Collaborations, and B. A. et al., "Tests of general relativity with gw150914," *Phys.Rev.Lett. 116 (2016) no.22, 221101*, 2016.

[44] V. Cardoso, E. Franzin, and P. Pani, "Is the gravitational-wave ringdown a probe of the event horizon?," *Phys.Rev.Lett. 116 (2016) no.17, 171101*, 2016.

[45] D. Birmingham, I. Sachs, and S. N. Solodukhin, "Conformal field theory interpretation of black hole quasinormal modes," *Phys. Rev. Lett.*, vol. 88, p. 151301, 2002.

[46] M. Cvetic and G. W. Gibbons, "Conformal Symmetry of a Black Hole as a Scaling Limit: A Black Hole in an Asymptotically Conical Box," *JHEP*, vol. 07, p. 014, 2012.

[47] M. Baggio, J. de Boer, J. I. Jottar, and D. R. Mayerson, "Conformal Symmetry for Black Holes in Four Dimensions and Irrelevant Deformations," *JHEP*, vol. 04, p. 084, 2013.

[48] M. Cvetic, G. W. Gibbons, and Z. H. Saleem, "Quasinormal modes for subtracted rotating and magnetized geometries," *Phys. Rev.*, vol. D90, no. 12, p. 124046, 2014.

[49] M. Cvetic, G. W. Gibbons, and Z. H. Saleem, "Thermodynamics of Asymptotically Conical Geometries," *Phys. Rev. Lett.*, vol. 114, no. 23, p. 231301, 2015.

[50] M. Cvetic, G. W. Gibbons, Z. H. Saleem, and A. Satz, "Vacuum Polarization of STU Black Holes and their Subtracted Geometry Limit," *JHEP*, vol. 01, p. 130, 2015.

[51] O. S. An, M. Cvetic, and I. Papadimitriou, "Black hole thermodynamics from a variational principle: Asymptotically conical backgrounds," *JHEP*, vol. 03, p. 086, 2016.

[52] A. Chakraborty and C. Krishnan, "Subttractors," *JHEP*, vol. 08, p. 057, 2013.

[53] A. Chakraborty and C. Krishnan, "Attraction, with Boundaries," *Class. Quant. Grav.*, vol. 31, p. 045009, 2014.

[54] B. Carter, "Global structure of the kerr family of gravitational fields," *Phys.Rev. 174 (1968) 1559-1571*, 1968.

[55] J. M. Maldacena and A. Strominger, "AdS(3) black holes and a stringy exclusion principle," *JHEP*, vol. 12, p. 005, 1998.

[56] Y. Matsuo, T. Tsukioka, and C. M. Yoo, "Another realization of kerr/cft correspondence," *Nucl.Phys. B825 (2010) 231-241*, 2009.

[57] A. Strominger, "Black hole entropy from near horizon microstates," *JHEP 9802 (1998) 009*, 1997.

[58] M. Cvetic and D. Youm, "All the static spherically symmetric black holes of heterotic string on a six torus," *Nucl.Phys. B472 (1996) 249-267*, 1995.

[59] R. Tolman and P. Ehrenfest, "Temperature equilibrium in a static gravitational field," *Physical Review*, 1930.

[60] R. M. Wald, "Gravitation, thermodynamics, and quantum theory," *Class.Quant.Grav. 16 (1999) A177-A190*, 1999.

[61] J. M. Bardeen and G. T. Horowitz, "The extreme kerr throat geometry: A vacuum analog of ads(2) x s**2," *Phys.Rev. D60 (1999) 104030*, 1999.

[62] G. Papadopoulos and P. Townsend, "Intersecting m-branes," *Phys.Lett. B380 (1996) 273-279*, 1996.

[63] A. A. Tseytlin, "Harmonic superpositions of m-branes," *Nucl.Phys. B475 (1996) 149-163*, 1996.

[64] J. M. Maldacena, A. Strominger, and E. Witten, "Black hole entropy in m theory," *JHEP 9712 (1997) 002*, 1997.

[65] I. Bena, M. Guica, and W. Song, "Un-twisting the nhek with spectral flows," *JHEP 1303 (2013) 028*, 2012.

[66] H. Kodama and A. Ishibashi, "Master equations for perturbations of generalized static black holes with charge in higher dimensions," *Prog. Theor. Phys.*, vol. 111, pp. 29–73, 2004.

[67] H. Kodama, A. Ishibashi, and O. Seto, "Brane world cosmology: Gauge invariant formalism for perturbation," *Phys.Rev. D62 (2000) 064022*, 2000.

[68] S. Mukohyama, "Gauge invariant gravitational perturbations of maximally symmetric spacetimes," *Phys.Rev. D62 (2000) 084015*, 2000.

[69] A. Higuchi, "Symmetric tensor spherical harmonics on the nn sphere and their application to the de sitter group so(nn ,1)," *J.Math.Phys. 28 (1987) 1553*, 1987.

[70] S. Chandrasekhar and S. L. Detweiler, "The quasi-normal modes of the schwarzschild black hole," *Proc.Roy.Soc.Lond. A344 (1975) 441-452*, 1975.

[71] D. L. Gunter, "A study of the coupled gravitational and electromagnetic perturbations to the reissner–nordstrom black hole: The scattering matrix, energy conversion, and quasi-normal modes," *Phil. Trans. Roy. Soc. Lond. A296, 497*, 1980.

[72] K. Kokkotas and B. F. Schutz, "Black hole normal modes: A WKB approach. 3. the Reissner-Nordstrom black hole," *Phys.Rev. D37 (1988) 3378-3387*, 1988.

[73] E. W. Leaver, "Quasinormal modes of reissner-nordstrom black holes," *Phys.Rev. D41 (1990) 2986-2997*, 1990.

[74] H. Onozawa, T. Mishima, T. Okamura, and H. Ishihara, "Quasinormal modes of maximally charged black holes," *Phys.Rev. D53 (1996) 7033-7040*, 1996.

[75] N. Andersson and H. Onozawa, "Quasinormal modes of nearly extreme reissner-nordstrom black holes," *Phys.Rev. D54 (1996) 7470-7475*, 1996.

[76] L. Motl and A. Neitzke, "Asymptotic black hole quasinormal frequencies," *Adv.Theor.Math.Phys. 7 (2003) no.2, 307-330*, 2003.

[77] N. Andersson and C. Howls, "The asymptotic quasinormal mode spectrum of nonrotating black holes," *Class.Quant.Grav. 21 (2004) 1623-1642*, 2003.

[78] S. Ferrara, R. Kallosh, and A. Strominger, "N=2 extremal black holes," *Phys. Rev.*, vol. D52, pp. R5412–R5416, 1995.

[79] S. Ferrara and R. Kallosh, "Supersymmetry and attractors," *Phys. Rev.*, vol. D54, pp. 1514–1524, 1996.

[80] S. Ferrara and R. Kallosh, "Universality of supersymmetric attractors," *Phys. Rev.*, vol. D54, pp. 1525–1534, 1996.

[81] V. Balasubramanian, P. Kraus, and A. E. Lawrence, "Bulk versus boundary dynamics in anti-de Sitter space-time," *Phys. Rev.*, vol. D59, p. 046003, 1999.

[82] B. Chen, Z. Xue, and J.-J. Zhang, "Note on Thermodynamic Method of Black Hole/CFT Correspondence," *JHEP*, vol. 03, p. 102, 2013.

[83] B. Chen, S.-x. Liu, and J.-j. Zhang, "Thermodynamics of Black Hole Horizons and Kerr/CFT Correspondence," *JHEP*, vol. 11, p. 017, 2012.

[84] A. Castro, J. M. Lapan, A. Maloney, and M. J. Rodriguez, "Black Hole Monodromy and Conformal Field Theory," *Phys. Rev.*, vol. D88, p. 044003, 2013.

[85] A. Castro, J. M. Lapan, A. Maloney, and M. J. Rodriguez, "Black Hole Scattering from Monodromy," *Class. Quant. Grav.*, vol. 30, p. 165005, 2013.

[86] T. Andrade, C. Keeler, A. Peach, and S. F. Ross, "Schrödinger holography with z = 2," *Class. Quant. Grav.*, vol. 32, no. 8, p. 085006, 2015.

[87] W. Chemissany and I. Papadimitriou, "Lifshitz holography: The whole shebang," *JHEP*, vol. 01, p. 052, 2015.

[88] H. Kodama and A. Ishibashi, "A Master equation for gravitational perturbations of maximally symmetric black holes in higher dimensions," *Prog. Theor. Phys.*, vol. 110, pp. 701–722, 2003.

[89] M. Cvetic and I. Papadimitriou, "AdS_2 Holographic Dictionary," 2016.

[90] E. Cremmer, C. Kounnas, A. Van Proeyen, J. P. Derendinger, S. Ferrara, B. de Wit, and L. Girardello, "Vector Multiplets Coupled to N=2 Supergravity: SuperHiggs Effect, Flat Potentials and Geometric Structure," *Nucl. Phys.*, vol. B250, pp. 385–426, 1985.

[91] M. J. Duff, J. T. Liu, and J. Rahmfeld, "Four-dimensional string-string-string triality," *Nucl. Phys.*, vol. B459, pp. 125–159, 1996.

[92] L. Huijse, S. Sachdev, and B. Swingle, "Hidden Fermi surfaces in compressible states of gauge-gravity duality," *Phys. Rev.*, vol. B85, p. 035121, 2012.

[93] X. Dong, S. Harrison, S. Kachru, G. Torroba, and H. Wang, "Aspects of holography for theories with hyperscaling violation," *JHEP*, vol. 06, p. 041, 2012.

[94] F.-F. Yuan and Y.-C. Huang, "Harrison metrics for the Schwarzschild black hole," *Commun. Theor. Phys.*, vol. 60, pp. 551–555, 2013.

[95] D. Anninos, S. A. Hartnoll, and D. M. Hofman, "Static Patch Solipsism: Conformal Symmetry of the de Sitter Worldline," *Class. Quant. Grav.*, vol. 29, p. 075002, 2012.

[96] R. J. Anantua, S. A. Hartnoll, V. L. Martin, and D. M. Ramirez, "The Pauli exclusion principle at strong coupling: Holographic matter and momentum space," *JHEP*, vol. 03, p. 104, 2013.

[97] R. A. Davison and B. Goutéraux, "Momentum dissipation and effective theories of coherent and incoherent transport," *JHEP*, vol. 01, p. 039, 2015.

[98] M. Guica, K. Skenderis, M. Taylor, and B. C. van Rees, "Holography for Schrodinger backgrounds," *JHEP*, vol. 02, p. 056, 2011.

[99] G. Compère, M. Guica, and M. J. Rodriguez, "Two Virasoro symmetries in stringy warped AdS_3," *JHEP*, vol. 12, p. 012, 2014.

[100] N. Iqbal, H. Liu, and M. Mezei, "Semi-local quantum liquids," *JHEP*, vol. 04, p. 086, 2012.

[101] G. T. Horowitz and V. E. Hubeny, "Quasinormal modes of AdS black holes and the approach to thermal equilibrium," *Phys. Rev.*, vol. D62, p. 024027, 2000.

[102] S. D. Mathur, "The fuzzball proposal for black holes: An elementary review," *Fortsch.Phys. 53 (2005) 793-827*, 2005.

[103] K. Skenderis and M. Taylor, "The fuzzball proposal for black holes," *Phys.Rept. 467 (2008) 117-171*, 2008.

[104] V. Balasubramanian, J. de Boer, S. El-Showk, and I. Messamah, "Black holes as effective geometries," *Class.Quant.Grav. 25 (2008) 214004*, 2008.

[105] S. D. Mathur, "The information paradox: A pedagogical introduction," *Class.Quant.Grav. 26 (2009) 224001*, 2009.

[106] B. D. Chowdhury and A. Virmani, "Modave lectures on fuzzballs and emission from the d1-d5 system," *arXiv:1001.1444*, 2010.

[107] I. Bena and N. P. Warner, "Resolving the Structure of Black Holes: Philosophizing with a Hammer," 2013.

[108] P. Berglund, E. G. Gimon, and T. S. Levi, "Supergravity microstates for bps black holes and black rings," *JHEP 0606 (2006) 007*, 2005.

[109] I. Bena and N. P. Warner, "Bubbling supertubes and foaming black holes," *Phys.Rev. D74 (2006) 066001*, 2005.

[110] I. Bena and N. P. Warner, "Black holes, black rings and their microstates," *Lect.Notes Phys. 755 (2008) 1-92*, 2007.

[111] J. de Boer, S. El-Showk, I. Messamah, and D. V. den Bleeken, "Quantizing n=2 multicenter solutions," *JHEP 0905 (2009) 002*, 2008.

[112] I. Bena, J. de Boer, M. Shigemori, and N. P. Warner, "Double, double supertube bubble," *JHEP 1110 (2011) 116*, 2011.

[113] I. Bena, S. Giusto, R. Russo, M. Shigemori, and N. P. Warner, "Habemus superstratum! a constructive proof of the existence of superstrata," *JHEP 1505 (2015) 110*, 2015.

[114] I. Bena, S. Giusto, E. J. Martinec, R. Russo, M. Shigemori, D. Turton, and N. P. Warner, "Smooth horizonless geometries deep inside the black-hole regime," *Phys.Rev.Lett. 117 (2016) no.20, 201601*, 2016.

[115] F. Denef, "Supergravity flows and d-brane stability," *JHEP 0008 (2000) 050*, 2000.

[116] I. Bena and N. P. Warner, "One ring to rule them all ... and in the darkness bind them?," *Adv.Theor.Math.Phys. 9 (2005) no.5, 667-701*, 2004.

[117] J. B. Gutowski and H. S. Reall, "General supersymmetric ads(5) black holes," *JHEP 0404 (2004) 048*, 2004.

[118] J. P. Gauntlett and J. B. Gutowski, "General concentric black rings," *Phys.Rev. D71 (2005) 045002*, 2004.

[119] H. Elvang, R. Emparan, D. Mateos, and H. S. Reall, "Supersymmetric black rings and three-charge supertubes," *Phys.Rev. D71 (2005) 024033*, 2004.

[120] I. Bena, S. Giusto, M. Shigemori, and N. P. Warner, "Supersymmetric solutions in six dimensions: A linear structure," *JHEP 1203 (2012) 084*, 2011.

[121] V. Jejjala, O. Madden, S. F. Ross, and G. Titchener, "Non-supersymmetric smooth geometries and d1-d5-p bound states," *Phys.Rev. D71 (2005) 124030*, 2005.

[122] S. Giusto, S. F. Ross, and A. Saxena, "Non-supersymmetric microstates of the d1-d5-kk system," *JHEP 0712 (2007) 065*, 2007.

[123] J. H. Al-Alawi and S. F. Ross, "Spectral flow of the non-supersymmetric microstates of the d1-d5-kk system," *JHEP 0910 (2009) 082*, 2009.

[124] I. Bena, S. Giusto, C. Ruef, and N. P. Warner, "A (running) bolt for new reasons," *JHEP 0911 (2009) 089*, 2009.

[125] N. Bobev and C. Ruef, "The nuts and bolts of einstein-maxwell solutions," *JHEP 1001 (2010) 124*, 2009.

[126] I. Bena, A. Puhm, and B. Vercnocke, "Metastable Supertubes and non-extremal Black Hole Microstates," *JHEP*, vol. 04, p. 100, 2012.

[127] I. Bena, A. Puhm, and B. Vercnocke, "Non-extremal Black Hole Microstates: Fuzzballs of Fire or Fuzzballs of Fuzz ?," *JHEP*, vol. 12, p. 014, 2012.

[128] G. Bossard and S. Katmadas, "Floating jmart," *JHEP 1504 (2015) 067*, 2014.

[129] G. Bossard and S. Katmadas, "A bubbling bolt," *JHEP 1407 (2014) 118*, 2014.

[130] I. Bena, G. Bossard, S. Katmadas, and D. Turton, "Non-BPS multi-bubble microstate geometries," *JHEP*, vol. 02, p. 073, 2016.

[131] I. Bena, G. Bossard, and S. Katmadas, "Bolting multicenter solutions," *JHEP 1701 (2017) 127*, 2016.

[132] S. Kachru, J. Pearson, and H. L. Verlinde, "Brane / flux annihilation and the string dual of a nonsupersymmetric field theory," *JHEP*, vol. 06, p. 021, 2002.

[133] S. Kachru, R. Kallosh, A. D. Linde, and S. P. Trivedi, "De sitter vacua in string theory," *Phys.Rev. D68 (2003) 046005*, 2003.

[134] S. P. et al. [Supernova Cosmology Project Collaboration], "Measurements of omega and lambda from 42 high-redshift supernovae," *Astrophys. J. 517, 565*, 1999.

[135] A. G. R. et al. [Supernova Search Team Collaboration], "Observational evidence from supernovae for an accelerating universe and a cosmological constant," *Astron. J. 116, 1009*, 1998.

[136] B. de Wit, D. Smit, and N. H. Dass, "Residual supersymmetry of compactified d=10 supergravity," *Nucl.Phys. B283 (1987) 165*, 1986.

[137] J. M. Maldacena and C. Nunez, "Supergravity description of field theories on curved manifolds and a no go theorem," *Int.J.Mod.Phys. A16 (2001) 822-855*, 2000.

[138] S. B. Giddings, S. Kachru, and J. Polchinski, "Hierarchies from fluxes in string compactifications," *Phys. Rev.*, vol. D66, p. 106006, 2002.

[139] C. Burgess, R. Kallosh, and F. Quevedo, "De sitter string vacua from supersymmetric d terms," *JHEP 0310 (2003) 056*, 2003.

[140] L. Aalsma, J. P. van der Schaar, and B. Vercnocke, "Constrained superfields on metastable anti-d3-branes," *JHEP 1705 (2017) 089*, 2017.

[141] E. McDonough and M. Scalisi, "Inflation from nilpotent kähler corrections," *JCAP 1611 (2016) no.11, 028*, 2016.

[142] R. Kallosh, A. Linde, D. Roest, and Y. Yamada, "D3 induced geometric inflation," *JHEP 1707 (2017) 057*, 2017.

[143] J. M. Maldacena and H. S. Nastase, "The Supergravity dual of a theory with dynamical supersymmetry breaking," *JHEP*, vol. 09, p. 024, 2001.

[144] R. Argurio, M. Bertolini, S. Franco, and S. Kachru, "Gauge/gravity duality and meta-stable dynamical supersymmetry breaking," *JHEP*, vol. 01, p. 083, 2007.

[145] R. Argurio, M. Bertolini, S. Franco, and S. Kachru, "Meta-stable vacua and D-branes at the conifold," *JHEP*, vol. 06, p. 017, 2007.

[146] O. DeWolfe, S. Kachru, and M. Mulligan, "A Gravity Dual of Metastable Dynamical Supersymmetry Breaking," *Phys. Rev.*, vol. D77, p. 065011, 2008.

[147] I. Bena, M. Graña, and N. Halmagyi, "On the Existence of Meta-stable Vacua in Klebanov-Strassler," *JHEP*, vol. 09, p. 087, 2010.

[148] P. McGuirk, G. Shiu, and Y. Sumitomo, "Non-supersymmetric infrared perturbations to the warped deformed conifold," *Nucl. Phys.*, vol. B842, pp. 383–413, 2011.

[149] I. Bena, M. Graña, S. Kuperstein, and S. Massai, "Giant Tachyons in the Landscape," *JHEP*, vol. 02, p. 146, 2015.

[150] I. Bena and S. Kuperstein, "Brane polarization is no cure for tachyons," *JHEP*, vol. 09, p. 112, 2015.

[151] I. Bena, D. Junghans, S. Kuperstein, T. V. Riet, T. Wrase, and M. Zagermann, "Persistent anti-brane singularities," *JHEP 1210 (2012) 078*, 2012.

[152] J. Blåbäck, U. H. Danielsson, and T. Van Riet, "Resolving anti-brane singularities through time-dependence," *JHEP*, vol. 02, p. 061, 2013.

[153] U. H. Danielsson and T. Van Riet, "Fatal attraction: more on decaying anti-branes," *JHEP*, vol. 03, p. 087, 2015.

[154] J. Polchinski, "Brane/antibrane dynamics and KKLT stability," 2015.

[155] B. Michel, E. Mintun, J. Polchinski, A. Puhm, and P. Saad, "Remarks on brane and antibrane dynamics," *JHEP*, vol. 09, p. 021, 2015.

[156] J. Polchinski and M. J. Strassler, "The String dual of a confining four-dimensional gauge theory," 2000.

[157] J. McGreevy, L. Susskind, and N. Toumbas, "Invasion of the giant gravitons from anti-de sitter space," *JHEP 0006 (2000) 008*, 2000.

[158] C. V. Johnson, A. W. Peet, and J. Polchinski, "Gauge theory and the excision of repulson singularities," *Phys.Rev. D61 (2000) 086001*, 1999.

[159] R. C. Myers and O. Tafjord, "Superstars and giant gravitons," *JHEP 0111 (2001) 009*, 2001.

[160] O. J. C. Dias, G. S. Hartnett, B. E. Niehoff, and J. E. Santos, "Mass-deformed m2 branes in stenzel space," *arXiv:1704.02323*, 2017.

[161] I. R. Klebanov and S. S. Pufu, "M-Branes and Metastable States," *JHEP*, vol. 08, p. 035, 2011.

[162] I. Bena, G. Giecold, and N. Halmagyi, "The Backreaction of Anti-M2 Branes on a Warped Stenzel Space," *JHEP*, vol. 04, p. 120, 2011.

[163] R. C. Myers, "Dielectric branes," *JHEP*, vol. 12, p. 022, 1999.

[164] J. Madore, "The fuzzy sphere," *Class.Quant.Grav. 9 (1992) 69-88*, 1991.

[165] I. R. Klebanov and M. J. Strassler, "Supergravity and a confining gauge theory: Duality cascades and chi SB resolution of naked singularities," *JHEP*, vol. 08, p. 052, 2000.

[166] J. Blåbäck, U. H. Danielsson, D. Junghans, T. Van Riet, and S. C. Vargas, "Localised anti-branes in non-compact throats at zero and finite T," *JHEP*, vol. 02, p. 018, 2015.

[167] E. A. Bergshoeff, K. Dasgupta, R. Kallosh, A. Van Proeyen, and T. Wrase, "$\overline{\mathrm{D3}}$ and dS," *JHEP*, vol. 05, p. 058, 2015.

[168] F. F. Gautason, D. Junghans, and M. Zagermann, "Cosmological Constant, Near Brane Behavior and Singularities," *JHEP*, vol. 09, p. 123, 2013.

[169] S. S. Gubser, "Curvature singularities: The Good, the bad, and the naked," *Adv. Theor. Math. Phys.*, vol. 4, pp. 679–745, 2000.

[170] I. Bena, A. Buchel, and O. J. C. Dias, "Horizons cannot save the Landscape," *Phys. Rev.*, vol. D87, no. 6, p. 063012, 2013.

[171] A. Buchel and D. A. Galante, "Cascading gauge theory on dS_4 and String Theory landscape," *Nucl.Phys.*, vol. B883, pp. 107–148, 2014.

[172] I. Bena, J. Blåbäck, U. H. Danielsson, and T. Van Riet, "Antibranes cannot become black," *Phys. Rev.*, vol. D87, no. 10, p. 104023, 2013.

[173] G. S. Hartnett, "Localised Anti-Branes in Flux Backgrounds," *JHEP*, vol. 06, p. 007, 2015.

[174] D. Z. Freedman and J. A. Minahan, "Finite temperature effects in the supergravity dual of the N=1* gauge theory," *JHEP*, vol. 0101, p. 036, 2001.

[175] A. Dymarsky, "On gravity dual of a metastable vacuum in klebanov-strassler theory," *JHEP 1105 (2011) 053*, 2011.

[176] G. W. Gibbons and N. P. Warner, "Global structure of five-dimensional fuzzballs," *Class. Quant. Grav.*, vol. 31, p. 025016, 2014.

[177] D. Junghans, "Dynamics of warped flux compactifications with backreacting antibranes," *Phys.Rev. D89 (2014) no.12, 126007*, 2014.

[178] I. Bena, M. Graña, S. Kuperstein, and S. Massai, "Polchinski-Strassler does not uplift Klebanov-Strassler," *JHEP*, vol. 09, p. 142, 2013.

[179] F. F. Gautason, B. Truijen, and T. Van Riet, "Smeared antibranes polarise in AdS," *JHEP*, vol. 07, p. 165, 2015.

[180] R. Emparan and H. S. Reall, "Black rings," *Class.Quant.Grav. 23 (2006) R169*, 2006.

[181] M. Cvetic, G. Gibbons, D. Kubiznak, and C. Pope, "Black hole enthalpy and an entropy inequality for the thermodynamic volume," *Phys.Rev. D84 (2011) 024037*, 2010.

[182] K. Copsey and G. T. Horowitz, "The Role of dipole charges in black hole thermodynamics," *Phys. Rev.*, vol. D73, p. 024015, 2006.

[183] S. W. Hawking and G. T. Horowitz, "The Gravitational Hamiltonian, action, entropy and surface terms," *Class. Quant. Grav.*, vol. 13, pp. 1487–1498, 1996.

[184] M. Cvetič, G. W. Gibbons, H. Lü, and C. N. Pope, "Ricci flat metrics, harmonic forms and brane resolutions," *Commun. Math. Phys.*, vol. 232, pp. 457–500, 2003.

[185] S. Kachru, R. Kallosh, A. D. Linde, J. M. Maldacena, L. P. McAllister, and S. P. Trivedi, "Towards inflation in string theory," *JCAP*, vol. 0310, p. 013, 2003.

[186] S. Massai, "Metastable Vacua and the Backreacted Stenzel Geometry," *JHEP*, vol. 06, p. 059, 2012.

[187] W. Cottrell, J. Gaillard, and A. Hashimoto, "Gravity dual of dynamically broken supersymmetry," *JHEP*, vol. 08, p. 105, 2013.

[188] G. Giecold, F. Orsi, and A. Puhm, "Insane Anti-Membranes?," *JHEP*, vol. 03, p. 041, 2014.

[189] J. Blåbäck, "Note on M2-branes in opposite charge," *Phys. Rev.*, vol. D89, no. 6, p. 065004, 2014.

[190] R. Emparan and H. S. Reall, "A Rotating black ring solution in five-dimensions," *Phys. Rev. Lett.*, vol. 88, p. 101101, 2002.

[191] T. Eguchi and A. J. Hanson, "Asymptotically Flat Selfdual Solutions to Euclidean Gravity," *Phys. Lett.*, vol. B74, p. 249, 1978.

[192] P. Candelas and X. C. de la Ossa, "Comments on Conifolds," *Nucl. Phys.*, vol. B342, pp. 246–268, 1990.

[193] M. Stenzel, "Ricci-flat metrics on the complexification of a compact rank one symmetric space," *manuscripta mathematica*, vol. 80, no. 1, pp. 151–163, 1993.

[194] P. K. Townsend and M. Zamaklar, "The First law of black brane mechanics," *Class. Quant. Grav.*, vol. 18, pp. 5269–5286, 2001.

[195] R. C. Myers and M. J. Perry, "Black Holes in Higher Dimensional Space-Times," *Annals Phys.*, vol. 172, p. 304, 1986.

[196] F. Ferrari and A. Rovai, "Gravity and On-Shell Probe Actions," 2016.

[197] T. Ortin, *Gravity and strings*. Cambridge Univ. Press, 2004.

[198] L. F. Abbott and S. Deser, "Stability of Gravity with a Cosmological Constant," *Nucl. Phys.*, vol. B195, p. 76, 1982.

[199] A. Bergman and C. P. Herzog, "The Volume of some nonspherical horizons and the AdS / CFT correspondence," *JHEP*, vol. 01, p. 030, 2002.

[200] T. Andrade, C. Keeler, A. Peach, and S. F. Ross, "Schrödinger holography for z ¡ 2," *Class.Quant.Grav. 32 (2015) no.3, 035015*, 2014.

[201] D. Son, "Toward an ads/cold atoms correspondence: A geometric realization of the schrodinger symmetry," *Phys.Rev. D78 (2008) 046003*, 2008.

[202] K. Balasubramanian and J. McGreevy, "Gravity duals for non-relativistic cfts," *Phys.Rev.Lett. 101 (2008) 061601*, 2008.

[203] S. Kachru, X. Liu, and M. Mulligan, "Gravity duals of lifshitz-like fixed points," *Phys.Rev. D78 (2008) 106005*, 2008.